Centro Brasileiro de Pesquisas Físicas
Programa de Doutorado

Rodrigo Galhardo Rana

$\mathbb{Z}_2^n$ graded (super)algebras and n-bit physics: a framework for parastatistics

Rio de Janeiro/RJ

2025

$\mathbb{Z}_2^n$ GRADED (SUPER)ALGEBRAS AND n-BIT PHYSICS: A FRAMEWORK FOR PARASTATISTICS

Rodrigo Galhardo Rana

Defesa de Doutorado submetida a coordenação de formação científica do Centro Brasileiro de Pesquisas Físicas como parte dos requisitos para a obtenção do título de Doutor em Física.
Orientador: Prof. Dr. Francesco Toppan

Rio de Janeiro/RJ

2025

"Z 2^n GRADED (SUPER) ALGEBRAS AND n-bit PHYSICS: A FRAMEWORK FOR PARASTATISTICS"

RODRIGO GALHARDO RANA

Tese de Doutorado em Física apresentada no Centro Brasileiro de Pesquisas Físicas do Ministério da Ciência Tecnologia e Inovação. Fazendo parte da banca examinadora os seguintes professores:

gov.br Documento assinado digitalmente
FRANCESCO TOPPAN
Data: 03/07/2025 16:18:51-0300
Verifique em https://validar.iti.gov.br

Francesco Toppan - Orientador/CBPF

Joris Van der Jeugt

Joris Van der Jeugt – UGent

gov.br Documento assinado digitalmente
SERGIO AUGUSTO GIARDINO FILHO
Data: 30/06/2025 15:30:22-0300
Verifique em https://validar.iti.gov.br

Sergio Giardino - UFRGS

gov.br Documento assinado digitalmente
ALEKSANDR NIKOLAIEVICH PINZUL
Data: 01/07/2025 21:16:20-0300
Verifique em https://validar.iti.gov.br

Aleksandr Nikolaievich Pinzul - UnB

Andrei Mikhailov - UNESP

Rio de Janeiro, 25 de junho de 2025.

Abstract

This thesis explores the algebraic foundations of Z_2^n-graded Lie (super)algebras and their physical applications in quantum mechanics and quantum field theory. By employing a Boolean logic framework, we classify all inequivalent graded brackets via mappings $\mathbb{Z}_2^n \times \mathbb{Z}_2^n \to \mathbb{Z}_2$, leading to

$$b_n = n + \lfloor n/2 \rfloor + 1$$

distinct Lie-type structures. These mappings, constructed through Karnaugh maps and logical operations (AND, OR, XOR), define the commutation and anticommutation relations of n-bit parastatistics, generalizing conventional Bose-Fermi statistics.

The physical implications of these structures manifest in Z_2^n-graded quantum Hamiltonians, which support inequivalent multiparticle quantizations. Depending on the graded algebra, particles are categorized into bosonic, fermionic, parabosonic, and parafermionic sectors, each with unique exchange symmetries. Crucially, statistical transmutations arising from the graded brackets lead to physically distinguishable parastatistics, measurable through eigenvalues of specific observables.

A key application of this formalism is to $\mathcal{N}$-extended supersymmetric and superconformal quantum mechanics, where the graded structures induce $s_{\mathcal{N}}$ inequivalent formulations (with $s_{\mathcal{N}} = 2, 6, 10, 14$ for $\mathcal{N} = 1, 2, 4, 8$, respectively). These inequivalences correspond to alternative statistical transmutations of supercharges, modifying the energy spectra of supersymmetric systems. In particular, in the $\mathcal{N} = 2$ superconformal model with an $sl(2|1)$ spectrum-generating algebra, the $\mathbb{Z}_2^2$-graded parastatistics introduce an energy level degeneracy that cannot be realized within standard Bose-Fermi statistics.

This work establishes Boolean representations as a fundamental tool for constructing and classifying graded symmetries, offering new perspectives on exotic quantum statistics and their experimental signatures. The results have potential applications in quantum field theory, higher-dimensional supersymmetry, and quantum information science.

Resumo

Esta tese explora os fundamentos algébricos das álgebras de Lie (super)graduadas por $\mathbb{Z}_2^n$ e suas aplicações físicas em mecânica quântica e teoria quântica de campos. Utilizando uma estrutura lógica booleana, classificamos todos os *brackets* graduados inequivocamente distintos por meio de aplicações $\mathbb{Z}_2^n \times \mathbb{Z}_2^n \to \mathbb{Z}_2$, o que conduz a

$$b_n = n + \lfloor n/2 \rfloor + 1$$

estruturas distintas do tipo Lie. Essas aplicações, construídas com auxílio de mapas de Karnaugh e operações lógicas (AND, OR, XOR), definem as relações de comutação e anticomutação das parastatísticas de n bits, generalizando as estatísticas convencionais de Bose–Fermi.

As implicações físicas dessas estruturas manifestam-se em hamiltonianos quânticos $\mathbb{Z}_2^n$-graduados, os quais admitem quantizações multipartículas inequivocamente distintas. Dependendo da álgebra graduada considerada, as partículas são classificadas em setores bosônicos, fermiônicos, parabosônicos e parafermiônicos, cada um com simetrias de troca características. Essencialmente, as transmutações estatísticas induzidas pelos *brackets* graduados dão origem a parastatísticas fisicamente distinguíveis, mensuráveis por meio dos autovalores de certos observáveis.

Uma aplicação central desse formalismo encontra-se na mecânica quântica supersimétrica e superconforme com $\mathcal{N}$ extensões, onde as estruturas graduadas geram $s_{\mathcal{N}}$ formulações inequivocamente distintas (com $s_{\mathcal{N}} = 2, 6, 10, 14$ para $\mathcal{N} = 1, 2, 4, 8$, respectivamente). Tais inequivalências correspondem a diferentes transmutações estatísticas das supercargas, modificando os espectros de energia dos sistemas supersimétricos. Em particular, no modelo superconformal com $\mathcal{N} = 2$ e álgebra de geração espectral $sl(2|1)$, as parastatísticas graduadas por $\mathbb{Z}_2^2$ introduzem uma degenerescência nos níveis de energia que não pode ser reproduzida no contexto das estatísticas de Bose–Fermi padrão.

Este trabalho estabelece as representações booleanas como uma ferramenta fundamental para a construção e classificação de simetrias graduadas, oferecendo novas perspectivas sobre estatísticas quânticas exóticas e suas assinaturas experimentais. Os resultados obtidos possuem aplicações potenciais em teoria quântica de campos, supersimetria em dimensões elevadas e ciência da informação quântica.

Key-words: Estruturas algébricas. Superalgebras. Parastatística.

Table of contents

1 Introduction

Symmetry and algebraic structures play a fundamental role in modern theoretical physics, shaping our understanding of fundamental interactions, quantum mechanics, and quantum field theory. Lie algebras and their graded extensions, particularly Lie superalgebras, have been extensively explored in the context of supersymmetry (SUSY), string theory, and quantum field theory [1, 2, 3, 4]. While conventional SUSY relies on $\mathbb{Z}_2$-graded algebras, more generalized grading structures, such as $\mathbb{Z}_2^n$-graded algebras, have recently gained attention due to their potential to describe exotic quantum symmetries, non-standard statistics, and higher-order generalizations of supersymmetry.

We focus on $\mathbb{Z}_2^n$-graded structures, examining both their mathematical foundations and their physical consequences [5, 6, 7, 8, 9, 10, 11, 12, 13, 14, 15, 16, 17]. These graded structures provide a natural extension of supersymmetry and introduce alternative symmetry transformations that go beyond traditional Lie superalgebras. One of the key motivations behind their study is their appearance in dynamical symmetries of physical systems, including classical and quantum mechanics, as well as field-theoretic models.

In non-relativistic quantum mechanics, $\mathbb{Z}_2^2$-graded symmetries naturally emerge as dynamical invariances in the Lévy-Leblond equations, which describe non-relativistic spin-$\frac{1}{2}$ particles [18, 19]. Recent advancements in this direction include the classification of Lévy-Leblond spinors [20], highlighting the potential physical relevance of these generalized symmetries. Extensions to classical mechanics have also been considered, where worldline models incorporating $\mathbb{Z}_2^2$ gradings have been explored as an extension of phase-space dynamics [21]. In quantum field theory, similar generalizations have been studied in two-dimensional sigma models, where $\mathbb{Z}_2^2$-graded supersymmetry has been explicitly constructed [22]. Moreover, quantum mechanical formulations incorporating $\mathbb{Z}_2^2$-graded algebras have been analyzed in various models [23, 24, 25]. Superspace extensions of these graded structures have also been systematically studied, revealing their role in generalized SUSY models [26, 27, 28, 29, 30, 31, 32]. While most studies focus on $n = 2$, important advancements have been made for higher-order generalizations ($n \geq 3$), as explored in [33, 34, 35, 36, 37, 38].

A particularly intriguing consequence of $\mathbb{Z}_2^n$-graded algebras is their connection to paraparticles, exotic quantum states that generalize conventional bosons and fermions [39, 40, 41, 42, 43, 44]. Paraparticles obey intermediate statistics that differ from Bose-Fermi symmetry, leading to novel algebraic and physical properties. One of the most pressing questions in this context is whether paraparticles are physically distinguishable from ordinary bosons and fermions. This problem has been tackled using exchange operators that measure statistical properties in multiparticle quantum states [39, 40]. In conventional quantum mechanics, the eigenvalues of such operators reflect wavefunction symmetry: $+1$ for bosons and -1 for fermions. However, in $\mathbb{Z}_2^n$-graded systems, the nature of exchange operators becomes significantly more intricate, requiring a deeper analysis of the statistical transmutations that arise from these algebraic structures [45], also [46, 47].

A critical aspect of these statistical transmutations is their effect on physical observables, particularly in quantum mechanics and field theory. Understanding how these transmutations alter wavefunction symmetrization rules is essential for uncovering their implications in condensed matter physics, quantum information theory, and high-energy physics.

To systematically classify inequivalent $\mathbb{Z}_2^n$-graded Lie brackets, we employ a Boolean logic gate representation through Karnaugh maps [48] (a diagram method to simplify Boolean expressions), which provides a computationally efficient framework to encode the commutation and anticommutation relations of graded algebras. This approach is based on the observation that graded Jacobi identities and associative compatibility conditions naturally translate into Boolean operations. In this formulation, elements of the algebra are assigned binary grading labels, and their commutation properties, whether they commute, anticommute, are determined by logical AND, OR, and XOR operations on their grading vectors. This allows for a straightforward method to generate and classify all possible graded brackets, ensuring that the entire space of inequivalent structures is exhaustively explored.

Beyond their abstract classification, we explore the physical consequences of $\mathbb{Z}_2^n$-graded algebras in quantum mechanics and quantum field theory. A particularly relevant application is their impact on statistical transmutations, which lead to novel multiparticle wavefunction symmetrization rules. Unlike conventional Bose-Fermi statistics, these transmutations introduce alternative forms of quantum statistics, fundamentally modifying the structure of quantum states.

One of the key results of this work is the application of these statistical transmutations to supersymmetric quantum mechanics (SQM). We analyze how different $\mathbb{Z}_2^n$-graded brackets lead to inequivalent Lie (super)algebras associated with supersymmetry, resulting in observable modifications to energy spectra and degeneracy structures in quantum systems. A particularly striking example is found in superconformal quantum mechanics with the de Alfaro-Fubini-Furlan (DFF) oscillator term [49]. We demonstrate that for certain choices of $\mathbb{Z}_2^n$-graded brackets, the resulting paraparticle statistics produce energy spectra that cannot be reproduced by standard bosons and fermions, providing a concrete and testable prediction for $\mathbb{Z}_2^n$-graded symmetries.

This thesis is structured as follows. Section 2 introduces the mathematical foundations of color (super)algebras and their generalization beyond Lie superalgebras. Section 3 presents the classification of $\mathbb{Z}_2^n$-graded Lie brackets and the Boolean logic representation. Section 4 explores the physical consequences of these algebras, focusing on quantum Hamiltonians. Section 5 is about paraparticle detectability as a consequence of statistical transmutations. Section 6 develops applications in quantum field theory. Section 7 summarizes our findings and discusses future research directions.

This study contributes to the growing interest in higher-graded algebraic structures and their physical realizations, establishing a firm foundation for further exploration of exotic symmetries in physics.

2 Color (Super)algebras

Algebraic structures play a central role in mathematical physics, particularly in understanding and modeling symmetries within physical systems. Among these structures, Color (Super)algebras generalize the concepts of Lie algebras and superalgebras by incorporating graded symmetries and exotic commutation relations. These algebras extend traditional frameworks by allowing elements to be assigned "grades", which dictate how they interact with one another under multiplication or bracket operations. This chapter develops the foundational principles of Color (Super)algebras, preparing the ground for their application and further generalization in subsequent chapters.

2.1 Graded Algebras and Symmetries

To understand Color (Super)algebras, we begin with the concept of a graded algebra. Let V be a vector space over a field $\mathbb{K}$. The space V is said to be graded if it can be decomposed into a direct sum of subspaces indexed by elements of a grading set G:

$$V = \bigoplus_{g \in G} V_g. \tag{2.1}$$

The elements of V_g are referred to as homogeneous elements of grade g. A graded algebra is a graded vector space equipped with a bilinear product $\cdot : V \times V \to V$ that preserves the grading:

$$V_g \cdot V_h \subseteq V_{g+h}, \quad \forall g, h, g+h \in G. \tag{2.2}$$

Here, the addition $g + h$ is defined within the grading set G, which is typically chosen to reflect the symmetries under consideration.

In the context of Color (Super)algebras, the grading set G introduces a key distinction between different types of algebraic structures. The simplest example is a Z_2-graded algebra, where $G = \{0, 1\}$. This grading distinguishes even elements ($g = 0$) from odd elements ($g = 1$), a characteristic feature of superalgebras. On the other hand, color (super)algebras use more general grading sets, allowing for a richer classification of elements and their interactions.

2.2 Commutation Relations and Generalized Symmetry

A defining feature of Color (Super)algebras is the modification of traditional commutation relations to accommodate the grading. For two homogeneous elements

$A \in V_g$ and $B \in V_h$, the commutator is replaced by a graded commutator:

$$[A, B] = A \cdot B - (-1)^{\langle g,h \rangle} B \cdot A, \tag{2.3}$$

where $\langle g, h\rangle$ is a bilinear mapping that determines the interaction between grades g and h. The sign factor $(-1)^{\langle g,h\rangle}$ encodes the symmetry properties of the algebra. For instance, in a $\mathbb{Z}_2$-graded algebra, $\langle g, h\rangle$ often corresponds to the product of g and h modulo 2.

The choice of $\langle g, h\rangle$ determines whether the algebra exhibits commutative or anti-commutative behavior for certain pairs of elements. If $\langle g, h\rangle = 0$, the graded commutator reduces to the standard commutator, while if $\langle g, h\rangle = 1$, the graded commutator behaves like an anticommutator. This flexibility allows Color (Super)algebras to describe a wide range of symmetries, from those seen in bosonic systems to those characteristic of fermionic or parastatistic systems.

2.3 Jacobi Identity and Algebraic Consistency

To ensure that the structure of a graded algebra remains consistent, its elements must satisfy a generalized form of the Jacobi identity. For three homogeneous elements $A \in V_g$, $B \in V_h$, and $C \in V_k$, the graded Jacobi identity is given by:

$$(-1)^{\langle k,g\rangle}[A, [B, C]] + (-1)^{\langle g,h\rangle}[B, [C, A]] + (-1)^{\langle h,k\rangle}[C, [A, B]] = 0. \tag{2.4}$$

This identity guarantees that the bracket operation is well-defined and compatible with the algebra's grading. The bilinear form $\langle g, h\rangle$ plays a critical role here, influencing how terms interact and ensuring that the structure is closed under the bracket operation.

2.4 Applications and Physical Relevance

Color (Super)algebras are of significant interest in physics due to their ability to model exotic symmetries and generalized statistics. For example, superalgebras, an important subclass of Color (Super)algebras, are central to supersymmetry, where bosonic and fermionic degrees of freedom are unified within a single theoretical framework. The graded structure of these algebras allows for the coexistence of commutative and anti-commutative behaviors, reflecting the fundamental properties of these systems.

Beyond supersymmetry, Color (Super)algebras provide a natural framework for describing parastatistics, where particles obey generalized commutation relations that extend beyond the standard Bose-Einstein and Fermi-Dirac statistics. The grading structure encodes the interactions between different particle types, offering insights into the underlying symmetries of these systems.

From a mathematical perspective, graded algebras serve as a foundation for studying representation theory and category theory, where the grading set G facilitates the classification of representations and morphisms. These tools are increasingly relevant in areas such as topological quantum field theory, quantum computing, and digital logic, where graded structures naturally align with the underlying mathematical framework.

2.5 Towards $\mathbb{Z}_2^n$-Graded Algebras

The Color (Super)algebras discussed in this chapter provide a versatile framework for studying graded symmetries, but their scope is limited by the choice of grading set G. In the next chapter, we extend these concepts to $\mathbb{Z}_2^n$-graded algebras, where $G = \mathbb{Z}_2^n$ represents the n-dimensional vector space over $\mathbb{Z}_2$. This generalization introduces new possibilities for classifying elements and defining commutation relations, enabling the description of more complex symmetries and higher-dimensional grading structures.

$\mathbb{Z}_2^n$-graded algebras not only generalize the properties of Color (Super)algebras but also connect directly to physical applications, such as parastatistics and quantum field theories with quaternionic or exotic scalar fields. The following chapter formalizes the construction of $\mathbb{Z}_2^n$-graded Lie brackets, exploring their mathematical properties and their relevance to contemporary theoretical physics.

3 Construction of $\mathbb{Z}_2^n$-Graded Lie Brackets

The generalization of algebraic structures to $\mathbb{Z}_2^n$-graded Lie brackets provides a versatile mathematical framework for studying systems with graded symmetries. These brackets extend the concepts of Lie algebras and superalgebras by introducing higher-dimensional grading groups, allowing for richer interactions and more intricate classification schemes. In this chapter, we formalize the construction of $\mathbb{Z}_2^n$-graded Lie brackets, focusing on their foundational properties, computational representations, and their role as the basis for equivalence classes in graded algebras.

3.1 Definitions and Framework

The $\mathbb{Z}_2^n$-grading structure extends the familiar notion of grading in $\mathbb{Z}_2$-graded algebras (superalgebras) by using the group $G = \mathbb{Z}_2^n$, which consists of n-dimensional binary vectors. The group operation is component-wise addition modulo 2, denoted as:

$$g + h = (g_1 + h_1, g_2 + h_2, \ldots, g_n + h_n) \mod 2. \tag{3.1}$$

Each vector $g \in G$ serves as a grade that determines the behavior of elements in a graded algebra.

3.2 Canonical Forms and Generalized Brackets

The study of $\mathbb{Z}_2^n$-graded Lie brackets often begins by specifying canonical forms for the bilinear form $\langle g, h \rangle$. These forms influence the behavior of the bracket and the classification of the algebra.

3.2.1 Standard Bilinear Forms

One common choice for $\langle g, h \rangle$ is the standard dot product modulo 2:

$$\langle g, h \rangle = g \cdot h \mod 2, \tag{3.2}$$

where $g \cdot h$ is the dot product of the binary vectors g and h. This form encodes the parity of the interaction between grades, determining whether the bracket behaves as a commutator or an anticommutator.

3.2.2 Generalized Brackets and Mixed Symmetries

The flexibility of $\mathbb{Z}_2^n$-graded Lie brackets allows for the definition of generalized brackets that interpolate between purely commutative and purely anticommutative behavior. For homogeneous elements $A \in V_g$ and $B \in V_h$, the generalized bracket can be written as:

$$[A, B] = \begin{cases} A \cdot B - B \cdot A, & \text{if } \langle g, h \rangle = 0, \\ A \cdot B + B \cdot A, & \text{if } \langle g, h \rangle = 1. \end{cases} \tag{3.3}$$

Such brackets are particularly useful in modeling systems with mixed symmetries, such as parastatistics or extended supersymmetry.

The complete list of inequivalent canonical forms for $\langle \alpha, \beta \rangle$ can be expressed as follows:

I - For $\mathbb{Z}_2^n$-graded compatible Lie algebras:

$$\langle g, h \rangle_0 = 0 \quad \text{(it is an ordinary Lie algebra induced by a vanishing scalar product matrix)}, \tag{3.4}$$

and

$$\langle g, h \rangle_{n+1+k} = \sum_{j=0}^{k} (g_{2j+1}h_{2j+2} + g_{2j+2}h_{2j+1}) \mod 2, \quad k = 0, 1, 2, \ldots, \left\lfloor \frac{n}{2} \right\rfloor - 1, \tag{3.5}$$

where the maximal value for k is expressed in terms of the floor function.

II - For $\mathbb{Z}_2^n$-graded compatible Lie superalgebras:

$$\langle g, h \rangle_k = \sum_{j=1}^{k} (g_j h_j) \mod 2, \quad \text{for } k = 1, 2, \ldots, n. \tag{3.6}$$

Therefore, the total number b_n of inequivalent, $\mathbb{Z}_2^n$-graded compatible Lie (super)algebras which obey definitions I and II is given by:

$$b_n = n + \left\lfloor \frac{n}{2} \right\rfloor + 1. \tag{3.7}$$

3.2.3 Boolean Representations of Graded Brackets

Boolean algebra provides a natural framework for representing the $\mathbb{Z}_2^n$-graded structure of Lie brackets. By interpreting the components of the grading vectors $\alpha = (\alpha_1, \alpha_2, \ldots, \alpha_n)$ and $\beta = (\beta_1, \beta_2, \ldots, \beta_n)$ as binary inputs, the bilinear map $\langle \alpha, \beta \rangle$ can be expressed as a Boolean function (where we changed the notation to greek letters to specifically refers to boolean expressions). This allows the interaction between graded elements to be modeled using logical operations such as AND ($\wedge$), OR ($\vee$), XOR ($\oplus$), and NOT ($\neg$).

Boolean Expressions for $\mathbb{Z}_2^n$-Graded Brackets

For homogeneous elements $A \in V_\alpha$ and $B \in V_\beta$, the graded antisymmetry of the bracket is defined as:

$$[A, B] = -(-1)^{\langle\alpha,\beta\rangle}[B, A]. \tag{3.8}$$

Here, $(-1)^{\langle\alpha,\beta\rangle}$ determines the sign factor and depends on the Boolean expression for $\langle\alpha, \beta\rangle$, a bilinear form defined on the components of α and β.

The most common Boolean expressions for $\langle\alpha, \beta\rangle$ include:

$$\langle\alpha, \beta\rangle = \bigoplus_{i=1}^{n}(\alpha_i \wedge \beta_i), \tag{3.9}$$

where the XOR operation combines the pairwise AND operations on the components, and

$$\langle\alpha, \beta\rangle = \bigoplus_{i\neq j}(\alpha_i \wedge \beta_j), \tag{3.10}$$

representing antisymmetric cross terms. Fully symmetric contributions may combine these forms:

$$\langle\alpha, \beta\rangle = \bigoplus_{i=1}^{n}(\alpha_i \wedge \beta_i) + \bigoplus_{i\neq j}(\alpha_i \wedge \beta_j). \tag{3.11}$$

Logical Operations in $\mathbb{Z}_2^n$

Boolean algebra supports the operations required to model graded interactions. The key operations are:
- AND ($\wedge$ or .): Represents the logical intersection of two inputs. For example, $\alpha_1 \wedge \beta_1 = 1$ if both $\alpha_1 = 1$ and $\beta_1 = 1$.
- OR ($\vee$ or $+$): Represents the union of inputs. $\alpha_1 \vee \beta_1 = 1$ if $\alpha_1 = 1$ or $\beta_1 = 1$.
- XOR ($\oplus$): Represents exclusive disjunction, where $\alpha_1 \oplus \beta_1 = 1$ if $\alpha_1 \neq \beta_1$.
- NOT ($\neg$): Represents negation, flipping the binary value ($\neg\alpha_1 = 1-\alpha_1$). Also represented by a overline as $\overline{\alpha_1}$.

These operations enable the compact representation of bilinear maps, which can be further analyzed using truth tables, Karnaugh maps, and circuit diagrams.

Truth Tables for $\mathbb{Z}_2^2$, example of the color (super)algebra

The truth table for the symmetric mapping $\langle\alpha, \beta\rangle = \alpha_1 \cdot \beta_1 \oplus \alpha_2 \cdot \beta_2$ is:

α_1	α_2	β_1	β_2	$\langle\alpha,\beta\rangle$
0	0	0	0	0
0	0	0	1	0
0	0	1	0	0
0	0	1	1	0
0	1	0	0	0
0	1	0	1	1
0	1	1	0	0
0	1	1	1	1
1	0	0	0	0
1	0	0	1	0
1	0	1	0	1
1	0	1	1	1
1	1	0	0	0
1	1	0	1	1
1	1	1	0	1
1	1	1	1	0

This table shows all possible combinations of $\alpha_1, \alpha_2, \beta_1, \beta_2$ and their corresponding $\langle\alpha,\beta\rangle$.

Karnaugh Maps and Simplification of Boolean Expressions

Karnaugh maps (K-maps) are a graphical tool used to simplify Boolean expressions systematically. They represent truth table outputs in a two-dimensional grid format, where adjacent cells differ by only one variable (according to Gray code ordering). This adjacency property makes it easier to visually identify terms that can be combined to simplify the expression. Karnaugh maps are widely used in digital logic design and computational modeling to minimize the number of logic gates required in circuit implementations.

To construct a Karnaugh map for the bilinear map $\langle\alpha,\beta\rangle$, we follow these steps:

1. Identify the variables (here, $\alpha_1, \alpha_2, \beta_1, \beta_2$) and their combinations, which define the rows and columns of the map.

2. Fill in the grid using the values of $\langle\alpha,\beta\rangle$ from the truth table.

3. Group adjacent cells with the same output value (e.g., 1) into blocks. These groups should be powers of two in size (1, 2, 4, 8, etc.).

4. Use the groups to write the simplified Boolean expression, where each group corresponds to a term that can be factored out.

In this case, the Karnaugh map for the bilinear map $\langle \alpha, \beta \rangle = \alpha_1 \cdot \beta_1 \oplus \alpha_2 \cdot \beta_2$ is as follows:

$\alpha_1\alpha_2 \backslash \beta_1\beta_2$	00	01	11	10
00	0	0	0	0
01	0	1	1	0
11	0	1	0	1
10	0	0	1	1

The rows represent the combinations of α_1 and α_2, while the columns correspond to β_1 and β_2. The value in each cell is the output of the bilinear map $\langle \alpha, \beta \rangle$ for the given input combination.

Next, we group adjacent 1s:

- A group of size 2 in the row $\alpha_1\alpha_2 = 01$ and columns $\beta_1\beta_2 = 11, 10$.
- Another group of size 2 in the row $\alpha_1\alpha_2 = 11$ and columns $\beta_1\beta_2 = 01, 10$.

From these groups, the simplified Boolean expression can be written as:

$$\langle \alpha, \beta \rangle = (\alpha_1.\beta_1) \oplus (\alpha_2.\beta_2). \tag{3.12}$$

This process significantly reduces the complexity of Boolean expressions by eliminating redundant terms. The use of Karnaugh maps is particularly advantageous for simplifying expressions in higher dimensions, such as those arising in $\mathbb{Z}_2^n$-graded algebras, where direct inspection of truth tables becomes impractical.

Boolean Circuits

The circuit diagram for the above expression consists of:
1. Two AND gates to compute $\alpha_1 \wedge \beta_1$ and $\alpha_2 \wedge \beta_2$.
2. An XOR gate to combine their outputs.

This circuit effectively implements the bilinear map for $\mathbb{Z}_2^2$-graded algebras.

Practical Implications

Boolean representations provide several advantages:
1. Digital Simulations: Graded structures can be directly simulated using digital logic. Each component of α and β is treated as a binary input, and the bilinear map is implemented as a logical function.
2. Quantum Computing: Boolean algebra aligns with the binary nature of qubits, enabling

the modeling of $\mathbb{Z}_2^n$-graded algebras in quantum systems.
3. Efficient Analysis: Tools such as truth tables, Karnaugh maps, and Boolean circuits streamline the study of graded algebras, particularly in applications like parastatistics.

Boolean algebra thus serves as both a conceptual and practical framework for $\mathbb{Z}_2^n$-graded Lie brackets, bridging abstract algebra with computational methods.

3.3 $\mathbb{Z}_2^n$ Structures

For $\mathbb{Z}_2^n$, the graded vectors of n-components are associated with gradings in powers of 2, as are the related generators. Specifically, there are 2^n gradations. For example:

- For $n = 1$ ($\mathbb{Z}_2$):
$$[I] = 0, \quad [A] = 1,$$
where the identity I has grading 0 and the single generator A has grading 1.
- For $n = 2$ ($\mathbb{Z}_2^2$):
$$[I] = 00, \quad [A] = 01, \quad [B] = 10, \quad [C] = 11.$$
- For $n = 3$ ($\mathbb{Z}_2^3$):
$$[I] = 000, [A] = 001, [B] = 010, [C] = 011, [D] = 100, [E] = 101, [F] = 110, [G] = 111,$$
with each generator assigned a unique binary grading.

3.3.1 Structure for $n = 1$: $\mathbb{Z}_2$

For $n = 1$, the vector space G is divided into two homogeneous subspaces:

$$G = G_0 \oplus G_1.$$

The possible mappings that respect these restrictions are:

1. $\langle \alpha, \beta \rangle = 0$, corresponding to an ordinary Lie algebra.
2. $\langle \alpha, \beta \rangle = \alpha \cdot \beta \mod 2$, defining a $\mathbb{Z}_2$-graded superalgebra.

3.3.2 Structure for $n = 2$: $\mathbb{Z}_2^2$

Consider the generators I, A, B, C with respective gradations $00, 01, 10, 11$. Following the construction for $n = 1$, there are four possible mappings:

1. $\langle \alpha, \beta \rangle = 0$, representing an ordinary Lie algebra.

2. $\langle \alpha, \beta \rangle = \alpha_1 \cdot \beta_1$, defining a $\mathbb{Z}_2$-graded superalgebra embedded in $\mathbb{Z}_2^2$.
3. $\langle \alpha, \beta \rangle = \alpha_1 \cdot \beta_2 - \alpha_2 \cdot \beta_1$, corresponding to a $\mathbb{Z}_2^2$-graded color algebra with antisymmetric properties.
4. $\langle \alpha, \beta \rangle = \alpha_1 \cdot \beta_1 + \alpha_2 \cdot \beta_2$, defining a $\mathbb{Z}_2^2$-graded superalgebra with symmetric contributions.

3.3.3 Structure for $n = 3$: $\mathbb{Z}_2^3$

For $n = 3$, there are five inequivalent mappings, including:

1. $\langle \alpha, \beta \rangle = 0$, corresponding to an ordinary Lie algebra.
2. $\langle \alpha, \beta \rangle = \alpha_1 \cdot \beta_1$, defining an embedded $\mathbb{Z}_2$-graded superalgebra.
3. $\langle \alpha, \beta \rangle = \alpha_1 \cdot \beta_1 + \alpha_2 \cdot \beta_2$, describing an embedded $\mathbb{Z}_2^2$-graded superalgebra.
4. $\langle \alpha, \beta \rangle = \alpha_1 \cdot \beta_2 - \alpha_2 \cdot \beta_1$, defining an embedded $\mathbb{Z}_2^2$-graded algebra.
5. $\langle \alpha, \beta \rangle = \alpha_1 \cdot \beta_1 + \alpha_2 \cdot \beta_2 + \alpha_3 \cdot \beta_3$, representing a generalized $\mathbb{Z}_2^3$-graded superalgebra.

These structures provide the foundation for n-bit parastatistics.

3.3.4 Practical Implications

These results provide a pathway to simulate exotic quantum systems using digital logic. For example:

- Boolean circuits can represent n-bit parastatistics.
- Logic gates such as AND, OR, XOR, and NOT encode the behavior of graded Lie algebras.

These digital representations could have applications in modeling, simulating, and controlling systems involving paraparticles such as parabosons and parafermions. In the Appendix, we will present all the details.

3.4 Connection to Equivalence Classes and Physical Interpretation

The construction of $\mathbb{Z}_2^n$-graded Lie brackets establishes the mathematical basis for understanding equivalence classes of graded algebras. Equivalence classes naturally arise from the properties of the bilinear form $\langle g, h \rangle$, which determines how elements interact and how the algebra behaves under transformations.

In the next chapter, we delve into the equivalence and inequivalence of $\mathbb{Z}_2^n$-graded Lie algebras. This includes an analysis of graded sectors and their role in defining equivalence classes, as well as the concept of marked operators that lead to inequivalent algebras. These equivalence classes have profound implications for physical systems, as they manifest in phenomena such as parastatistics, energy spectrum degeneracy, and the classification of quantum symmetries.

3.5 Classes of Equivalence of the Graded Sectors

The $2^n - 1$ nonzero graded sectors of an associative $\mathbb{Z}_2^n$-graded ring of operators are, by default, treated as equivalent. This equivalence implies that the graded sectors are on equal footing, and their roles in the algebraic structure can be interchanged without altering the fundamental properties of the system. The symmetry among the graded sectors is particularly well-demonstrated in lower-dimensional cases, such as $n = 3$.

In this case, the assignment of nonvanishing entries in 8×8 matrices, as detailed in Appendix, illustrates the equality of these sectors. Geometrically, this configuration is represented by the vertices of a Fano plane. The Fano plane provides a visual depiction of the relationships among the graded sectors, highlighting their interconnectedness and the absence of a natural hierarchy among them.

3.5.1 Impact of the $\mathbb{Z}_2^n$-Graded Bracket

The introduction of a $\mathbb{Z}_2^n$-graded bracket disrupts the equivalence of the graded sectors. As defined in Equation (2.3), the bracket determines the symmetry or antisymmetry of the interaction between graded sectors, remembering:

$$[A, B] = -(-1)^{\langle\alpha,\beta\rangle}[B, A], \tag{3.13}$$

where $\langle\alpha, \beta\rangle$ is the bilinear map associated with the grading. This bilinear map assigns specific symmetry properties to interactions between elements of different graded sectors.

For instance, in the 3_4 case (Appendix), the grading 001 exhibits a distinct behavior. The corresponding row and column in the matrix representation are entirely populated by zeros, indicating that this sector commutes with all others. As a result, the 001-graded sector describes bosons, which are particles that commute with every other particle. In contrast, other graded sectors exhibit nontrivial interactions. For example, the 110 and 111-graded sectors define parabosons, characterized by partially symmetric commutators, while $101, 011, 100$, and 010-graded sectors define parafermions, which are associated with antisymmetric commutators.

This distinction illustrates how the introduction of the $\mathbb{Z}_2^n$-graded bracket splits the graded sectors into distinct classes of equivalence. For the 3_4-superalgebra, three classes of equivalence emerge: bosons, parabosons, and parafermions. These equivalence classes reflect the underlying symmetries of the algebra and their implications for the physical behavior of particles.

3.5.2 General Patterns in $\mathbb{Z}_2^n$-Graded Algebras

This analysis generalizes to all $\mathbb{Z}_2^n$-graded Lie (super)algebras with $n = 1, 2, 3$, and 4. The number of distinct equivalence classes for each case is summarized as follows:

n	Equivalence Class	Count
1	$1_1, 1_2$	$1, 1$
2	$2_1, 2_2, 2_3, 2_4$	$1, 2, 1, 2$
3	$3_1, 3_2, 3_3, 3_4, 3_5$	$1, 2, 2, 3, 2$
4	$4_1, 4_2, 4_3, 4_4, 4_5, 4_6, 4_7$	$1, 2, 1, 2, 3, 3, 2$

The equivalence classes define the possible configurations of particles (e.g., bosons, parabosons, and parafermions) and their relationships within $\mathbb{Z}_2^n$-graded rings. For a given algebra, operators in the same equivalence class can be interchanged without altering the multiplication table, up to a normalization factor. However, the existence of inequivalent classes introduces distinct roles for certain operators, leading to richer algebraic structures.

3.5.3 Graded Quantum Hamiltonians and Parastatistics

A single-particle quantum Hamiltonian belonging to a $\mathbb{Z}_2^n$-graded associative ring of operators admits, following the construction presented above, a total number of:

$$c_n \geq b_n, \tag{3.14}$$

where c_n is the model-dependent number of inequivalent $\mathbb{Z}_2^n$-graded Lie (super)algebras, and b_n represents the lower bound determined in Equation (3.7). For single-particle systems, these alternatives are physically indistinguishable. As such, c_n inequivalent graded algebras describe the same quantum model, with the choice among them being a matter of convenience or mathematical simplicity.

In the first-quantized formulation, however, the multiparticle sector of the $\mathbb{Z}_2^n$-graded quantum Hamiltonian allows for the discrimination of the alternatives. Specifically, different (anti)commutation relations among particles lead to several consistent n-bit parastatistics. These distinct parastatistical configurations produce measurable physical consequences.

3.5.4 Marked Operators and Their Effects

The distinction between equivalence and inequivalence is often influenced by the presence of marked operators. Marked operators are those that disrupt the symmetry among graded sectors by introducing specific properties that distinguish them from others. For example, in the $\mathbb{Z}_2^2$-graded quaternions, the three imaginary quaternionic generators are on equal footing, resulting in a single equivalence class. However, for split-quaternions, one generator is marked, splitting the graded sectors into two equivalence classes, with the generators divided as $1+2$. Similarly, for $\mathbb{Z}_2^3$-graded biquaternions, the graded sectors split into three equivalence classes: one marked generator and two groups of three equivalent generators each.

The number of equivalence classes in these cases exceeds the minimum number of inequivalent algebras. For instance:

$$\begin{aligned}
&\text{Quaternions:} && c_2 = b_2 = 4, \\
&\text{Split-quaternions:} && c_2 = 6 > b_2 = 4, \\
&\text{Biquaternions:} && c_3 = 16 > b_3 = 5.
\end{aligned}$$

Marked operators thus play a critical role in creating inequivalent structures, enriching the variety of graded algebras and their applications.

3.5.5 Physical Applications of Equivalence Classes

Equivalence classes in $\mathbb{Z}_2^n$-graded algebras have profound physical implications. The classification of bosons, parabosons, and parafermions is directly tied to these classes. Bosons, which commute with all other particles, occupy a single equivalence class. Parabosons and parafermions, defined by partially symmetric and antisymmetric commutators respectively, occupy separate equivalence classes.

In quantum mechanics, equivalence classes influence the behavior of multiparticle systems, including their symmetry properties and statistical behaviors. For example, in the 3_4-superalgebra, the separation of graded sectors into three equivalence classes explains the coexistence of bosonic, parabosonic, and parafermionic states in the same system. These distinctions extend to quantum Hamiltonians, where the number of inequivalent classes determines the supported parastatistics.

Beyond particle physics, equivalence classes have implications for supersymmetric quantum mechanics and superconformal systems. The distribution of supercharges across graded sectors, along with their interactions, creates unique statistical transmutations, further enriching the study of $\mathbb{Z}_2^n$-graded systems.

4 Applications to Quantum Mechanics

The algebraic structures of $\mathbb{Z}_2^n$-graded algebras find profound applications in quantum mechanics, particularly in constructing Hamiltonians with exotic statistics and exploring statistical transmutations within supersymmetric frameworks. This chapter investigates these applications, emphasizing the mathematical and physical implications of $\mathbb{Z}_2^n$-graded operators.

4.0.1 Braided Tensor Products and Multiparticle Construction

To analyze $\mathbb{Z}_2^n$-graded quantum models, we introduce the framework of braided tensor products. Let A, B, C, D be $\mathbb{Z}_2^n$-graded operators with n-bit gradings $\alpha, \beta, \gamma, \delta$, respectively. The braided tensor product, denoted $\otimes_{\mathrm{br}}$, satisfies the relation:

$$(A \otimes_{\mathrm{br}} B) \cdot (C \otimes_{\mathrm{br}} D) = (-1)^{\langle \beta, \gamma \rangle} (AC) \otimes_{\mathrm{br}} (BD), \tag{4.1}$$

where the sign on the right-hand side depends on the symmetric scalar product $\langle \cdot, \cdot \rangle$.

This braided tensor product applies consistently to a $\mathbb{Z}_2^n$-graded compatible Lie (super)algebra $\mathfrak{g}$ and its Universal Enveloping Algebra $\mathcal{U} := \mathcal{U}(\mathfrak{g})$, which is a graded Hopf algebra. Among the operations in the Hopf algebra, the coproduct Δ is particularly relevant for constructing multiparticle states. The coproduct map:

$$\Delta : \mathcal{U} \to \mathcal{U} \otimes_{\mathrm{br}} \mathcal{U}, \tag{4.2}$$

satisfies the coassociativity property:

$$\Delta^{(m+1)} := (\Delta \otimes_{\mathrm{br}} 1)\Delta^{(m)} = (1 \otimes_{\mathrm{br}} \Delta)\Delta^{(m)}, \tag{4.3}$$

with $\Delta^{(1)} \equiv \Delta$. For any $u_1, u_2 \in \mathcal{U}$, the comultiplication is:

$$\Delta(u_1 u_2) = \Delta(u_1) \cdot \Delta(u_2). \tag{4.4}$$

The coproduct acts on the identity $1 \in \mathcal{U}(\mathfrak{g})$ and primitive elements $g \in \mathfrak{g}$ as follows:

$$\Delta(1) = 1 \otimes_{\mathrm{br}} 1, \quad \Delta(g) = 1 \otimes_{\mathrm{br}} g + g \otimes_{\mathrm{br}} 1. \tag{4.5}$$

From these rules, the action of $\Delta(u)$ on any $u \in \mathcal{U}$ can be derived using the comultiplication. Primitive elements such as Hamiltonians and creation/annihilation operators play a central role in constructing multiparticle systems. The coproduct $\Delta = \Delta^{(1)}$ is used to construct two-particle states, while $\Delta^{(m)}$ is applied to construct $(m+1)$-particle states.

4.0.2 Nilpotent Operators and Pauli Exclusion Principle

Let $A \in \mathfrak{g}$ be a nilpotent creation operator with n-bit grading α, satisfying:

$$A^2 = 0, \quad [A] = \alpha, \quad \langle \alpha, \alpha \rangle = 0 \text{ or } 1. \tag{4.6}$$

The corresponding two-particle creation operator is:

$$\Delta(A) = 1 \otimes_{\mathrm{br}} A + A \otimes_{\mathrm{br}} 1. \tag{4.7}$$

The comultiplication implies:

$$A^2 = 0 \implies \Delta(A^2) = \Delta(A) \cdot \Delta(A) = 1 + (-1)^{\langle \alpha, \alpha \rangle}(A \otimes_{\mathrm{br}} A). \tag{4.8}$$

For parafermions with $\langle \alpha, \alpha \rangle = 1$, this equation reduces to:

$$A^2 = 0 \quad \text{and} \quad \Delta(A^2) = 0. \tag{4.9}$$

This result encodes the Pauli exclusion principle for parafermions in the multiparticle sector.

4.0.3 Observables and Measurable Parastatistics

In a $\mathbb{Z}_2^n$-graded compatible Lie (super)algebra, an observable operator $\Omega \in \mathrm{End}(\mathcal{H}_m)$ must satisfy the following conditions:

1) Ω is Hermitian: $\Omega^\dagger = \Omega$.
2) Ω is zero-graded: $[\Omega] = 0$.

These properties ensure that Ω has real eigenvalues, making it a valid physical observable. For the quantum Hamiltonians supporting b_n inequivalent parastatistics, these observables produce the signs from the braided tensor product as measurable eigenvalues. The inequivalent parastatistics thus become physically distinguishable. The graded Hopf algebra formalism, endowed with a braided tensor product, provides a powerful tool for constructing multiparticle quantum systems. By encoding the parastatistics in the algebra's structure, this approach connects mathematical symmetry to measurable physical phenomena. The signs from the braided tensor product appear in eigenvalues, enabling the detection of inequivalent parastatistics and their contributions to the energy spectrum.

4.0.4 Construction of $\mathbb{Z}_2^n$-Graded Quantum Hamiltonians

In this section, we construct a class of quantum Hamiltonians within the framework of an associative $\mathbb{Z}_2^n$-graded ring of operators. These Hamiltonians are associated with b_n

inequivalent graded Lie (super)algebras that satisfy the lower bound $c_n \geq b_n$ established in Equation (5.1). Through explicit computations for $n = 2$ and $n = 3$, we demonstrate that these graded Lie (super)algebras lead to detectable parastatistics, resulting in $b_2 = 4$ and $b_3 = 5$ inequivalent multiparticle quantizations.

For a general n, the construction involves introducing 2^n pairs of annihilation and creation operators, denoted by $a_{i;n}$ and $a^\dagger_{i;n}$, where $i = 0, 1, \ldots, 2^n - 1$. These operators are represented by $2^{n+1} \times 2^{n+1}$ matrices with binary entries (0 and 1). The matrices are expressed as tensor products of 2×2 matrices, specifically:

$$I = \begin{pmatrix} 1 & 0 \\ 0 & 1 \end{pmatrix}, \quad Y = \begin{pmatrix} 0 & 1 \\ 1 & 0 \end{pmatrix}, \quad \beta = \begin{pmatrix} 0 & 0 \\ 1 & 0 \end{pmatrix}, \quad \gamma = \begin{pmatrix} 0 & 1 \\ 0 & 0 \end{pmatrix}. \tag{4.10}$$

Case $n = 1$: The 1-Bit Operators

For $n = 1$, the creation and annihilation operators are 4×4 matrices constructed as:

$$a^\dagger_{0;1} = I \otimes \gamma, \quad a_{0;1} = (a^\dagger_{0;1})^\dagger = I \otimes \beta, \tag{4.11}$$

$$a^\dagger_{1;1} = Y \otimes \gamma, \quad a_{1;1} = (a^\dagger_{1;1})^\dagger = Y \otimes \beta. \tag{4.12}$$

Case $n = 2$: The 2-Bit Operators

For $n = 2$, the operators are 8×8 matrices constructed similarly, with combinations of I and Y in the first two tensor products and γ in the third:

$$a^\dagger_{0;2} = I \otimes I \otimes \gamma, \quad a_{0;2} = (a^\dagger_{0;2})^\dagger = I \otimes I \otimes \beta, \tag{4.13}$$

$$a^\dagger_{1;2} = I \otimes Y \otimes \gamma, \quad a_{1;2} = (a^\dagger_{1;2})^\dagger = I \otimes Y \otimes \beta, \tag{4.14}$$

$$a^\dagger_{2;2} = Y \otimes I \otimes \gamma, \quad a_{2;2} = (a^\dagger_{2;2})^\dagger = Y \otimes I \otimes \beta, \tag{4.15}$$

$$a^\dagger_{3;2} = Y \otimes Y \otimes \gamma, \quad a_{3;2} = (a^\dagger_{3;2})^\dagger = Y \otimes Y \otimes \beta. \tag{4.16}$$

4.0.5 General Construction for n-Bit Operators

The general pattern for n-bit annihilation and creation operators $a_{i;n}$ and $a^\dagger_{i;n}$ becomes evident from the cases above:

- The annihilation operator $a_{i;n}$ is the Hermitian conjugate of the creation operator:
$$a_{i;n} = \left(a^\dagger_{i;n}\right)^\dagger.$$
- For the creation operators $a^\dagger_{i;n}$, the matrix in the $(n+1)$-th tensor product is always γ, while the first n tensor products consist of all possible combinations of I and Y.

This systematic construction ensures a consistent representation of $\mathbb{Z}_2^n$-graded operators, setting the foundation for analyzing their quantum mechanical properties.

4.0.6 Creation Operators for $n = 3$

Following the general rules of construction, for $n = 3$, the eight 16×16 creation operators are:

$$\begin{aligned} a^\dagger_{0;3} &= I \otimes I \otimes I \otimes \gamma, \quad a^\dagger_{1;3} = I \otimes I \otimes Y \otimes \gamma, \\ a^\dagger_{2;3} &= I \otimes Y \otimes I \otimes \gamma, \quad a^\dagger_{3;3} = I \otimes Y \otimes Y \otimes \gamma, \\ a^\dagger_{4;3} &= Y \otimes I \otimes I \otimes \gamma, \quad a^\dagger_{5;3} = Y \otimes I \otimes Y \otimes \gamma, \\ a^\dagger_{6;3} &= Y \otimes Y \otimes I \otimes \gamma, \quad a^\dagger_{7;3} = Y \otimes Y \otimes Y \otimes \gamma. \end{aligned} \tag{4.17}$$

Due to the nilpotency of the operators β and γ, satisfying $\beta^2 = \gamma^2 = 0$, each pair $(a_{i;n}, a^\dagger_{i;n})$ defines a fermionic oscillator. These operators obey the relations:

$$\{a_{i;n}, a_{i;n}\} = \{a^\dagger_{i;n}, a^\dagger_{i;n}\} = 0, \quad \{a_{i;n}, a^\dagger_{i;n}\} = I_{2^{n+1}}, \tag{4.18}$$

and

$$a^\dagger_{i;n} a^\dagger_{j;n} = 0, \quad \forall\, i, j = 0, 1, \ldots, 2^n - 1. \tag{4.19}$$

4.0.7 $\mathbb{Z}_2^n$-Grading of Operators

The $\mathbb{Z}_2^n$-grading is assigned based on the tensor products of the diagonal (I) and antidiagonal (Y) matrices appearing in $a^\dagger_{i;n}$ and $a_{i;n}$. For $n = 1, 2$, the gradings are:

$$\begin{aligned} &[a^\dagger_{0;1}] = 0, \quad [a^\dagger_{1;1}] = 1, \\ &[a^\dagger_{0;2}] = 00, \quad [a^\dagger_{1;2}] = 01, \quad [a^\dagger_{2;2}] = 10, \quad [a^\dagger_{3;2}] = 11. \end{aligned} \tag{4.20}$$

For $n \geq 3$, the extension is straightforward, with $a^\dagger_{0;n}$ assigned to the zero-graded sector:

$$[a^\dagger_{0;n}] = 0. \tag{4.21}$$

4.0.8 Hamiltonian Construction and Hilbert Space

The Hermitian n-bit Hamiltonian operator H_n is defined as:

$$H_n := a^\dagger_{0;n} a_{0;n}, \tag{4.22}$$

with the first few cases being:

$$H_1 = \mathrm{diag}(0, 1), \quad H_2 = \mathrm{diag}(0, 1, 0, 1), \quad H_3 = \mathrm{diag}(0, 1, 0, 1, 0, 1, 0, 1). \tag{4.23}$$

By construction, the Hamiltonian satisfies:

$$[H_n, a_{i;n}] = -a_{i;n}, \quad [H_n, a^\dagger_{i;n}] = +a^\dagger_{i;n}, \tag{4.24}$$

for all i. The single-particle n-bit Hilbert space $\mathcal{H}_{1;n}$ is spanned by the creation operators acting on the n-bit Fock vacuum $|\mathrm{vac}\rangle_n$, which satisfies:

$$a_{i;n}|\mathrm{vac}\rangle_n = 0, \quad \forall\, i. \tag{4.25}$$

The Fock vacuum $|\mathrm{vac}\rangle_n$ is a 2^{n+1}-component column vector:

$$|\mathrm{vac}\rangle_n = r_1, \tag{4.26}$$

where r_j denotes a column vector with 1 in the j-th position and 0 elsewhere.

The excited states are given by:

$$v_{i;n} = a^\dagger_{i;n}|\mathrm{vac}\rangle_n. \tag{4.27}$$

The $\mathbb{Z}_2^n$-graded 2^{n+1}-dimensional Hilbert space is:

$$\mathcal{H}_{1;n} = \{|\mathrm{vac}\rangle_n, v_{i;n}\}, \tag{4.28}$$

with $|\mathrm{vac}\rangle_n$ and $v_{0;n}$ belonging to the zero-graded sector.

The energy spectrum is:

$$H_n|\mathrm{vac}\rangle_n = 0, \quad H_n v_{i;n} = v_{i;n}, \quad \forall\, i, \tag{4.29}$$

where the excited state is 2^n-degenerate.

4.0.9 Generalized Diagonal Operators

A more general zero-graded diagonal Hermitian operator $H_{d;n}$ is defined as:

$$H_{d;n} := \mathrm{diag}(x_0, x_1, \ldots, x_{2^n-1}) \otimes (\beta\gamma). \tag{4.30}$$

For example:

$$H_{d;1} = \mathrm{diag}(0, x_0, 0, x_1), \quad H_{d;2} = \mathrm{diag}(0, x_0, 0, x_1, 0, x_2, 0, x_3). \tag{4.31}$$

The eigenvalues of $H_{d;n}$ are:

$$H_{d;n}|\mathrm{vac}\rangle_n = 0, \quad H_{d;n}v_{i;n} = x_i v_{i;n}. \tag{4.32}$$

4.0.10 Exchange Operators

To analyze particle exchanges, we define the graded exchange operators $X_{ij;n}$:

$$X_{ij;n} = e_{i,j} + e_{j,i}, \quad X_{ij;n} = X_{ij} \otimes I, \tag{4.33}$$

where $e_{i,j}$ is a matrix with 1 at the (i,j)-th entry and 0 elsewhere. These operators are symmetric $2^{n+1} \times 2^{n+1}$ matrices, with their gradings given by:

$$[X_{ij;n}] = [a^\dagger_{i;n}] + [a^\dagger_{j;n}] \mod 2. \tag{4.34}$$

For $n = 2$, the three exchange operators are:

$$X_{12;2} = \begin{pmatrix} 0 & 0 & 0 & 0 \\ 0 & 0 & 1 & 0 \\ 0 & 1 & 0 & 0 \\ 0 & 0 & 0 & 0 \end{pmatrix} \otimes I, \tag{4.35}$$

$$X_{13;2} = \begin{pmatrix} 0 & 0 & 0 & 0 \\ 0 & 0 & 0 & 1 \\ 0 & 0 & 0 & 0 \\ 0 & 1 & 0 & 0 \end{pmatrix} \otimes I, \tag{4.36}$$

$$X_{23;2} = \begin{pmatrix} 0 & 0 & 0 & 0 \\ 0 & 0 & 0 & 0 \\ 0 & 0 & 0 & 1 \\ 0 & 0 & 1 & 0 \end{pmatrix} \otimes I. \tag{4.37}$$

Their respective gradings are:

$$[X_{12;2}] = 11, \quad [X_{13;2}] = 01, \quad [X_{23;2}] = 10. \tag{4.38}$$

4.0.11 The Inequivalent Two-Particle Quantizations

Having outlined the construction of multi-particle sectors from graded Hopf algebras above, this discussion focuses on presenting the results. As noted earlier, for the system under consideration, demonstrating the distinguishability of the b_n parastatistics requires an analysis of only the two-particle sector. We specifically examine the cases $n = 2$ and $n = 3$, with the extension to $n > 3$ being a natural and straightforward progression.

The n-bit two-particle vacuum $|\text{vac}\rangle^{(2)}_n$ is represented as the 2^{2n+2}-component column vector:

$$|\text{vac}\rangle^{(2)}_n = |\text{vac}\rangle_n \otimes |\text{vac}\rangle_n. \tag{4.39}$$

The 2^n first-excited states (with energy level 1) are denoted as $v^{(2)}_i; n$ and given by:

$$v^{(2)}_{i;n} = \left(a^\dagger_{i;n} \otimes I_{2^{n+1}} + I_{2^{n+1}} \otimes a^\dagger_{i;n}\right) |\text{vac}\rangle^{(2)}_n. \tag{4.40}$$

The maximal number of second-excited states (energy level 2), denoted as $v^{(2)}_{ij;n}$ for $0 \leq i \leq j \leq 2^n - 1$, is $2^{n-1}(2^n - 1)$. These states are given by:

$$v^{(2)}_{ij;n} = \left(a^\dagger_{i;n} \otimes I_{2^{n+1}} + I_{2^{n+1}} \otimes a^\dagger_{i;n}\right) \left(a^\dagger_{j;n} \otimes I_{2^{n+1}} + I_{2^{n+1}} \otimes a^\dagger_{j;n}\right) |\text{vac}\rangle^{(2)}_n, \tag{4.41}$$

or equivalently:

$$v_{ij}^{(2)};n = \left(a_{i;n}^\dagger \otimes a_{j;n}^\dagger + (-1)^{\epsilon_{ij}} a_{j;n}^\dagger \otimes a_{i;n}^\dagger\right) |\mathrm{vac}\rangle_n^{(2)}, \tag{4.42}$$

where the factor $(-1)^{\epsilon_{ij}}$ depends on the mutual (anti)commutation properties of the i-th and j-th particles. This expression ensures that there are no third-excited states in the two-particle sector.

The parastatistics are determined by the signs $(-1)^{\epsilon_{ij}}$, and their inequivalence appears only in the second-excited states $v_{ij;n}^{(2)}$.

The two-particle Hamiltonian and the extension of the diagonal operator are:

$$H_n^{(2)} = H_n \otimes I_{2^{n+1}} + I_{2^{n+1}} \otimes H_n, \quad H_{d;n}^{(2)} = H_{d;n} \otimes I_{2^{n+1}} + I_{2^{n+1}} \otimes H_{d;n}. \tag{4.43}$$

The two-particle Hilbert space $\mathcal{H}_{2;n}$ is spanned by the states:

$$\mathcal{H}_{2;n} = \left\{|\mathrm{vac}\rangle_n^{(2)}, v_i^{(2)};n, v_{ij}^{(2)};n\right\}. \tag{4.44}$$

Analysis for $n = 2$

The total number of states in the $\mathcal{H}_{2;n=2}$ Hilbert space, depending on the graded Lie (super)algebras in Appendix, is:

a) For 2_1 and 2_3 (para)bosonic algebras: $1 + 4 + 10 = 15$,

b) For 2_2 and 2_4 parafermionic superalgebras: $1 + 4 + 8 = 13$.

These counts include contributions from energy eigenstates with $E = 0, 1, 2$. The difference in the a) and b) cases is due to the Pauli exclusion principle, which enforces $v_{11;2} = v_{22;2} = 0$ for the graded superalgebras.

The inequivalence of the $2_1, 2_3$ (para)bosonic statistics versus the $2_2, 2_4$ parafermionic statistics is reflected in the degeneracy of the second-excited states. Discriminating 2_1 bosons from 2_3 parabosons or 2_2 fermions from 2_4 parafermions requires additional observables.

Let w_{12}, w_{13}, w_{23} represent normalized states of the second-excited sector:

$$w_{ij} = \frac{1}{\sqrt{2}} v_{ij;2}. \tag{4.45}$$

The states w_{12}, w_{13}, w_{23} for the four cases are:

$$\begin{aligned}
&\text{For } 2_1: \quad w_{12} = \frac{1}{\sqrt{2}}(r_{30} + r_{44}), \quad w_{13} = \frac{1}{\sqrt{2}}(r_{32} + r_{60}), \quad w_{23} = \frac{1}{\sqrt{2}}(r_{48} + r_{62}),\\
&\text{For } 2_3: \quad w_{12} = \frac{1}{\sqrt{2}}(r_{30} - r_{44}), \quad w_{13} = \frac{1}{\sqrt{2}}(r_{32} + r_{60}), \quad w_{23} = \frac{1}{\sqrt{2}}(r_{48} - r_{62}),\\
&\text{For } 2_2: \quad w_{12} = \frac{1}{\sqrt{2}}(r_{30} - r_{44}), \quad w_{13} = \frac{1}{\sqrt{2}}(r_{32} + r_{60}), \quad w_{23} = \frac{1}{\sqrt{2}}(r_{48} - r_{62}),\\
&\text{For } 2_4: \quad w_{12} = \frac{1}{\sqrt{2}}(r_{30} + r_{44}), \quad w_{13} = \frac{1}{\sqrt{2}}(r_{32} - r_{60}), \quad w_{23} = \frac{1}{\sqrt{2}}(r_{48} - r_{62}).
\end{aligned} \tag{4.46}$$

To distinguish the cases, the observable $Y_{12;2} = X_{12;2} \otimes X_{12;2}$ is measured on the state w_{12}. The eigenvalues ± 1 of $Y_{12;2}$ allow discrimination among the four cases.

Analysis for $n = 3$

For $n = 3$, the total number of states in the $\mathcal{H}_{2;n=3}$ Hilbert space is:

$$\begin{aligned} \text{a) For } 3_1 \text{ and } 3_2 \text{ (para)bosonic algebras:} \quad & 1 + 8 + 36 = 45, \\ \text{b) For } 3_3, 3_4, 3_5 \text{ parafermionic superalgebras:} \quad & 1 + 8 + 32 = 41. \end{aligned}$$

Similar measurements using observables $Y_{ij;3}$ provide the necessary eigenvalue distinctions to differentiate among the parastatistics.

5 Parastatistics detectability: A statistical transmutation approach

In this chapter, we extend the framework of induced graded Lie (super)algebras to the study of Supersymmetric Quantum Mechanics (SQM), a formalism that has proven to be highly influential in both physics and mathematics. Since its inception in [50], where it was introduced as a reformulation of the Atiyah-Singer index theorem, SQM has served as a foundational tool for understanding complex algebraic and topological structures. Within this context, we explore the concept of n-bit parastatistics associated with SQM. To describe these parastatistics, we adopt the term *statistical transmutation*, which has been used in condensed matter physics to refer to related phenomena (see [51] for additional discussions and references). Here, statistical transmutation refers specifically to the algebraic transformations governed by $\mathbb{Z}_2^n$-graded Lie (super)algebras that are induced by the operators in SQM.

5.1 Statistical Transmutations in $\mathcal{N} = 1, 2, 4, 8$-Extended Supersymmetric Quantum Mechanics

To further elucidate this framework, consider the construction of an $\mathcal{N} = 2$ supersymmetric quantum model, as presented in [52]. This model exhibits invariance under a $\mathbb{Z}_2^2$-graded superalgebra. The emergence of this graded symmetry naturally prompted the question: what is the physical role of such a $\mathbb{Z}_2^2$-graded invariant superalgebra? This inquiry was addressed in [39], where it was demonstrated that the $\mathbb{Z}_2^2$-graded invariance leads to observable parafermionic statistics within the multiparticle sector. This finding underscores the direct physical implications of graded algebraic symmetries in quantum systems.

The present framework generalizes this analysis, providing a systematic and model-independent approach to $\mathbb{Z}_2^n$-graded structures. This generalization applies to any positive integer n, enabling a unified description of algebraic statistical transmutations. By leveraging these results, we can uncover new classes of parastatistics and their physical manifestations, offering deeper insights into the interplay between symmetry, algebra, and quantum mechanics.

For any positive integer n, $\mathbb{Z}_2^n$-gradings can be applied. In particular, for a positive integer $\mathcal{N} = 1, 2, 3, 4, 5, \ldots$, the superalgebra $\mathrm{sqm}_{\mathcal{N}}$ of the $\mathcal{N}$-extended one-dimensional supersymmetric quantum mechanics is defined by the following (anti)commutators:

$$\{Q_i, Q_j\} = 2\delta_{ij} H, \quad [H, Q_i] = 0, \tag{5.1}$$

where $i, j = 1, \ldots, \mathcal{N}$.

Here, Q_i are the generators of supersymmetry transformations, known as the supercharges, and H is the Hamiltonian, which is invariant under these transformations. Both Q_i and H are assumed to be Hermitian, satisfying:

$$Q_i^\dagger = Q_i, \quad H^\dagger = H. \tag{5.2}$$

We denote the corresponding Universal Enveloping Superalgebra as $U_\mathcal{N} := \mathcal{U}(\text{sqm}_\mathcal{N})$. For $m = 0, 1, 2, \ldots$, these superalgebras are spanned by the following sets of operators:

$$\begin{aligned}
&U_{\mathcal{N}=1} = \{H^m, H^m Q_1\},\\
&U_{\mathcal{N}=2} = \{H^m, H^m Q_1, H^m Q_2, H^m Q_1 Q_2\},\\
&U_{\mathcal{N}=3} = \{H^m, H^m Q_1, H^m Q_2, H^m Q_3, H^m Q_1 Q_2, H^m Q_1 Q_3, H^m Q_2 Q_3, H^m Q_1 Q_2 Q_3\},\\
&\qquad \vdots
\end{aligned} \tag{5.3}$$

In general, for $\mathcal{N}$-extended supersymmetric quantum mechanics, the number of operators included in $U_\mathcal{N}$ at any given m is $2^\mathcal{N}$.

The subsequent analysis relies on the matrix differential representations of the Q_i and H operators as defined in (5.1). The $\text{sqm}_\mathcal{N}$ superalgebras admit two distinct types of differential representations. At the classical level, there are the time-dependent worldline D-module representations introduced in [53, 54], which are used for constructing invariant worldline sigma models. At the quantum level, differential representations are employed where the Hamiltonian H acts as a second-order differential operator in the spatial coordinates. The relationship between these two types of representations is clarified in [55] and, specifically within a $\mathbb{Z}_2^2$-graded framework, in [24].

As outlined in [53], the minimal and irreducible D-module representations of the $\text{sqm}_\mathcal{N}$ superalgebra express the $\mathcal{N}$ supercharges Q_i as $d_\mathcal{N} \times d_\mathcal{N}$ matrix operators. These are first-order differential operators in the time variable t, where $d_\mathcal{N}$ is given by the following expression.

Let us parametrize $\mathcal{N}$ as

$$\mathcal{N} = 8k + r, \tag{5.4}$$

where

$$k = 0, 1, 2, \cdots \in \mathbb{N}_0, \quad r = 1, 2, 3, 4, 5, 6, 7, 8. \tag{5.5}$$

The size of the $d_\mathcal{N}$ matrix is then determined by the formula:

$$d_\mathcal{N} = 2^{(4k + z(r) + 1)}, \tag{5.6}$$

where $z(r)$ is given by

$$z(r) = \lceil \log_2 r \rceil. \tag{5.7}$$

In the above formula, the ceiling function $\lceil \cdot \rceil$ is used, resulting in the following specific values:

$$\begin{aligned} &z(1) = 0, \\ &z(2) = 1, \\ &z(3) = z(4) = 2, \\ &z(5) = z(6) = z(7) = z(8) = 3. \end{aligned} \tag{5.8}$$

The dimensionality $d_{\mathcal{N}}$ of the bosonic and fermionic subspaces corresponds to sequence A034583 in the OEIS (Online Encyclopedia of Integer Sequences), available at https://oeis.org. The sequence begins as follows:

$$1 \times d_{\mathcal{N}} \quad \Rightarrow \quad 1, 2, 4, 4, 8, 8, 8, 8, 16, 32, 64, 64, 128, 128, 128, 128, 256, \ldots \tag{5.9}$$

For values $\mathcal{N} \geq 4$, it has been demonstrated in [56] that the $\mathrm{sqm}_{\mathcal{N}}$ superalgebra supports D-module representations that may be reducible but remain indecomposable. The statistical transmutations associated with these representations can, in principle, be calculated for any D-module, whether it corresponds to a reducible or irreducible representation of the $\mathcal{N}$-extended $\mathrm{sqm}_{\mathcal{N}}$ superalgebra.

For irreducible representations, it is useful to introduce the parameter:

$$n_{\mathcal{N}} := 4k + z(r) + 1, \tag{5.10}$$

where $n_{\mathcal{N}}$ determines the dimensionality of the matrix space:

$$d_{\mathcal{N}} \times d_{\mathcal{N}} = 2^{n_{\mathcal{N}}} \times 2^{n_{\mathcal{N}}}. \tag{5.11}$$

In this context, the irreducible supercharges Q_i can be associated with the nonzero graded sectors of a $\mathbb{Z}_2^{n_{\mathcal{N}}}$-grading. Meanwhile, the Hamiltonian H is assigned to the $n_{\mathcal{N}}$-bit zero vector, denoted by 0.

To simplify the discussion, we will focus on irreducible representations of $\mathcal{N} = 1, 2, 4, 8$-extended one-dimensional Supersymmetric Quantum Mechanics. These specific cases of $\mathcal{N}$, which are intimately connected to the division algebras, have been the subject of extensive study in the literature and serve as significant examples for exploring the algebraic framework.

Before advancing further, it is important to highlight a few key observations. For the cases $\mathcal{N} = 1, 2, 4, 8$, the minimal D-module representations correspond to matrix sizes of 2×2, 4×4, 8×8, and 16×16, respectively. These representations are valid for both the classical and quantum settings. From the relationship provided in (5.10) and (5.11), we find the values of $n_{\mathcal{N}}$ for each case as follows:

$$n_{\mathcal{N}=1} = 1, \quad n_{\mathcal{N}=2} = 2, \quad n_{\mathcal{N}=4} = 3, \quad n_{\mathcal{N}=8} = 4. \tag{5.12}$$

These values of $n_{\mathcal{N}}$ are significant because they define the number of bits in the $\mathbb{Z}_2^{n_{\mathcal{N}}}$-grading associated with the supercharges Q_i. The graded Lie (super)algebras induced by different grading assignments for the supercharges are classified based on the $n = 1, 2, 3, 4$-bit cases, as detailed in the tables provided in Appendix. Each table outlines the inequivalent structures arising from these gradings.

At this point, we are ready to compute the number of inequivalent graded Lie (super)algebras, denoted $s_{\mathcal{N}}$, induced by the minimal set of H and Q_i operators satisfying the defining relations in (5.1). These computations focus specifically on $\mathcal{U}(\mathrm{sqm}_{\mathcal{N}})$, the universal enveloping algebra of the $\mathrm{sqm}_{\mathcal{N}}$ superalgebra.

The methodology for this analysis draws on techniques previously applied to (split-)quaternions and biquaternions, which are discussed in detail in Appendices. However, the computation here incorporates unique features stemming from the $\mathbb{Z}_2^{n_{\mathcal{N}}}$-grading of the supercharges. The distinctions in these assignments lead to structural differences in the resulting graded Lie (super)algebras. These variations will be carefully outlined in the following sections to provide a complete picture of the classification.

5.1.1 The $\mathcal{N} = 1$ Statistical Transmutations

In the case of $\mathcal{N} = 1$, the Hamiltonian H is assigned to the zero grading, $[H] = 0$, and the single supercharge Q_1 is assigned the grading $[Q_1] = 1$. The inequivalent graded Lie (super)algebras can be classified based on the information from the 1-bit tables provided in Appendix.

The distinct cases and their corresponding properties are summarized in Table 1:

Case	**Algebra Type**	**Relations**
1_1	Lie algebra	$[H, Q_1] = 0$
1_2	Lie superalgebra	$[H, Q_1] = 0, \quad \{Q_1, Q_1\} = 2H$

Table 1 – Classification of inequivalent graded Lie (super)algebras for $\mathcal{N} = 1$.

From the above classification, the number of inequivalent graded Lie (super)algebras for $\mathcal{N} = 1$ is:

$$s_{\mathcal{N}=1} = 2. \tag{5.13}$$

5.1.2 The $\mathcal{N} = 2$ Statistical Transmutations

For $\mathcal{N} = 2$, the Hamiltonian H is assigned the zero grading, $[H] = 00$. The supercharges Q_1 and Q_2 are assigned to the nonzero gradings, denoted as $[Q_1] = \alpha$ and $[Q_2] = \beta$, where $\alpha \neq \beta$ and $\alpha, \beta \in \{10, 01, 11\}$. The grading assignments of the operators in the Universal Enveloping (Super)algebra $\mathcal{U}(\mathrm{sqm}_{\mathcal{N}=2})$ are as follows:

$$\begin{aligned} [H^m] &= 00, \\ [H^m Q_1] &= \alpha, \\ [H^m Q_2] &= \beta, \\ [H^m Q_1 Q_2] &= \alpha + \beta \mod 2. \end{aligned} \tag{5.14}$$

An important feature of this setup is the presence of an empty $\alpha + \beta$-graded sector, denoted as $\varnothing$, which can be interpreted as a generator associated with a matrix of all zero entries. This marked generator plays a key role in distinguishing the graded Lie (super)algebras. The computation of the inequivalent graded Lie (super)algebras $s_{\mathcal{N}=2}$ mirrors that of the split-quaternions, as discussed in Appendix, which involves a $1 + 2$ decomposition of the 2-bit nonvanishing graded sectors.

The cases and their properties are summarized in Table 2:

Case	Type of Algebra	Grading Assignment	Description
2_1	Lie algebra	$[Q_1] = 10, [Q_2] = 01$	Bosonic case: $2B$, infinite generators
$2_2\alpha$	Lie superalgebra	$[Q_1] = 10, [Q_2] = 11$	Mixed case: $1F + 1B$, infinite generators
$2_2\beta$	Lie superalgebra	$[Q_1] = 10, [Q_2] = 01$	Fermionic case: $2F$, infinite generators
2_3	Parabosonic algebra	$[Q_1] = 10, [Q_2] = 01$	Parabosonic case: $2PB$, 3 generators
$2_4\alpha$	Parafermionic superalgebra	$[Q_1] = 10, [Q_2] = 11$	Mixed case: $1PF + 1PB$, 3 generators
$2_4\beta$	Parafermionic superalgebra	$[Q_1] = 10, [Q_2] = 01$	Parafermionic case: $2PF$, 4 generators

Table 2 – Classification of inequivalent graded Lie (super)algebras for $\mathcal{N} = 2$.

From the contributions of the four 2-bit cases, the total number of inequivalent graded Lie (super)algebras for $\mathcal{N} = 2$ is:

$$s_{\mathcal{N}=2} = 1 + 2 + 1 + 2 = 6. \tag{5.15}$$

5.1.3 The $\mathcal{N} = 4$ Statistical Transmutations

The $\mathcal{N} = 4$ statistical transmutations are derived from the 3-bit tables. The four supercharges, Q_i, along with the three null matrices representing the empty slots ($\emptyset$), are distributed among the seven non-zero graded sectors. This arrangement leads to two distinct classes of equivalence for the marked generators, encompassing $4 + 3 = 7$ elements. The non-zero graded sectors can be visualized as encoded within a Fano plane diagram.

Two key observations are critical for the analysis:

1. **Alignment of Empty Slots**: The three null matrices ($\emptyset$) are aligned along an edge of the Fano plane since the product of two null matrices always results in another null matrix.

2. **(Para)Bosonic Alignment**: In the 3_1 to 3_5 tables of (Appendix), the product of two (para)bosonic sectors yields a third (para)boson. Consequently, these bosonic sectors are also aligned along an edge of the Fano plane.

These two principles simplify the combinatorial analysis necessary to compute $s_{\mathcal{N}=4}$, the total number of inequivalent graded Lie (super)algebras.

Case	**Graded Sectors Split**	**Grading Assignment for Q_i**	**Transmutation Description**
3_1	7 bosons	$[Q_1] = 001, [Q_2] = 101, [Q_3] = 011, [Q_4] = 111$	$4B$: 4 bosonic supercharges
3_2^α	1 boson, 6 parabosons	$[Q_1] = 001, [Q_2] = 101, [Q_3] = 011, [Q_4] = 111$	$1B + 3PB$: 1 bosonic, 3 parabosonic
3_2^β	7 parabosons	$[Q_1] = 110, [Q_2] = 010, [Q_3] = 011, [Q_4] = 111$	$4PB$: 4 parabosonic supercharges
3_3^α	3 bosons, 4 fermions	$[Q_1] = 001, [Q_2] = 011, [Q_3] = 101, [Q_4] = 111$	$2B + 2F$: 2 bosonic, 2 fermionic
3_3^β	7 fermions	$[Q_1] = 100, [Q_2] = 110, [Q_3] = 101, [Q_4] = 111$	$4F$: 4 fermionic supercharges (identity transmutation)
3_4^α	1 boson, 2 parabosons, 4 parafermions	$[Q_1] = 001, [Q_2] = 110, [Q_3] = 100, [Q_4] = 011$	$1B + 1PB + 2PF$: 1 bosonic, 1 parabosonic, 2 parafermionic
3_4^β	2 parabosons, 4 parafermions	$[Q_1] = 111, [Q_2] = 110, [Q_3] = 010, [Q_4] = 011$	$2PB + 2PF$: 2 parabosonic, 2 parafermionic
3_4^γ	7 parafermions	$[Q_1] = 101, [Q_2] = 010, [Q_3] = 100, [Q_4] = 011$	$4PF$: 4 parafermionic supercharges
3_5^α	3 parabosons, 4 parafermions	$[Q_1] = 101, [Q_2] = 011, [Q_3] = 010, [Q_4] = 001$	$2PB + 2PF$: 2 parabosonic, 2 parafermionic
3_5^β	7 parafermions	$[Q_1] = 100, [Q_2] = 111, [Q_3] = 010, [Q_4] = 001$	$4PF$: 4 parafermionic supercharges

Table 3 – Classification of $\mathcal{N} = 4$ statistical transmutations based on 3-bit graded Lie (super)algebras.

Using the properties above (alignment of empty slots and (para)bosonic alignment), the inequivalent statistical transmutations are categorized into ten distinct cases, each corresponding to a different graded Lie (super)algebra structure. The assignments of gradings to the supercharges determine whether they behave as bosons, parabosons, fermions, or parafermions.

- **Bosonic Cases:** The cases 3_1 and 3_2^β correspond to purely bosonic or parabosonic assignments, with 3_1 featuring four bosonic supercharges and 3_2^β describing a purely parabosonic system.
- **Fermionic Cases:** The case 3_3^β recovers the original $\mathcal{N} = 4$ supersymmetric quantum mechanics with four fermionic supercharges.
- **Mixed Cases:** The remaining cases present different mixtures of bosons, parabosons, fermions, and parafermions, leading to diverse transmutation patterns such as $(2B + 2F)$, $(1B + 3PB)$, $(2PB + 2PF)$, and $(4PF)$.

The total number of inequivalent transmutations is given by

$$s_{\mathcal{N}=4} = 1 + 2 + 2 + 3 + 2 = 10. \tag{5.16}$$

These results generalize previous studies on $\mathcal{N} = 2$ systems and extend the framework of statistical transmutations to higher-dimensional graded Lie (super)algebras.

5.1.4 The $\mathcal{N} = 8$ Statistical Transmutations and Fano Plane Encoding

The $\mathcal{N} = 8$ transmutations are derived from the 4-bit tables (Appendix). The eight supercharges Q_i, along with the seven vanishing matrices representing the empty slots $\emptyset$, must be distributed among the fifteen nonzero graded sectors. This classification follows from the structure of the *generalized* Fano plane, a key geometric tool used to organize the graded sectors. The implications of the Fano plane for the classification of graded Lie (super)algebras and the corresponding statistical transmutations are outlined below.

5.1.5 Fano Planes and Graded Structures

The Fano plane is a finite projective geometry that naturally encodes the algebraic structure of graded Lie (super)algebras. In the $\mathcal{N} = 4$ case, the seven nonzero graded sectors can be represented as the seven points of the standard Fano plane, where each line represents a graded multiplication rule.

For $\mathcal{N} = 8$, the structure extends to a generalized Fano plane, encoding fifteen nonzero graded sectors within a higher-dimensional incidence geometry.

5.1.6 Properties of the $\mathcal{N} = 4$ Fano Plane

1. Alignment of Empty Slots ($\emptyset$): Since the product of two empty slots remains an empty slot, the corresponding vanishing matrices align along an edge of the Fano plane.
2. Parafermion and Paraboson Alignment: The graded multiplication rules enforce the condition that the product of two (para)bosons must generate a third (para)boson. This requirement constrains their placement within the Fano structure.
3. Supercharge Assignments: The four supercharges Q_i must be positioned such that they complement an edge of the Fano plane, leading to multiple inequivalent grading assignments.

5.1.7 The $\mathcal{N} = 8$ Generalized Fano Plane

For $\mathcal{N} = 8$, the graded sectors increase from seven to fifteen, forming a higher-dimensional analog of the Fano plane. This extension represents an incidence structure in projective geometry over $\mathbb{Z}_2$, enforcing additional constraints on graded Lie (super)algebras.

The key properties are:

1. Expanded Empty Slots: With seven empty slots, the generalized Fano structure enforces additional constraints on the grading assignments.
2. Multiple Parafermionic Subspaces: Unlike $\mathcal{N} = 4$, where a single edge aligns parafermions, $\mathcal{N} = 8$ allows for multiple parafermionic alignments.
3. Higher-Dimensional Projection: The fifteen graded sectors correspond to an incidence geometry that extends the standard Fano plane into a higher-dimensional configuration.

For 4_4 and 4_7, we have two inequivalent contributions from unmarked vertices, as follows,

α diagram:

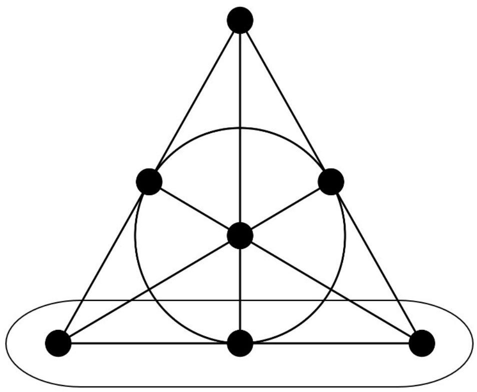

β diagram:

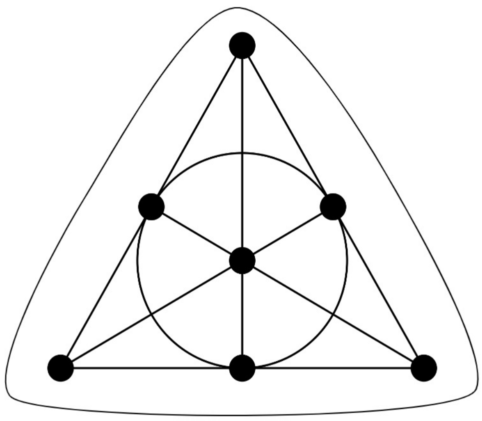

For 4_5 we have three inequivalent contributions with three marked vertices,

α diagram:

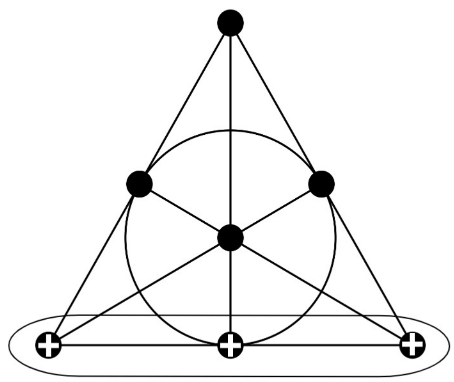

β diagram:

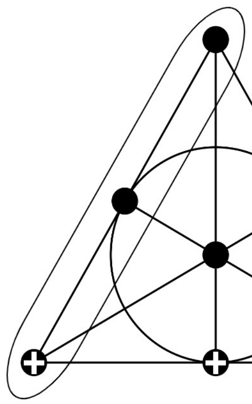

γ diagram:

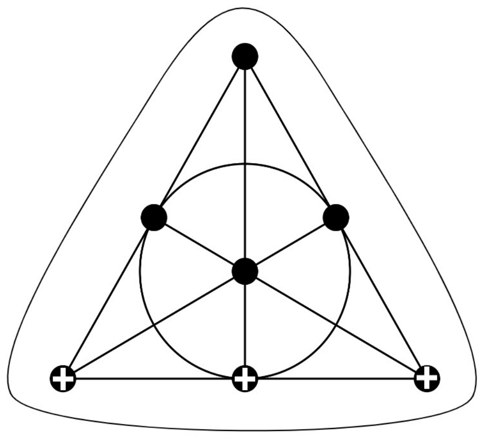

For 4_6 we have three inequivalent contributions with one marked vertice,

α diagram:

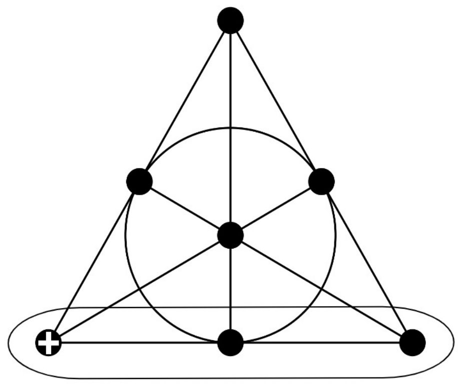

β diagram:

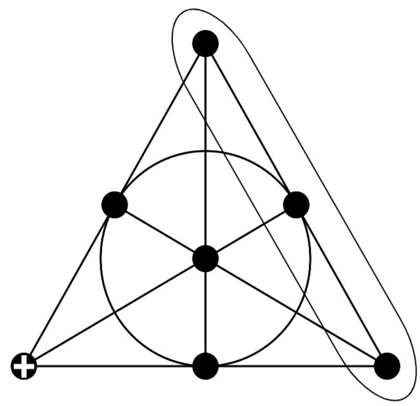

γ diagram:

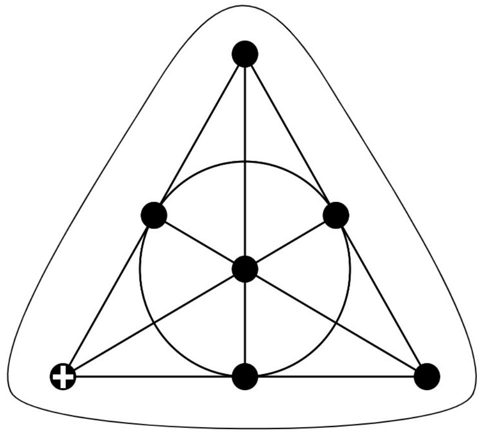

5.1.8 Statistical Transmutation Classification

The transmutations for $\mathcal{N} = 8$ follow the 4-bit classification scheme, where the fifteen nonzero graded sectors accommodate the eight supercharges and seven empty slots. The resulting transmutations are summarized in the following table.

Case	**Supercharges (8 sectors)**	**Empty Slots (7 sectors)**	**Transmutation Type**
4_1	$8B$	$7B$	Fully bosonic
4_2^α	$2B + 6PB$	$1B + 6PB$	Mixed bosonic-parabosonic
4_2^β	$8PB$	$3B + 4PB$	Fully parabosonic
4_3	$8PB$	$7PB$	Fully parabosonic
4_4^α	$4B + 4F$	$3B + 4F$	Boson-fermion mixed
4_4^β	$8F$	$7B$	Fully fermionic
4_5^α	$4PB + 4PF$	$3B + 4PF$	Paraboson-parafermion mixed
4_5^β	$2B + 2PB + 4PF$	$1B + 2PB + 4PF$	Hybrid bosonic-parastatistics
4_5^γ	$8PF$	$3B + 4PB$	Fully parafermionic
4_6^α	$4PB + 4PF$	$1B + 2PB + 4PF$	Mixed paraboson-parafermion
4_6^β	$1B + 3PB + 4PF$	$3PB + 4PF$	Higher parabosonic-parafermionic
4_6^γ	$8PF$	$1B + 6PB$	Fully parafermionic
4_7^α	$4PB + 4PF$	$3PB + 4PF$	Mixed high-order paraboson-parafermion
4_7^β	$8PF$	$7PB$	Fully parafermionic

Table 4 – Complete classification of $\mathcal{N} = 8$ statistical transmutations with 14 inequivalent cases.

By summing all the contributions from the seven 4-bit tables, we obtain

$$s_{\mathcal{N}=8} = 1 + 2 + 1 + 2 + 3 + 3 + 2 = 14. \tag{5.17}$$

The Fano planes provide an underlying geometric structure that dictates how graded multiplication rules operate in supersymmetric quantum mechanics. For $\mathcal{N} = 4$, the standard Fano plane organizes the seven nonzero graded sectors, while for $\mathcal{N} = 8$, a generalized Fano structure emerges.

The key findings are:

- The Fano structure determines how graded sectors interact, enforcing parafermionic and parabosonic constraints.
- The $\mathcal{N} = 8$ case introduces a higher-dimensional incidence geometry, increasing the number of transmutation possibilities.
- The inequivalent graded Lie (super)algebras lead to physically distinct parafermionic statistics, which may be detectable in multiparticle quantum systems.

These results demonstrate that the geometric encoding of graded sectors is fundamental to understanding supersymmetric quantum mechanics and statistical transmutations.

In this section, we have demonstrated that the Universal Enveloping Superalgebras $U_{\mathcal{N}} \equiv \mathcal{U}(\mathrm{sqm}_{\mathcal{N}})$ associated with the one-dimensional $\mathcal{N}$-extended Supersymmetric Quantum Mechanics can accommodate alternative gradings beyond the conventional supersymmetric grading. These alternative gradings define distinct and inequivalent graded Lie (super)algebra structures on $U_{\mathcal{N}}$, each leading to a different formulation of (para)statistics.

As established in this section, each specific graded Lie (super)algebra structure determines its own set of statistical transmutations. Consequently, the classification of $\mathcal{N} = 1, 2, 4, 8$ supersymmetric theories results in a corresponding number $s_{\mathcal{N}}$ of inequivalent graded Lie (super)algebras:

$$\begin{aligned} \mathcal{N} = 1: &\qquad n_1 = 1, \quad s_1 = 1 + 1 = 2, \\ \mathcal{N} = 2: &\qquad n_2 = 2, \quad s_2 = 1 + 2 + 1 + 2 = 6, \\ \mathcal{N} = 4: &\qquad n_4 = 3, \quad s_4 = 1 + 2 + 2 + 3 + 2 = 10, \\ \mathcal{N} = 8: &\qquad n_8 = 4, \quad s_8 = 1 + 2 + 1 + 2 + 3 + 3 + 2 = 14. \end{aligned} \tag{5.18}$$

In this classification, the numbers $s_{\mathcal{N}}$ are systematically partitioned into their respective contributions, which originate from each of the inequivalent $n_{\mathcal{N}}$-bit graded brackets listed in Appendix. As discussed in Section 3, the presence of "marked" generators increases the number of possible inequivalent structures, ensuring that $s_{\mathcal{N}} \geq b_{\mathcal{N}}$.

The values of $s_{\mathcal{N}}$ obtained above quantify the total number of allowed statistical transmutations affecting the supercharges Q_i in each case. The next fundamental question is whether these inequivalent parastatistics produce observable physical effects. This issue is examined in the subsequent section, where we explore how parastatistics can manifest in measurable quantities. In particular, we analyze whether these parastatistics influence the degeneracy structure of energy levels in multiparticle states. To facilitate this analysis, we work within the framework of Superconformal Quantum Mechanics, augmented by the de Alfaro-Fubini-Furlan (DFF) oscillator term [49]. This formulation preserves the spectrum-generating superconformal algebra while providing a well-defined vacuum state and discrete energy spectrum, thereby offering a natural setting to investigate the physical implications of graded statistical transmutations.

5.2 Detectable Parastatistics in Superconformal Quantum Mechanics with de Alfaro-Fubini-Furlan Oscillator Terms

In this section, we explore the physical detectability of the statistical transmutations introduced in Supersymmetric Quantum Mechanics (SQM). As emphasized before, each graded Lie (super)algebra defined on a Universal Enveloping Algebra, such as

$$U_{\mathcal{N}} \equiv \mathcal{U}(\mathrm{sqm}_{\mathcal{N}}) \tag{5.19}$$

from equation (5.3) induces a distinct (para)statistics in the multiparticle sector of a corresponding quantum model.

From a single-particle perspective, these different graded Lie (super)algebras merely provide alternative formulations of the same physical system. However, in a multiparticle sector, their physical equivalence or inequivalence becomes a model-dependent question, requiring direct analysis of how these structures impact observable quantities.

5.2.1 Detectability of Statistical Transmutations

A fundamental question arises: are the $s_{\mathcal{N}}$ statistical transmutations (given in equation (5.18)) physically measurable?

A complete resolution of this issue demands an extensive investigation, as the physical effects of graded parastatistics depend on the multiparticle dynamics of the specific quantum system under study. Such an in-depth analysis extends beyond the scope of this work. Instead, we focus here on the simplest nontrivial case the two-particle sector of an $\mathcal{N}=2$ supersymmetric quantum model to illustrate the key ideas and establish a concrete example of detectable parastatistics.

Our findings indicate a striking result:

- The $s_{\mathcal{N}=2}=6$ distinct parastatistics obtained in equation (5.15) naturally split into two sets:
  1. Three cases correspond to conventional statistics, associated with standard bosonic and fermionic states (from tables 2_1 and 2_2 in Appendix).
  2. Three cases correspond to genuine parastatistics, which involve paraparticles, parabosons and parafermions, associated with the graded structures 2_3, 2_4^{α}, and 2_4^{β}.

A crucial observation is that the energy-level degeneracies in the two-particle system exhibit measurable differences between these two groups. Specifically, the genuine parastatistics yield an energy spectrum that cannot be reproduced by ordinary bosons or fermions, providing an observable signature of paraparticles.

This discovery represents the first known example where the $\mathbb{Z}_2^2$-graded parabosons and parafermions, originally introduced by Rittenberg and Wyler, explicitly alter the energy spectrum of a quantum system.

The mechanism of parastatistics detection presented here differs fundamentally from that found in the models analyzed at the beginning of this section, and in the references [39, 40]. In those cases, distinguishing between n-bit paraparticles and ordinary particles required measuring an observable distinct from the Hamiltonian, as both species shared the same energy spectrum. In contrast, in the present model, the impact of parastatistics is directly reflected in the energy spectrum itself, making detection more straightforward.

5.2.2 The Role of Superconformal Symmetry in Statistical Transmutations

To systematically analyze the effects of statistical transmutations, we adopt the framework of Superconformal Quantum Mechanics (SCQM). This approach offers several advantages. It introduces superconformal Lie superalgebras, which serve as spectrum-generating superalgebras, allowing for an algebraic classification of energy levels. The algebraic structure simplifies the identification of energy-level degeneracies arising from different graded Lie (super)algebras.

The superalgebra governing SCQM depends on the number of supercharges $\mathcal{N}$:

- $\mathcal{N} = 1$: The superalgebra $\mathfrak{osp}(1|2)$
- $\mathcal{N} = 2$: The superalgebra $\mathfrak{sl}(2|1)$
- $\mathcal{N} = 4$: The exceptional superalgebra $D(2,1;\alpha)$ (see [55])
- $\mathcal{N} = 8$: The exceptional superalgebra $F(4)$ (see [57])

For a comprehensive review of superconformal mechanics and its implications, see Ref. [58] and references therein.

5.2.3 The Importance of the de Alfaro-Fubini-Furlan (DFF) Oscillator Term

A central challenge in studying parastatistics in quantum mechanics is constructing a model that provides a clear and computable framework. This challenge is addressed by incorporating the de Alfaro-Fubini-Furlan (DFF) oscillator term into the Hamiltonian.

This term plays a crucial role in the following ways:

1. It preserves the spectrum-generating superconformal algebra, ensuring that the structure of the quantum theory remains intact.

2. It introduces a well-defined ground state and a discrete energy spectrum, which greatly simplifies the analysis of energy-level degeneracies.

3. It allows for a direct comparison between ordinary statistics and parastatistics, making it possible to observe physical distinctions between them.

Given these advantages, our investigation will focus on analyzing the statistical transmutations within the framework of superconformal quantum mechanics, incorporating the DFF oscillator term. This setting provides the ideal structure for identifying and understanding the physical consequences of inequivalent graded Lie (super)algebras.

5.2.4 Summary of Key Findings

The study of parastatistics in supersymmetric quantum mechanics reveals that their physical relevance manifests primarily in the multiparticle sector. While different graded Lie (super)algebras yield equivalent descriptions at the single-particle level, their impact becomes nontrivial when considering systems involving multiple interacting particles. The structural differences between inequivalent statistical transmutations influence the symmetry properties and observable features of the quantum states, making it possible to distinguish distinct parastatistical behaviors in multi-particle sectors.

A particularly striking result emerges in the case of $\mathcal{N} = 2$ supersymmetric quantum mechanics. The presence of $\mathbb{Z}_2^2$-graded parastatistics introduces modifications to the energy spectrum that are absent in conventional bosonic and fermionic systems. These modifications manifest as shifts in the degeneracies of energy levels, indicating that particles governed by such alternative statistics obey fundamentally different combinatorial occupancy rules compared to standard quantum particles. This represents the first explicit demonstration that $\mathbb{Z}_2^2$-graded parastatistics have a tangible effect on quantum energy spectra, providing a novel avenue for their potential experimental verification.

A crucial component of this analysis is the incorporation of the de Alfaro-Fubini-Furlan (DFF) oscillator term into the Hamiltonian. This term serves a dual purpose: first, it ensures that the quantum system possesses a normalized ground state, which is essential for defining a well-structured Hilbert space. Second, it introduces a discrete energy spectrum, significantly simplifying the study of level degeneracies and allowing for a precise identification of statistical transmutations. Without the DFF term, the continuous nature of the spectrum would make it considerably more difficult to isolate the effects of parastatistics from other dynamical features of the system.

Furthermore, the formalism of Superconformal Quantum Mechanics provides a powerful framework for analyzing statistical transmutations systematically. By leveraging the structure of superconformal Lie superalgebras, it becomes possible to classify the energy spectra of different inequivalent graded Lie (super)algebras. The mathematical consistency of this approach enables a rigorous characterization of how distinct parastatistical properties manifest in quantum systems. The connection between graded parastatistics and superconformal symmetry suggests deeper algebraic structures at play, which may have implications beyond quantum mechanics, extending into quantum field theory and higher-dimensional models of supersymmetry.

These findings collectively underscore the importance of parastatistics as a physically meaningful extension of conventional quantum statistics. The explicit demonstration that energy spectra can encode signatures of inequivalent statistical transmutations provides strong motivation for further theoretical and experimental investigations into the role of graded Lie (super)algebras in quantum mechanics.

Building on these insights, we now turn our attention to the implications of graded parastatistics within the framework of $\mathcal{N} = 1, 2, 4, 8$ Superconformal Quantum Mechanics. By leveraging the structure of superconformal algebras, we systematically explore how statistical transmutations manifest in these theories and affect the symmetry properties, energy spectra, and multiparticle dynamics. This analysis not only reinforces the physical significance of inequivalent graded Lie (super)algebras but also provides a deeper connection between parastatistics and the mathematical foundations of supersymmetric quantum mechanics.

5.3 On $\mathcal{N} = 1, 2, 4, 8$ Superconformal Quantum Mechanics

A one-dimensional $\mathcal{N}$-extended superconformal algebra is a simple Lie superalgebra $\mathfrak{g}$ that appears in Kac's classification [1], with generators satisfying additional structural properties. In addition to the standard $\mathbb{Z}_2$-grading, these generators are characterized by their scaling dimensions $s = -1, -\frac{1}{2}, 0, \frac{1}{2}, 1$, such that the algebra decomposes as

$$\mathfrak{g} = \mathfrak{g}_{-1} \oplus \mathfrak{g}_{-\frac{1}{2}} \oplus \mathfrak{g}_0 \oplus \mathfrak{g}_{\frac{1}{2}} \oplus \mathfrak{g}_1. \tag{5.20}$$

Here, the generators in $\mathfrak{g}_{\pm\frac{1}{2}}$ are odd (fermionic), while those in $\mathfrak{g}_0$, $\mathfrak{g}_{\pm 1}$ are even (bosonic). The (anti)commutators obey the relation

$$[\mathfrak{g}_r, \mathfrak{g}_s\} \subseteq \mathfrak{g}_{r+s}. \tag{5.21}$$

The positive subalgebra $\mathfrak{g}_{>0} = \mathfrak{g}_{\frac{1}{2}} \oplus \mathfrak{g}_1$ is isomorphic to the supersymmetric quantum mechanics algebra $\mathfrak{sqm}_{\mathcal{N}}$ defined in Eq. (5.1). Specifically, the Hamiltonian H is housed in $\mathfrak{g}_1$, while the $\mathcal{N}$ supercharges Q_i reside in $\mathfrak{g}_{\frac{1}{2}}$. Their respective conformal partners, the generator K and the $\mathcal{N}$ additional generators $\widetilde{Q}_i$, are assigned to $\mathfrak{g}_{-1}$ and $\mathfrak{g}_{-\frac{1}{2}}$, respectively. Finally, the subalgebra $\mathfrak{g}_0$ contains the dilatation operator D and an additional structure known as the R-symmetry subalgebra. The generators $\{H, D, K\}$ close an $\mathfrak{sl}(2)$ subalgebra, with D playing the role of the Cartan element.

For a given $\mathcal{N}$-extended superconformal algebra, the total number of generators is given by

$$d = 2\mathcal{N} + 3 + r, \tag{5.22}$$

where r represents the number of R-symmetry generators. The most relevant cases include:

- $\mathfrak{osp}(1|2)$, which has 5 generators ($\mathcal{N} = 1$ with $r = 0$, meaning no R-symmetry),
- $\mathfrak{sl}(2|1)$, which has 8 generators ($\mathcal{N} = 2$ with $r = 1$, where R-symmetry forms a $\mathfrak{u}(1)$ subalgebra),
- $D(2, 1; \alpha)$, which, for generic values of α [59], contains 17 generators ($\mathcal{N} = 4$ with $r = 6$, where R-symmetry corresponds to $\mathfrak{su}(2) \oplus \mathfrak{su}(2)$),
- $F(4)$, which has 40 generators ($\mathcal{N} = 8$ with $r = 21$, where R-symmetry is given by $\mathfrak{so}(7)$).

To construct explicit differential matrix representations of these superconformal algebras, we consider their irreducible realizations satisfying the constraints outlined earlier in this chapter for their respective $\mathfrak{sqm}_{\mathcal{N}}$ subalgebras. These representations, expressed in terms of the space coordinate x, are conveniently written using tensor products of the fundamental 2×2 matrices

$$I = \begin{pmatrix} 1 & 0 \\ 0 & 1 \end{pmatrix}, \quad X = \begin{pmatrix} 1 & 0 \\ 0 & -1 \end{pmatrix}, \quad Y = \begin{pmatrix} 0 & 1 \\ 1 & 0 \end{pmatrix}, \quad A = \begin{pmatrix} 0 & 1 \\ -1 & 0 \end{pmatrix}, \tag{5.23}$$

as introduced in Appendix.

These representations play a crucial role in describing the structure and implications of superconformal algebras, particularly in the study of quantum mechanical systems with extended supersymmetry.

For $\mathcal{N} = 1$, the differential matrix representation of $\mathfrak{osp}(1|2)$ is given by

$$Q_1 = \frac{1}{\sqrt{2}} \left(\partial_x \cdot A + \frac{\beta}{x} \cdot Y \right), \tag{5.24}$$

$$\tilde{Q}_1 = \frac{i}{\sqrt{2}} x \cdot A, \tag{5.25}$$

$$H = \frac{1}{2} \left(-\partial_x^2 + \frac{\beta^2}{x^2} \right) \cdot I - \frac{\beta}{2x^2} \cdot X, \tag{5.26}$$

$$D = -\frac{i}{2} \left(x\partial_x + \frac{i}{2} \right) \cdot I, \tag{5.27}$$

$$K = \frac{1}{2} x^2 \cdot I, \tag{5.28}$$

where β is an arbitrary real parameter. The above operators are Hermitian.

The nonvanishing $\mathfrak{osp}(1|2)$ (anti)commutators are

$$\{Q_1, Q_1\} = 2H, \tag{5.29}$$

$$[D, Q_1] = 2iQ_1, \tag{5.30}$$

$$\{Q_1, \tilde{Q}_1\} = 2D, \tag{5.31}$$

$$[D, \tilde{Q}_1] = -i\tilde{Q}_1, \tag{5.32}$$

$$[D, H] = iH, \tag{5.33}$$

$$\{\tilde{Q}_1, \tilde{Q}_1\} = 2K, \tag{5.34}$$

$$[K, Q_1] = i\tilde{Q}_1, \tag{5.35}$$

$$[D, K] = -iK, \tag{5.36}$$

$$[K, \tilde{Q}_1] = -iQ_1, \tag{5.37}$$

$$[H, K] = -2iD. \tag{5.38}$$

For $\mathcal{N} = 2$, the differential matrix representation of $\mathfrak{sl}(2|1)$ is given by

$$Q_1 = \frac{1}{\sqrt{2}} \left(\partial_x \cdot A \otimes I + \frac{\beta}{x} \cdot Y \otimes I \right), \tag{5.39}$$

$$Q_2 = \frac{1}{\sqrt{2}} \left(\partial_x \cdot Y \otimes A + \frac{\beta}{x} \cdot A \otimes A \right), \tag{5.40}$$

$$\tilde{Q}_1 = \frac{i}{\sqrt{2}} x \cdot A \otimes I, \tag{5.41}$$

$$\tilde{Q}_2 = \frac{i}{\sqrt{2}} x \cdot Y \otimes A, \tag{5.42}$$

$$H = \frac{1}{2} \left(-\partial_x^2 + \frac{\beta^2}{x^2} \right) \cdot I \otimes I - \frac{\beta}{2x^2} \cdot X \otimes I, \tag{5.43}$$

$$D = -\frac{i}{2} \left(x\partial_x + \frac{1}{2} \right) \cdot I \otimes I, \tag{5.44}$$

$$K = \frac{1}{2} x^2 \cdot I \otimes I, \tag{5.45}$$

$$W = \frac{i}{4} (X \otimes A + 2\beta \cdot I \otimes A), \tag{5.46}$$

where W is the R-symmetry generator. As before, the operators are Hermitian, and β is an arbitrary real parameter.

The nonvanishing $\mathfrak{sl}(2|1)$ (anti)commutators are, for $j = 1, 2$:

$$\{Q_1, Q_1\} = \{Q_2, Q_2\} = 2H, \tag{5.47}$$

$$\{Q_1, \tilde{Q}_1\} = \{Q_2, \tilde{Q}_2\} = 2D, \tag{5.48}$$

$$[D, Q_j] = \frac{i}{2} Q_j, \tag{5.49}$$

$$[W, Q_1] = \frac{i}{2} Q_2, \tag{5.50}$$

$$[W, Q_2] = -\frac{i}{2} Q_1, \tag{5.51}$$

$$[D, \tilde{Q}_j] = -\frac{i}{2} \tilde{Q}_j, \tag{5.52}$$

$$[D, H] = iH, \tag{5.53}$$

$$\{\tilde{Q}_1, \tilde{Q}_1\} = \{\tilde{Q}_2, \tilde{Q}_2\} = 2K, \tag{5.54}$$

$$\{Q_1, \tilde{Q}_2\} = -\{Q_2, \tilde{Q}_1\} = 2W, \tag{5.55}$$

$$[K, Q_j] = i\tilde{Q}_j, \tag{5.56}$$

$$[W, \tilde{Q}_1] = \frac{i}{2} \tilde{Q}_2, \tag{5.57}$$

$$[W, \tilde{Q}_2] = -\frac{i}{2} \tilde{Q}_1, \tag{5.58}$$

$$[D, K] = -iK, \tag{5.59}$$

$$[K, \tilde{Q}_j] = -iQ_j, \tag{5.60}$$

$$[H, K] = -2iD. \tag{5.61}$$

For $\mathcal{N} = 4$, the differential matrix representation of $D(2, 1; \alpha)$ is constructed by evaluating the repeated (anti)commutators of the four supercharges Q_i and the generator K. These operators take the following explicit form:

$$Q_1 = \frac{1}{\sqrt{2}} \left(\partial_x \cdot A \otimes I \otimes I + \frac{\beta}{x} \cdot Y \otimes I \otimes I \right), \tag{5.62}$$

$$Q_2 = \frac{1}{\sqrt{2}} \left(\partial_x \cdot Y \otimes A \otimes X + \frac{\beta}{x} \cdot A \otimes A \otimes X \right), \tag{5.63}$$

$$Q_3 = \frac{1}{\sqrt{2}} \left(\partial_x \cdot Y \otimes A \otimes Y + \frac{\beta}{x} \cdot A \otimes A \otimes Y \right), \tag{5.64}$$

$$Q_4 = \frac{1}{\sqrt{2}} \left(\partial_x \cdot Y \otimes I \otimes A + \frac{\beta}{x} \cdot A \otimes I \otimes A \right). \tag{5.65}$$

The Hamiltonian's conformal partner, responsible for generating special conformal transformations, is given by:

$$K = \frac{1}{2} x^2 \cdot I \otimes I \otimes I. \tag{5.66}$$

This representation satisfies the structure of the $D(2, 1; \alpha)$ superalgebra, with the identification

$$\alpha = \beta - \frac{1}{2}. \tag{5.67}$$

For the $\mathcal{N} = 8$ case, the superalgebra extends to the exceptional Lie superalgebra $F(4)$, whose differential matrix representation has been constructed in [57].

When considering the statistical transmutations of supersymmetry, the fundamental bosonic generators, namely the Hamiltonian H, the dilatation operator D, and the special conformal generator K, are all assigned to the zero-graded sector:

$$[H] = [K] = [D] = 00. \tag{5.68}$$

In the presence of a conformal structure, each supercharge Q_i is accompanied by a conformal superpartner $\tilde{Q}_i$. Both of these generators reside in the same nonzero graded sector. Specifically, for $\mathcal{N} = 2$, the graded assignments take the form:

$$[Q_1] = [\tilde{Q}_1] = \mu, \quad [Q_2] = [\tilde{Q}_2] = \nu, \tag{5.69}$$

$$[W] = \mu + \nu \mod 2, \tag{5.70}$$

where μ and ν take distinct values in the set $\{10, 01, 11\}$. This classification reflects the interplay between supersymmetry and its underlying graded structure.

The de Alfaro-Fubini-Furlan (DFF) Hamiltonian H_{DFF} is introduced by modifying the standard Hamiltonian through the inclusion of the conformal generator K:

$$H_{\mathrm{DFF}} = H + K. \tag{5.71}$$

This modification introduces a β-dependent deformation of the quantum oscillator, altering its spectral properties while preserving the underlying superconformal symmetry.

Focusing on the $\mathcal{N} = 2$ case, the explicit form of the deformed Hamiltonian is given by:

$$H_{\mathrm{DFF}} = \frac{1}{2}\left(-\partial_x^2 + \frac{\beta^2}{x^2} + x^2\right) \cdot I \otimes I - \frac{\beta}{2x^2} \cdot X \otimes I. \tag{5.72}$$

This Hamiltonian is explicitly Hermitian, as required:

$$H_{\mathrm{DFF}}^{\dagger} = H_{\mathrm{DFF}}. \tag{5.73}$$

To analyze the system's spectrum, we introduce a set of creation and annihilation operators $a_j^{\dagger}$ and a_j for $j = 1, 2$, which are defined as:

$$a_j := Q_j - i\tilde{Q}_j, \quad a_j^\dagger := Q_j + i\tilde{Q}_j. \tag{5.74}$$

These operators exhibit the expected commutation relations with the Hamiltonian, confirming their role in raising and lowering the system's energy states:

$$[H_{\text{DFF}}, a_j] = -a_j, \quad [H_{\text{DFF}}, a_j^\dagger] = a_j^\dagger. \tag{5.75}$$

Additionally, the creation and annihilation operators satisfy the fundamental anti-commutation relations:

$$\{a_1, a_1^\dagger\} = \{a_2, a_2^\dagger\} = 2H_{\text{DFF}}. \tag{5.76}$$

An essential feature of this formulation is that each operator pair obeys a β-deformed Heisenberg algebra:

$$[a_1, a_1^\dagger] = [a_2, a_2^\dagger] = I_4 - 2\beta\overline{K}, \tag{5.77}$$

where $\overline{K}$ represents a Klein operator, defined as:

$$\overline{K} = X \otimes I. \tag{5.78}$$

This Klein operator satisfies key algebraic properties:

$$\overline{K}^2 = I_4, \quad \{a_j, \overline{K}\} = \{a_j^\dagger, \overline{K}\} = 0, \quad \text{for } j = 1, 2. \tag{5.79}$$

Furthermore, the creation operators exhibit additional anti-commutation relations:

$$\{a_i^\dagger, a_j^\dagger\} = 2\delta_{ij} Z, \quad [Z, a_j^\dagger] = 0, \quad \text{for } i, j = 1, 2, \tag{5.80}$$

where Z is given by:

$$Z = H + K + 2iD. \tag{5.81}$$

The algebraic structure described above recovers the fundamental (anti)commutation relations of $\mathcal{N} = 2$ supersymmetric quantum mechanics. However, a key difference lies in the fact that the operators $a_j^\dagger$ and Z are not Hermitian, leading to additional subtleties in their physical interpretation. This aspect plays a crucial role in distinguishing standard quantum statistics from the induced parastatistics in the presence of supersymmetry.

An in-depth study of the admissible Hilbert spaces associated with the Hamiltonian H_{DFF}, depending on the range of the parameter β, is provided in [59]. It is established that for

$$\beta > -\frac{1}{2}, \tag{5.82}$$

one can define a well-behaved single-particle Hilbert space $\mathcal{H}_\beta^{(1)}$, built from a properly normalized bosonic Fock vacuum Ψ_β. The explicit expression for the vacuum state, written in terms of the coordinate representation, is given by

$$\Psi_\beta(x) = \frac{1}{\sqrt{\Gamma(\beta+\frac{1}{2})}} x^\beta e^{-\frac{1}{2}x^2} \begin{pmatrix} 1 \\ 0 \\ 0 \\ 0 \end{pmatrix}. \tag{5.83}$$

Here, the prefactor ensures proper normalization, where the Gamma function in the denominator plays a crucial role in guaranteeing that the integral of the probability density remains finite. Specifically, as demonstrated in [59], this function satisfies the normalization condition

$$\int_{-\infty}^{\infty} dx \, \mathrm{Tr}\left(\Psi_\beta^\dagger \Psi_\beta\right) = 1. \tag{5.84}$$

The vacuum state $\Psi_\beta(x)$ is annihilated by both of the fundamental lowering operators:

$$a_1 \Psi_\beta(x) = a_2 \Psi_\beta(x) = 0. \tag{5.85}$$

This property establishes $\Psi_\beta(x)$ as the lowest-energy eigenstate of the system, from which the entire Hilbert space is constructed by applying the creation operators.

The single-particle Hilbert space $\mathcal{H}_\beta^{(1)}$ is then spanned by the basis states

$$|m; r, s\rangle := Z^m (a_1^\dagger)^r (a_2^\dagger)^s \Psi_\beta(x), \tag{5.86}$$

where the quantum numbers take values

$$r, s = 0, 1, \quad m = 0, 1, 2, \ldots. \tag{5.87}$$

Thus, the Hilbert space is formally given by

$$\mathcal{H}_\beta^{(1)} = \{|m; r, s\rangle\}. \tag{5.88}$$

Each of these basis vectors is an eigenstate of the de Alfaro-Fubini-Furlan Hamiltonian H_{DFF}, with corresponding eigenvalues

$$H_{\mathrm{DFF}}|m; r, s\rangle = E_{m;r,s}|m; r, s\rangle, \tag{5.89}$$

where the explicit form of the energy levels is

$$E_{m;r,s} = \frac{1}{2} + \beta + 2m + r + s. \tag{5.90}$$

A key feature of this spectrum is that, apart from the lowest energy state, the higher energy levels exhibit degeneracy. The ground state energy is given by

$$E_{\mathrm{vac}} := E_{0;0,0} = \frac{1}{2} + \beta. \tag{5.91}$$

Above the vacuum energy level, the remaining spectrum follows a characteristic pattern in which each excited state exhibits a twofold degeneracy:

$$E_n = \frac{1}{2} + \beta + n, \quad n = 0, 1, 2, \ldots. \tag{5.92}$$

This leads to a structured energy tower with degeneracies of the form $(1, 2, 2, 2, \ldots)$, where the first energy level is non-degenerate, and each subsequent level consists of two states with the same energy.

5.3.1 Statistical Transmutations of the $\mathcal{N} = 2$ DFF-Deformed Oscillator

We now extend the framework introduced in this section to the study of two-particle Hilbert spaces, constructed according to the six different $\mathcal{N} = 2$ parastatistics outlined in subsection 5.1.2. Each of these statistical transmutations modifies the structure of the Hilbert space and affects the resulting energy spectrum.

For a given deformation parameter β satisfying

$$\beta > -\frac{1}{2}, \tag{5.93}$$

the two-particle Hilbert spaces, denoted by $\mathcal{H}_{\beta,*}^{(2)}$ (where the asterisk labels the particular parastatistics), are properly constructed Fock spaces. These spaces are not arbitrary but must be subspaces of the tensor product of the single-particle Hilbert spaces:

$$\mathcal{H}_{\beta,*}^{(2)} \subset \mathcal{H}_{\beta}^{(1)} \otimes \mathcal{H}_{\beta}^{(1)}. \tag{5.94}$$

This condition ensures that the two-particle states are consistently built from the single-particle states while obeying the appropriate (para)statistics.

5.3.2 Two-Particle Operators and the Fock Vacuum

The extension to the two-particle sector is achieved by defining appropriate coproduct structures for the creation and annihilation operators, as well as for the Hamiltonian. The coproducts [60] for the fundamental operators are given by

$$\Delta(a_j^\dagger) = a_j^\dagger \otimes \mathbb{I}_4 + \mathbb{I}_4 \otimes a_j^\dagger, \quad \text{for } j = 1, 2. \tag{5.95}$$

$$\Delta(a_j) = a_j \otimes \mathbb{I}_4 + \mathbb{I}_4 \otimes a_j, \quad \text{for } j = 1, 2. \tag{5.96}$$

$$\Delta(H_{\text{DFF}}) = H_{\text{DFF}} \otimes \mathbb{I}_4 + \mathbb{I}_4 \otimes H_{\text{DFF}}. \tag{5.97}$$

These definitions ensure that the operators act consistently in the two-particle space while preserving the structure of the algebra.

The two-particle Fock vacuum, denoted by $\Psi_{\beta;0}(x, y)$, is explicitly given by

$$\Psi_{\beta;0}(x, y) = \frac{(xy)^\beta e^{-\frac{1}{2}(x^2+y^2)}}{\Gamma(\beta + \frac{1}{2})} \rho_1. \tag{5.98}$$

Here, ρ_1 is a 16-component column vector with 1 in the first position and 0 elsewhere, ensuring that the vacuum state is properly normalized. The normalization condition is chosen so that

$$\int_{-\infty}^{\infty} \int_{-\infty}^{\infty} dx\, dy\, \mathrm{Tr}\left(\Psi_{\beta;0}^\dagger \Psi_{\beta;0}\right) = 1. \tag{5.99}$$

This guarantees a unit norm for the vacuum state, consistent with the probabilistic interpretation of quantum mechanics.

The vacuum is annihilated by all two-particle lowering operators:

$$\Delta(a_1)\Psi_{\beta;0} = \Delta(a_2)\Psi_{\beta;0} = 0. \tag{5.100}$$

Thus, $\Psi_{\beta;0}$ is the lowest-energy state in the two-particle system.

5.3.3 Two-Particle Energy Spectrum

The two-particle Hilbert space $\mathcal{H}^{(2)}_{\beta,*}$ is spanned by states obtained by repeatedly applying the two-particle creation operators $\Delta(a_1^\dagger)$ and $\Delta(a_2^\dagger)$ on the vacuum:

$$\mathcal{H}^{(2)}_{\beta,*} = \mathrm{Span}\left\{\Delta(a_1^\dagger)^r\Delta(a_2^\dagger)^s\Psi_{\beta;0}\right\}, \quad r,s=0,1. \tag{5.101}$$

The corresponding energy eigenvalues in this two-particle sector are given by

$$E^{(2)}_\beta = 1+2\beta+n, \quad n=0,1,2,\ldots. \tag{5.102}$$

The vacuum energy is obtained for $n=0$:

$$E^{(2)}_{\beta;0} = 1+2\beta. \tag{5.103}$$

5.3.4 Two-Particle Excitations and Parastatistics Dependence

To systematically describe the energy eigenstates of the two-particle system, we introduce the following notation for the coproduct operators:

$$\Delta_1 = \Delta(a_1^\dagger), \quad \Delta_2 = \Delta(a_2^\dagger), \tag{5.104}$$

$$\Delta_{11} = \Delta_1\cdot\Delta_1, \quad \Delta_{22} = \Delta_2\cdot\Delta_2, \quad \Delta_{12} = \Delta_1\cdot\Delta_2, \quad \Delta_{21} = \Delta_2\cdot\Delta_1. \tag{5.105}$$

These operators generate the excited states from the two-particle vacuum, and their commutation/anticommutation properties depend on the underlying parastatistics.

5.3.5 Energy Eigenstates and Degeneracy Structure

Up to the second excited states, the two-particle Hilbert space $\mathcal{H}^{(2)}_\beta$ is spanned by the following energy eigenvectors:

$$E^{(2)}_{\beta,0} = 1+2\beta: \quad \Psi_{\beta;0}, \tag{5.106}$$

$$E^{(2)}_{\beta,1} = 2+2\beta: \quad \Psi_{\beta;1} = \Delta_1\Psi_{\beta;0}, \quad \Psi_{\beta;2} = \Delta_2\Psi_{\beta;0}, \tag{5.107}$$

$$E^{(2)}_{\beta,2} = 3+2\beta: \quad \Psi_{\beta;11} = \Delta_{11}\Psi_{\beta;0}, \quad \Psi_{\beta;22} = \Delta_{22}\Psi_{\beta;0}, \quad \Psi_{\beta;12} = \Delta_{12}\Psi_{\beta;0}, \quad \Psi_{\beta;21} = \Delta_{21}\Psi_{\beta;0}. \tag{5.108}$$

From this structure, we see that the vacuum state $\Psi_{\beta;0}$ is non-degenerate. The first excited energy level $E^{(2)}_{\beta,1}$ has a degeneracy of 2, while the degeneracy of the second excited level $E^{(2)}_{\beta,2}$ depends explicitly on the underlying parastatistics.

5.3.6 Effect of Parastatistics on Operator Structure

The influence of different parastatistics on the second excited states manifests in the explicit form of the creation operators:

$$\Delta_{11} = Z \otimes \mathbb{I}_4 + \mathbb{I}_4 \otimes Z + (1 + \delta_{11}) a_1^\dagger \otimes a_1^\dagger, \tag{5.109}$$

$$\Delta_{22} = Z \otimes \mathbb{I}_4 + \mathbb{I}_4 \otimes Z + (1 + \delta_{22}) a_2^\dagger \otimes a_2^\dagger, \tag{5.110}$$

$$\Delta_{12} = V \otimes \mathbb{I}_4 + \mathbb{I}_4 \otimes V + a_1^\dagger \otimes a_2^\dagger + \delta_{12} a_2^\dagger \otimes a_1^\dagger, \tag{5.111}$$

$$\Delta_{21} = -V \otimes \mathbb{I}_4 - \mathbb{I}_4 \otimes V + a_2^\dagger \otimes a_1^\dagger + \delta_{21} a_1^\dagger \otimes a_2^\dagger. \tag{5.112}$$

where we define

$$Z = a_1^\dagger a_1^\dagger = a_2^\dagger a_2^\dagger, \quad V = a_1^\dagger a_2^\dagger. \tag{5.113}$$

The parameters $\delta_{11}, \delta_{22}, \delta_{12}$ take values ± 1 and encode the commutation/anticommutation rules imposed by the graded structure. These signs are determined by the graded entries ε_{ij} from the classification tables in Appendix. Specifically, we set:

$$\delta_{ij} = (-1)^{\varepsilon_{ij}}. \tag{5.114}$$

5.3.7 Parastatistics and Sign Assignments

The explicit correspondence between the statistical transmutation types and the signs $\delta_{11}, \delta_{22}, \delta_{12}$ is summarized as follows:

Parastatistics	δ_{11}	δ_{22}	δ_{12}
2_1	$+1$	$+1$	$+1$
2_3	$+1$	$+1$	-1
2_2^α	$+1$	-1	$+1$
2_2^α	-1	$+1$	$+1$
2_2^β	-1	-1	-1
2_4^α	$+1$	-1	-1
2_4^α	-1	$+1$	-1
2_4^β	-1	-1	$+1$

Table 5 – Sign assignments for different $\mathcal{N} = 2$ parastatistics.

From equations (5.112), it follows that:

$$\Delta_{11} = \Delta_{22}, \quad \text{if } \delta_{11} = \delta_{22} = -1. \tag{5.115}$$

$$\Delta_{12} = -\Delta_{21}, \quad \text{if } \delta_{12} = -1. \tag{5.116}$$

These conditions imply that, when $\delta_{11} = \delta_{22} = -1$, the two states $\Psi_{\beta;11}$ and $\Psi_{\beta;22}$ collapse into the same ray vector. Similarly, when $\delta_{12} = -1$, the two states $\Psi_{\beta;12}$ and $\Psi_{\beta;21}$ become indistinguishable.

5.4 Energy Level Degeneracies and Statistical Transmutations

The degeneracy d_g of the energy levels varies depending on the choice of parastatistics, as summarized in Table 6. This table highlights the distinctions between the statistical transmutations arising in the $\mathcal{N} = 2$ deformed oscillator model.

Parastatistics	$E = 1 + 2\beta$	$E = 2 + 2\beta$	$E = 3 + 2\beta$	**Excitations**
2_1	1	2	4	$2B$ (bosons)
2_2^{α}	1	2	4	$1F + 1B$ (fermion + boson)
2_2^{β}	1	2	2	$2F$ (fermions)
2_3	1	2	3	$2PB$ (parabosons)
2_4^{α}	1	2	3	$1PF + 1PB$ (parafermion + paraboson)
2_4^{β}	1	2	3	$2PF$ (parafermions)

Table 6 – Energy level degeneracies d_g for different $\mathcal{N} = 2$ parastatistics. The last column describes the types of particles in each case, distinguishing ordinary bosons/fermions from paraparticles.

The effects of these transmutations become particularly evident in the multiparticle sector, where higher-order excitations will further differentiate the parastatistical properties of the system. The key observations from Table 6 are as follows:

The ground state ($E = 1 + 2\beta$) is always non-degenerate across all parastatistics, confirming a unique vacuum state in every case. The first excited level ($E = 2 + 2\beta$) consistently exhibits a degeneracy of 2, indicating the presence of a two-dimensional excitation space.

At the second excited level ($E = 3 + 2\beta$), significant differences emerge between the statistical transmutations:

- The standard bosonic case (2_1) and the mixed boson-fermion case (2_2^{α}) both yield a degeneracy of $d_g = 4$, implying that their underlying symmetry structures do not affect the counting of states at this level.

- The purely fermionic case (2_2^{β}) has only $d_g = 2$, in agreement with the Pauli exclusion principle, which restricts the available states.

- The three cases involving paraparticles (2_3, 2_4^α, 2_4^β) all exhibit $d_g = 3$, indicating that their statistical properties lead to a modified energy level structure that distinguishes them from standard bosons and fermions.

While measuring the degeneracy of the second-excited state does not distinguish between the 2_1 and 2_2^α statistics (both yielding $d_g = 4$), nor among the three parastatistical cases (2_3, 2_4^α, 2_4^β, each with $d_g = 3$), it is nevertheless sufficient to establish that the $\mathbb{Z}_2^2$-graded parastatistics yield a physical system with properties distinct from those of standard bosons or fermions.

These findings provide strong evidence that, at least within the framework of the $\mathcal{N} = 2$ deformed oscillator, parastatistics manifest in observable differences in the quantum energy spectrum. Further investigations may explore whether additional observables, such as correlation functions or selection rules, can offer further discrimination between different parastatistical behaviors.

Thus, we observe that the statistical transmutations induce a reorganization of the two-particle spectrum, reducing the number of independent states depending on the choice of δ_{ij}. This modification leads to distinct degeneracy structures, which provide a direct avenue to distinguish different types of (para)statistics through spectral measurements.

5.5 Summary and Comments

In this section, we presented a preliminary investigation into the physical consequences of algebraic statistical transmutations of supersymmetry, specifically in the context of Superconformal Quantum Mechanics with the inclusion of the de Alfaro-Fubini-Furlan (DFF) oscillator term. Our findings provide the first explicit evidence that $\mathbb{Z}_2^2$-graded parastatistics can directly influence the energy spectrum of a quantum model. This discovery represents a significant departure from previous cases where the presence of parastatistics had to be inferred through indirect measurements involving exchange operators.

The primary distinction between the mechanism discussed here and the one employed in the quantum models analyzed at the beginning of this section, as well as those in [39, 40], lies in the nature of the creation operators. In those previous cases, the quantum models relied on nilpotent creation operators, meaning that higher-order excitations would necessarily vanish beyond a certain threshold. As a consequence, distinguishing between ordinary statistics and parastatistics required constructing specific exchange operators and measuring their eigenvalues to extract statistical information.

In contrast, the creation operators associated with the DFF-deformed oscillator, as shown in equation (5.80), do not exhibit nilpotency. This fundamental difference allows the energy spectrum itself to encode information about the underlying parastatistics, making it possible to distinguish between different statistical transmutations through direct spectral measurements. The identification of this alternative detection mechanism opens new avenues for studying the physical implications of $\mathbb{Z}_2^2$-graded parastatistics in quantum systems.

The results presented here serve as a foundation for a systematic exploration of the detectability of inequivalent parastatistics arising from algebraic statistical transmutations of supersymmetry.

6 Applications in Quantum Field Theory

Building on the role of algebraic statistical transmutations in supersymmetric quantum mechanics, we now extend our analysis to quantum field theory. The integration of $\mathbb{Z}_2^n$-graded parastatistics into field-theoretic models introduces a platform for investigating exotic quantum statistics, extended symmetry algebras, and novel particle excitations. These generalizations challenge the canonical assumptions of quantum field theory, most notably, the Bose–Fermi dichotomy and its relation to spin.

To evaluate these extensions meaningfully, we must revisit the foundations of quantum field quantization, especially the intricate relationship between spin, statistics, and relativistic causality. The spin-statistics theorem, rigorously established by Pauli [61], asserts that integer-spin fields must commute and half-integer-spin fields must anticommute, ensuring compatibility with Lorentz invariance, locality, and positive energy. This result has since been formalized axiomatically by Streater and Wightman [62], and algebraically by Doplicher, Haag, and Roberts [63] using local observables and superselection sectors.

Recent developments have tested the limits of these foundational assumptions. In noncommutative field theory, where locality is modified, Chaichian et al. [64] showed that while C and T symmetries may be individually violated, the CPT theorem and spin-statistics connection can still hold in adapted forms.

The classification of allowable symmetries in quantum field theory is likewise evolving. The Coleman–Mandula theorem [65] constrains the unification of spacetime and internal symmetries within the S-matrix. However, its extension by Haag, Łopuszański, and Sohnius [66] demonstrates that supersymmetry, embodied in Lie superalgebras, can transcend these constraints. More recently, Ito and Nago [67] have proposed $\mathbb{Z}_2^n$-graded Lie superalgebras as a foundation for novel symmetry structures of the S-matrix.

These theoretical advances are increasingly supported by experiment. Para-particle oscillators have been realized using trapped-ion quantum simulators [68, 69], while statistical behavior beyond bosons and fermions has been explored [39, 40, 45, 70], hinting at a broader taxonomy of quantum statistics.

Alternative mathematical frameworks, such as quaternionic quantum mechanics, offer further generalization. Adler's foundational work [71] established a quaternionic formulation of quantum fields, and more recent contributions by Giardino [72, 73] have developed scalar and spinor field theories on real Hilbert spaces. These models suggest new internal symmetries, vacuum structures, and potential deviations from standard statistical behavior.

In the sections that follow, we develop the conventional spin-statistics connection, emphasizing its derivation from Lorentz symmetry, microcausality, and the positivity of the Hilbert space. This will serve as a benchmark for evaluating parastatistical and quaternionic field theories, allowing us to probe the boundaries of standard quantum field theory.

6.1 The Spin-Statistics Theorem and Microcausality

The spin-statistics theorem asserts that the spin of a quantum field dictates the algebraic relations its operators must satisfy: commutation relations for integer-spin fields (bosons), and anticommutation relations for half-integer-spin fields (fermions). These constraints ensure that quantum statistics are consistent with the core principles of relativistic quantum field theory, namely Lorentz invariance, locality, and positive energy.

First rigorously demonstrated by Pauli in 1940 [61], the theorem has since been reformulated in various frameworks. The Wightman axiomatic approach [62] and the algebraic quantum field theory program of Doplicher, Haag, and Roberts [74] offer mathematically rigorous perspectives based on local observables and superselection sectors. More recently, topological quantum field theories and lower-dimensional models have provided generalizations beyond the standard boson-fermion classification [75, 39, 40, 45].

Here, we adopt the constructive formalism of Weinberg [76], where quantum fields are derived from the unitary irreducible representations of the Poincaré group. Within this framework, the spin-statistics connection follows from the consistency of microcausality, Lorentz covariance, and the positivity of the Hilbert space norm, without invoking the full machinery of axiomatic field theory.

Let $\phi(x)$ denote a local quantum field transforming under a finite-dimensional representation of the Lorentz group. The requirement of microcausality imposes:

$$[\phi(x), \phi(y)]_{\mp} = 0 \quad \text{for} \quad (x-y)^2 < 0,$$

where the commutator or anticommutator is chosen according to the field's spin. This condition ensures that operators at spacelike separation do not influence each other, in accordance with relativistic causality.

Weinberg's formalism constructs fields from one-particle states $|\mathbf{p}, \sigma\rangle$ transforming under Lorentz transformations via Wigner rotations:

$$U(\Lambda)|\mathbf{p}, \sigma\rangle = \sum_{\sigma'} D^{(s)}_{\sigma'\sigma}(W(\Lambda, p))|\Lambda\mathbf{p}, \sigma'\rangle.$$

The corresponding quantum field is defined to create and annihilate these states:

$$\phi(x) = \int \frac{d^3p}{(2\pi)^3} \frac{1}{\sqrt{2E_{\mathbf{p}}}} \sum_{\sigma} \left[a(\mathbf{p}, \sigma) u(\mathbf{p}, \sigma) e^{-ip\cdot x} + a^\dagger(\mathbf{p}, \sigma) v(\mathbf{p}, \sigma) e^{ip\cdot x} \right].$$

To preserve causality, one demands:

$$[\phi(x), \phi^\dagger(y)]_\mp = 0 \quad \text{for} \quad (x-y)^2 < 0.$$

Weinberg shows that this constraint leads to a contradiction unless integer-spin fields use commutators and half-integer-spin fields use anticommutators. Violating this assignment leads either to a breakdown of causality or to negative-norm states.

Historical and Generalized Context

Although Pauli's original derivation [61] relied on heuristic field-theoretic arguments, later approaches grounded the theorem in rigorous mathematical structures. In algebraic quantum field theory, the connection emerges from properties of the local net of observables and the symmetry group of the vacuum [74]. In lower-dimensional theories, particularly in $2+1$ dimensions, the standard permutation group is replaced by the braid group, allowing for anyonic statistics and partial spin-statistics correlations [75].

It is crucial to note that the theorem depends fundamentally on Lorentz symmetry and microcausality. In non-relativistic quantum mechanics, or in nonlocal or noncommutative frameworks, the spin-statistics correspondence is no longer guaranteed and must be imposed by hand or justified separately.

Microcausality and the Dyson Expansion

In the interaction picture, the S-matrix is given by the Dyson series:

$$S = T \exp\left(-i \int d^4x \, \mathcal{H}_I(x)\right),$$

where T denotes time ordering. However, time ordering is not Lorentz invariant for spacelike-separated events unless the Hamiltonian density satisfies:

$$[\mathcal{H}_I(x), \mathcal{H}_I(y)] = 0 \quad \text{for} \quad (x-y)^2 > 0.$$

This condition, microcausality, is necessary for the Lorentz invariance of scattering amplitudes and ensures that observables remain frame-independent.

As Weinberg demonstrates [76], this requirement forces quantum fields to obey spin-dependent (anti)commutation relations to avoid acausal signal propagation and to preserve positivity. Incorrect statistics violate these properties, yielding inconsistencies in propagators and scattering amplitudes.

A complementary derivation by Duck and Sudarshan [77] analyzes unitarity through Feynman diagrams. They show that quantizing spin-1/2 fields with commutators (or spin-0 fields with anticommutators) leads to incorrect sign structure in loop corrections, violating the optical theorem. Although their focus is on unitarity rather than locality, the underlying principle is the same: incorrect statistics produce physically unacceptable behavior.

Thus, from both the algebraic and perturbative perspectives, the spin-statistics connection is not merely postulated but required by the internal consistency of relativistic quantum field theory.

6.2 Overview of Quaternionic Field Theories

Quaternionic field theory extends the foundations of quantum field theory by allowing fields to take values in the division algebra of quaternions, $\mathbb{H}$, rather than the real $\mathbb{R}$ or complex $\mathbb{C}$ numbers traditionally used. Quaternions, introduced by Hamilton in 1843, form a noncommutative four-dimensional algebra with basis $\{1, \mathbf{i}, \mathbf{j}, \mathbf{k}\}$ and multiplication rules $\mathbf{i}^2 = \mathbf{j}^2 = \mathbf{k}^2 = \mathbf{ijk} = -1$. Their noncommutativity introduces both mathematical richness and novel physical implications, making them attractive for theoretical investigations.

The formulation of quaternionic quantum mechanics (QQM) was pioneered by Adler in his seminal work *Quaternionic Quantum Mechanics and Quantum Fields* [71]. There, quaternionic Hilbert spaces and a generalization of canonical quantization were developed. Adler proposed that quaternionic structures might naturally encode internal symmetries, suggest mechanisms for CP violation, and even accommodate magnetic monopoles. His work laid the foundation for extending quaternionic techniques into interacting field theories.

Building on Adler's formalism, Giardino proposed a reformulation of quaternionic scalar and spinor fields within a real Hilbert space framework [72, 73]. This approach sidesteps interpretational challenges associated with quaternionic inner products and non-Hermitian operators. His two- and four-component formulations of quaternionic scalar fields lead to new vacuum structures and potential deviations from standard particle statistics. In particular, Giardino's quaternionic Dirac equation features an extended solution space with possible physical implications, including novel fermionic states.

Moreover, quaternionic electrodynamics has been shown to naturally incorporate magnetic monopoles through modified field strength tensors and conserved currents [72]. Giardino has also constructed a quaternionic conformal field theory (QCFT) [78], extending 2D conformal symmetries to four dimensions using quaternionic holomorphic functions. These developments open new directions in the study of symmetry, analyticity, and operator algebras in field theory.

Complementary contributions include Morita's early demonstration that a consistent quaternionic field theory can be constructed for bosonic and fermionic fields balanced under second-order dynamics [79], and De Leo's analysis of quaternionic groups in physics [80]. John Baez has further clarified the role of normed division algebras, including quaternions [81].

6.2.1 Motivations for Quaternionic Representations

Quaternionic representations offer several advantages over traditional complex field theories. First, quaternions generalize complex numbers while preserving a norm and supporting unitary evolution, enabling a natural extension of quantum theory. Because $\mathbb{H}$ contains $\mathbb{C}$ as a subalgebra, QQM may be viewed as an enrichment rather than a replacement of standard formalism.

Second, quaternionic Hilbert spaces admit richer symmetry structures. The automorphism group of $\mathbb{H}$ is SO(3), and quaternionic vector spaces are naturally aligned with SU(2) representations, central to the electroweak sector of the Standard Model. Quaternionic projective spaces also appear in extended supersymmetric theories [81], particularly in scalar manifold classifications.

Third, quaternionic frameworks support generalizations of quantum statistics. Their noncommutative scalar coefficients offer a natural algebraic setting for $\mathbb{Z}_2^n$-graded structures, relevant to parastatistics and exotic symmetry algebras [67]. Quaternion-valued operators are well-suited for encoding graded commutation relations and may lead to consistent quaternionic parastatistics field theories.

Fourth, in the context of conformal field theory, quaternionic analyticity permits an extension of 2D CFT structures to higher dimensions. Giardino's construction of QCFT [78] demonstrates that quaternionic holomorphic functions can play a role analogous to complex holomorphic functions in 2D, preserving essential aspects of conformal symmetry.

Finally, quaternionic models may provide insight into symmetry breaking, non-Hermitian dynamics, and emergent topological structures. In Adler's and Giardino's models, the generalization of propagators and conserved currents introduces new dynamics not easily captured by complex formulations.

In summary, quaternionic field theory offers a mathematically rigorous and physically compelling extension of standard quantum field theory. Its compatibility with internal symmetries, capacity for algebraic generalizations, and potential to reveal new particle phenomena make it a promising framework for future theoretical exploration.

6.3 Minimal Quaternionic Bosonic representation

First, we have to define a quaternionic basis. Considering,

$$e_0 = I \otimes I = \begin{pmatrix} 1 & 0 & 0 & 0 \\ 0 & 1 & 0 & 0 \\ 0 & 0 & 1 & 0 \\ 0 & 0 & 0 & 1 \end{pmatrix} \quad e_1 = X \otimes A = \begin{pmatrix} 0 & 1 & 0 & 0 \\ -1 & 0 & 0 & 0 \\ 0 & 0 & 0 & -1 \\ 0 & 0 & 1 & 0 \end{pmatrix} \tag{6.1}$$

$$e_2 = A \otimes I = \begin{pmatrix} 0 & 0 & 1 & 0 \\ 0 & 0 & 0 & 1 \\ -1 & 0 & 0 & 0 \\ 0 & -1 & 0 & 0 \end{pmatrix} \quad e_3 = Y \otimes A = \begin{pmatrix} 0 & 0 & 0 & 1 \\ 0 & 0 & -1 & 0 \\ 0 & 1 & 0 & 0 \\ -1 & 0 & 0 & 0 \end{pmatrix} \tag{6.2}$$

where we have used an alphabetical representation,

$$I = \begin{pmatrix} 1 & 0 \\ 0 & 1 \end{pmatrix}, \quad X = \begin{pmatrix} 1 & 0 \\ 0 & -1 \end{pmatrix}, \quad Y = \begin{pmatrix} 0 & 1 \\ 1 & 0 \end{pmatrix}, \quad A = \begin{pmatrix} 0 & 1 \\ -1 & 0 \end{pmatrix} \tag{6.3}$$

6.4 Quaternionic Bosonic Scalar Field Theory

For a scalar field theory in a minimal representation, we set,

$$\Phi_{\mathrm{B}} = e_0\tilde{\varphi}_0 + e_1\tilde{\varphi}_1 + e_2\tilde{\varphi}_2 + e_3\tilde{\varphi}_3 \tag{6.4}$$

where $\tilde{\varphi}_i$, for $i = 0, 1, 2, 3$ are the component scalar fields. In this case, bosonic. In order to construct the lagrangian density we have to construct $\overline{\Phi_{\mathrm{B}}}$, which is the quaternionic conjugate of Φ_{B}. Explicitly, we have,

$$\Phi_{\mathrm{B}} = \begin{pmatrix} \tilde{\varphi}_0 & \tilde{\varphi}_1 & \tilde{\varphi}_2 & \tilde{\varphi}_3 \\ -\tilde{\varphi}_1 & \tilde{\varphi}_0 & -\tilde{\varphi}_3 & \tilde{\varphi}_2 \\ -\tilde{\varphi}_2 & \tilde{\varphi}_3 & \tilde{\varphi}_0 & -\tilde{\varphi}_1 \\ -\tilde{\varphi}_3 & -\tilde{\varphi}_2 & \tilde{\varphi}_1 & \tilde{\varphi}_0 \end{pmatrix} \quad \overline{\Phi_{\mathrm{B}}} = \begin{pmatrix} \tilde{\varphi}_0 & -\tilde{\varphi}_1 & -\tilde{\varphi}_2 & -\tilde{\varphi}_3 \\ \tilde{\varphi}_1 & \tilde{\varphi}_0 & \tilde{\varphi}_3 & -\tilde{\varphi}_2 \\ \tilde{\varphi}_2 & -\tilde{\varphi}_3 & \tilde{\varphi}_0 & \tilde{\varphi}_1 \\ \tilde{\varphi}_3 & \tilde{\varphi}_2 & -\tilde{\varphi}_1 & \tilde{\varphi}_0 \end{pmatrix}. \tag{6.5}$$

6.4.1 Construction of the Lagrangian

For the free scalar field theory lagrangian density, we have,

$$\mathcal{L} = \frac{1}{4}\mathrm{Tr}\left[\partial^\mu\overline{\Phi_{\mathrm{B}}}\,\partial_\mu\Phi_{\mathrm{B}} - m^2\overline{\Phi_{\mathrm{B}}}\Phi_{\mathrm{B}}\right] \tag{6.6}$$

We can start with the kinect term,

$$\partial^{\mu}\overline{\Phi_{\mathrm{B}}}\,\partial_{\mu}\Phi_{\mathrm{B}} = \eta^{\mu\nu}\partial_{\nu}\overline{\Phi_{\mathrm{B}}}\,\partial_{\mu}\Phi_{\mathrm{B}} \tag{6.7}$$

where $\eta^{\mu\nu}$ is a diagonal matrix,

$$\eta^{\mu\nu} = \begin{pmatrix} r & 0 & 0 & 0 \\ 0 & 1 & 0 & 0 \\ 0 & 0 & 1 & 0 \\ 0 & 0 & 0 & 1 \end{pmatrix}. \tag{6.8}$$

The parameter r is for an arbitrary metric signature, that is, Minkowskian or Euclidian. Then,

$$\eta^{\mu\nu}\,\partial_{\mu}\overline{\Phi_{\mathrm{B}}}\,\partial_{\nu}\Phi_{\mathrm{B}} = \eta^{00}\,\partial_{0}\overline{\Phi_{\mathrm{B}}}\,\partial_{0}\Phi_{\mathrm{B}} + \sum_{i=1}^{3}\eta^{ii}\,\partial_{i}\overline{\Phi_{\mathrm{B}}}\,\partial_{i}\Phi_{\mathrm{B}} \tag{6.9}$$

$$= r\partial_{0}\overline{\Phi_{\mathrm{B}}}\,\partial_{0}\Phi_{\mathrm{B}} + \partial_{1}\overline{\Phi_{\mathrm{B}}}\,\partial_{1}\Phi_{\mathrm{B}} + \partial_{2}\overline{\Phi_{\mathrm{B}}}\,\partial_{2}\Phi_{\mathrm{B}} + \partial_{3}\overline{\Phi_{\mathrm{B}}}\,\partial_{3}\Phi_{\mathrm{B}} \tag{6.10}$$

Then we have,

$$\begin{aligned}\frac{1}{4}\,\mathrm{Tr}\left[\partial^{\mu}\overline{\Phi_{\mathrm{B}}}\,\partial_{\mu}\Phi_{\mathrm{B}}\right] = r\Big[&\partial_0\tilde{\varphi}_0\,\partial_0\tilde{\varphi}_0 + \partial_0\tilde{\varphi}_1\,\partial_0\tilde{\varphi}_1 + \partial_0\tilde{\varphi}_2\,\partial_0\tilde{\varphi}_2 + \partial_0\tilde{\varphi}_3\,\partial_0\tilde{\varphi}_3\Big] \\ &+ \partial_1\tilde{\varphi}_0\,\partial_1\tilde{\varphi}_0 + \partial_1\tilde{\varphi}_1\,\partial_1\tilde{\varphi}_1 + \partial_1\tilde{\varphi}_2\,\partial_1\tilde{\varphi}_2 + \partial_1\tilde{\varphi}_3\,\partial_1\tilde{\varphi}_3 \\ &+ \partial_2\tilde{\varphi}_0\,\partial_2\tilde{\varphi}_0 + \partial_2\tilde{\varphi}_1\,\partial_2\tilde{\varphi}_1 + \partial_2\tilde{\varphi}_2\,\partial_2\tilde{\varphi}_2 + \partial_2\tilde{\varphi}_3\,\partial_2\tilde{\varphi}_3 \\ &+ \partial_3\tilde{\varphi}_0\,\partial_3\tilde{\varphi}_0 + \partial_3\tilde{\varphi}_1\,\partial_3\tilde{\varphi}_1 + \partial_3\tilde{\varphi}_2\,\partial_3\tilde{\varphi}_2 + \partial_3\tilde{\varphi}_3\,\partial_3\tilde{\varphi}_3\end{aligned} \tag{6.11}$$

Mass term (auto interaction):

$$\frac{1}{4}\mathrm{Tr}\left[m^2\overline{\Phi_{\mathrm{B}}}\Phi_{\mathrm{B}}\right] = m^2(\tilde{\varphi}_0^2 + \tilde{\varphi}_1^2 + \tilde{\varphi}_2^2 + \tilde{\varphi}_3^2). \tag{6.12}$$

Now, for a higher order interaction term, we have,

$$\begin{aligned}\frac{1}{4}\mathrm{Tr}\left[\lambda(\overline{\Phi_{\mathrm{B}}}\Phi_{\mathrm{B}})^2\right] = {}&\lambda\left(\tilde{\varphi}_0^4 + \tilde{\varphi}_1^4 + \tilde{\varphi}_2^4 + \tilde{\varphi}_3^4\right) \\ &+ 2\lambda\left(\tilde{\varphi}_0^2\tilde{\varphi}_1^2 + \tilde{\varphi}_0^2\tilde{\varphi}_2^2 + \tilde{\varphi}_0^2\tilde{\varphi}_3^2\right) \\ &+ 2\lambda\left(\tilde{\varphi}_1^2\tilde{\varphi}_2^2 + \tilde{\varphi}_1^2\tilde{\varphi}_3^2 + \tilde{\varphi}_2^2\tilde{\varphi}_3^2\right).\end{aligned} \tag{6.13}$$

Moreover, quaternionic algebra presents a natural framework to accommodate $\mathbb{Z}_2^n$-graded structures, which generalize the usual fermionic/bosonic $\mathbb{Z}_2$-grading of superalgebras. In particular, this provides a suitable language for the formalism of parastatistics, where particles obey generalized symmetry relations extending beyond the Fermi-Dirac and Bose-Einstein cases. Because quaternionic structures support noncommutative scalar multiplication and generalized commutation relations, they provide a promising setting for constructing quaternionic parastatistical field theories.

However, to make meaningful comparisons with parabosonic scalar field theories, especially those with $\mathbb{Z}_2^n$-graded symmetry, one must go beyond the minimal representation of quaternionic bosonic fields. This is due to the fact that the minimal nontrivial parabosonic representation already requires a 16×16 matrix structure. Therefore, a non-minimal quaternionic bosonic representation is necessary to capture equivalent degrees of freedom and to faithfully reproduce the operator algebra structure of the parabosonic theory. This non-minimal embedding ensures a consistent mapping between the quaternionic bosonic and parabosonic fields. Hence, we set,

$$\Phi_{\mathrm{B}}^{16} = \Phi_{\mathrm{B}} \otimes \mathbb{I}_4. \tag{6.14}$$

Explicitly,

$$\Phi_{\mathrm{B}}^{16} = e_0 \otimes \mathbb{I}_4 \tilde{\varphi}_0 + e_1 \otimes \mathbb{I}_4 \tilde{\varphi}_1 + e_2 \otimes \mathbb{I}_4 \tilde{\varphi}_2 + e_3 \otimes \mathbb{I}_4 \tilde{\varphi}_3. \tag{6.15}$$

As in standard quaternionic field constructions, we must define the quaternionic conjugate of the field in order to construct covariant bilinear terms and invariant Lagrangians.

To proceed, we define the *quaternionic conjugate* of the field, denoted by $\overline{\Phi_{\mathrm{B}}^{16}}$. This operation acts by taking the quaternionic conjugate (i.e., reversing the sign of the imaginary components) of each entry.

This conjugate structure is essential in forming quaternionic inner products and kinetic terms, and it ensures hermiticity when constructing Lagrangian densities involving bosonic fields valued in quaternionic modules. Now, explicitly, we have,

$$
\Phi_{\mathrm{B}}^{16} = \begin{pmatrix}
\tilde{\varphi}_0 & 0 & 0 & 0 & \tilde{\varphi}_1 & 0 & 0 & 0 & \tilde{\varphi}_2 & 0 & 0 & 0 & \tilde{\varphi}_3 & 0 & 0 & 0 \\
0 & \tilde{\varphi}_0 & 0 & 0 & 0 & \tilde{\varphi}_1 & 0 & 0 & 0 & \tilde{\varphi}_2 & 0 & 0 & 0 & \tilde{\varphi}_3 & 0 & 0 \\
0 & 0 & \tilde{\varphi}_0 & 0 & 0 & 0 & \tilde{\varphi}_1 & 0 & 0 & 0 & \tilde{\varphi}_2 & 0 & 0 & 0 & \tilde{\varphi}_3 & 0 \\
0 & 0 & 0 & \tilde{\varphi}_0 & 0 & 0 & 0 & \tilde{\varphi}_1 & 0 & 0 & 0 & \tilde{\varphi}_2 & 0 & 0 & 0 & \tilde{\varphi}_3 \\
-\tilde{\varphi}_1 & 0 & 0 & 0 & \tilde{\varphi}_0 & 0 & 0 & 0 & -\tilde{\varphi}_3 & 0 & 0 & 0 & \tilde{\varphi}_2 & 0 & 0 & 0 \\
0 & -\tilde{\varphi}_1 & 0 & 0 & 0 & \tilde{\varphi}_0 & 0 & 0 & 0 & -\tilde{\varphi}_3 & 0 & 0 & 0 & \tilde{\varphi}_2 & 0 & 0 \\
0 & 0 & -\tilde{\varphi}_1 & 0 & 0 & 0 & \tilde{\varphi}_0 & 0 & 0 & 0 & -\tilde{\varphi}_3 & 0 & 0 & 0 & \tilde{\varphi}_2 & 0 \\
0 & 0 & 0 & -\tilde{\varphi}_1 & 0 & 0 & 0 & \tilde{\varphi}_0 & 0 & 0 & 0 & -\tilde{\varphi}_3 & 0 & 0 & 0 & \tilde{\varphi}_2 \\
-\tilde{\varphi}_2 & 0 & 0 & 0 & \tilde{\varphi}_3 & 0 & 0 & 0 & \tilde{\varphi}_0 & 0 & 0 & 0 & -\tilde{\varphi}_1 & 0 & 0 & 0 \\
0 & -\tilde{\varphi}_2 & 0 & 0 & 0 & \tilde{\varphi}_3 & 0 & 0 & 0 & \tilde{\varphi}_0 & 0 & 0 & 0 & -\tilde{\varphi}_1 & 0 & 0 \\
0 & 0 & -\tilde{\varphi}_2 & 0 & 0 & 0 & \tilde{\varphi}_3 & 0 & 0 & 0 & \tilde{\varphi}_0 & 0 & 0 & 0 & -\tilde{\varphi}_1 & 0 \\
0 & 0 & 0 & -\tilde{\varphi}_2 & 0 & 0 & 0 & \tilde{\varphi}_3 & 0 & 0 & 0 & \tilde{\varphi}_0 & 0 & 0 & 0 & -\tilde{\varphi}_1 \\
-\tilde{\varphi}_3 & 0 & 0 & 0 & -\tilde{\varphi}_2 & 0 & 0 & 0 & \tilde{\varphi}_1 & 0 & 0 & 0 & \tilde{\varphi}_0 & 0 & 0 & 0 \\
0 & -\tilde{\varphi}_3 & 0 & 0 & 0 & -\tilde{\varphi}_2 & 0 & 0 & 0 & \tilde{\varphi}_1 & 0 & 0 & 0 & \tilde{\varphi}_0 & 0 & 0 \\
0 & 0 & -\tilde{\varphi}_3 & 0 & 0 & 0 & -\tilde{\varphi}_2 & 0 & 0 & 0 & \tilde{\varphi}_1 & 0 & 0 & 0 & \tilde{\varphi}_0 & 0 \\
0 & 0 & 0 & -\tilde{\varphi}_3 & 0 & 0 & 0 & -\tilde{\varphi}_2 & 0 & 0 & 0 & \tilde{\varphi}_1 & 0 & 0 & 0 & \tilde{\varphi}_0
\end{pmatrix} \tag{6.16}
$$

and

$$
\overline{\Phi_{\mathrm{B}}^{16}} = \begin{pmatrix}
\tilde{\varphi}_0 & 0 & 0 & 0 & -\tilde{\varphi}_1 & 0 & 0 & 0 & -\tilde{\varphi}_2 & 0 & 0 & 0 & -\tilde{\varphi}_3 & 0 & 0 & 0 \\
0 & \tilde{\varphi}_0 & 0 & 0 & 0 & -\tilde{\varphi}_1 & 0 & 0 & 0 & -\tilde{\varphi}_2 & 0 & 0 & 0 & -\tilde{\varphi}_3 & 0 & 0 \\
0 & 0 & \tilde{\varphi}_0 & 0 & 0 & 0 & -\tilde{\varphi}_1 & 0 & 0 & 0 & -\tilde{\varphi}_2 & 0 & 0 & 0 & -\tilde{\varphi}_3 & 0 \\
0 & 0 & 0 & \tilde{\varphi}_0 & 0 & 0 & 0 & -\tilde{\varphi}_1 & 0 & 0 & 0 & -\tilde{\varphi}_2 & 0 & 0 & 0 & -\tilde{\varphi}_3 \\
\tilde{\varphi}_1 & 0 & 0 & 0 & \tilde{\varphi}_0 & 0 & 0 & 0 & \tilde{\varphi}_3 & 0 & 0 & 0 & -\tilde{\varphi}_2 & 0 & 0 & 0 \\
0 & \tilde{\varphi}_1 & 0 & 0 & 0 & \tilde{\varphi}_0 & 0 & 0 & 0 & \tilde{\varphi}_3 & 0 & 0 & 0 & -\tilde{\varphi}_2 & 0 & 0 \\
0 & 0 & \tilde{\varphi}_1 & 0 & 0 & 0 & \tilde{\varphi}_0 & 0 & 0 & 0 & \tilde{\varphi}_3 & 0 & 0 & 0 & -\tilde{\varphi}_2 & 0 \\
0 & 0 & 0 & \tilde{\varphi}_1 & 0 & 0 & 0 & \tilde{\varphi}_0 & 0 & 0 & 0 & \tilde{\varphi}_3 & 0 & 0 & 0 & -\tilde{\varphi}_2 \\
\tilde{\varphi}_2 & 0 & 0 & 0 & -\tilde{\varphi}_3 & 0 & 0 & 0 & \tilde{\varphi}_0 & 0 & 0 & 0 & \tilde{\varphi}_1 & 0 & 0 & 0 \\
0 & \tilde{\varphi}_2 & 0 & 0 & 0 & -\tilde{\varphi}_3 & 0 & 0 & 0 & \tilde{\varphi}_0 & 0 & 0 & 0 & \tilde{\varphi}_1 & 0 & 0 \\
0 & 0 & \tilde{\varphi}_2 & 0 & 0 & 0 & -\tilde{\varphi}_3 & 0 & 0 & 0 & \tilde{\varphi}_0 & 0 & 0 & 0 & \tilde{\varphi}_1 & 0 \\
0 & 0 & 0 & \tilde{\varphi}_2 & 0 & 0 & 0 & -\tilde{\varphi}_3 & 0 & 0 & 0 & \tilde{\varphi}_0 & 0 & 0 & 0 & \tilde{\varphi}_1 \\
\tilde{\varphi}_3 & 0 & 0 & 0 & \tilde{\varphi}_2 & 0 & 0 & 0 & -\tilde{\varphi}_1 & 0 & 0 & 0 & \tilde{\varphi}_0 & 0 & 0 & 0 \\
0 & \tilde{\varphi}_3 & 0 & 0 & 0 & \tilde{\varphi}_2 & 0 & 0 & 0 & -\tilde{\varphi}_1 & 0 & 0 & 0 & \tilde{\varphi}_0 & 0 & 0 \\
0 & 0 & \tilde{\varphi}_3 & 0 & 0 & 0 & \tilde{\varphi}_2 & 0 & 0 & 0 & -\tilde{\varphi}_1 & 0 & 0 & 0 & \tilde{\varphi}_0 & 0 \\
0 & 0 & 0 & \tilde{\varphi}_3 & 0 & 0 & 0 & \tilde{\varphi}_2 & 0 & 0 & 0 & -\tilde{\varphi}_1 & 0 & 0 & 0 & \tilde{\varphi}_0
\end{pmatrix} \tag{6.17}
$$

6.5 Quaternionic Parabosonic Scalar Field Theory

For this construction, we will use the same quaternionic basis, but additionally, we will introduce the parabosonic struture by the action of three matrices (M_1, M_2 and M_3), which are constructed with Pauli matrices in the following way.

$$M_1 = \mathbb{I}_2 \otimes \sigma_1, \quad M_2 = \sigma_1 \otimes \sigma_3, \quad M_3 = -\sigma_1 \otimes \sigma_3, \tag{6.18}$$

where

$$\sigma_1 = \begin{pmatrix} 0 & 1 \\ 1 & 0 \end{pmatrix}, \quad \sigma_2 = \begin{pmatrix} 0 & -i \\ i & 0 \end{pmatrix}, \quad \sigma_3 = \begin{pmatrix} 1 & 0 \\ 0 & -1 \end{pmatrix}. \tag{6.19}$$

Hence, explicitly, M_1, M_2 and M_3 are,

$$M_1 = \begin{pmatrix} 0 & 1 & 0 & 0 \\ 1 & 0 & 0 & 0 \\ 0 & 0 & 0 & 1 \\ 0 & 0 & 1 & 0 \end{pmatrix}, \quad M_2 = \begin{pmatrix} 0 & 0 & 1 & 0 \\ 0 & 0 & 0 & -1 \\ 1 & 0 & 0 & 0 \\ 0 & -1 & 0 & 0 \end{pmatrix}, \quad M_3 = \begin{pmatrix} 0 & 0 & 0 & i \\ 0 & 0 & -i & 0 \\ 0 & i & 0 & 0 \\ -i & 0 & 0 & 0 \end{pmatrix}. \tag{6.20}$$

Now, we can define a scalar field as,

$$\Phi^{16}_{\mathrm{PB}} = (e_0 \otimes \mathbb{I}_4)\tilde{\varphi}_0 + (e_1 \otimes M_1)\tilde{\varphi}_1 + (e_2 \otimes M_2)\tilde{\varphi}_2 + (e_3 \otimes M_3)\tilde{\varphi}_3 \tag{6.21}$$

where, again, $\tilde{\varphi}_i$, for $i = 0, 1, 2, 3$ are the component scalar fields. Explicitly, we have,

$$\Phi^{16}_{\mathrm{PB}} = \begin{pmatrix}
\varphi_0 & 0 & 0 & 0 & 0 & \varphi_1 & 0 & 0 & 0 & 0 & \varphi_2 & 0 & 0 & 0 & 0 & i\varphi_3 \\
0 & \varphi_0 & 0 & 0 & \varphi_1 & 0 & 0 & 0 & 0 & 0 & 0 & -\varphi_2 & 0 & 0 & -i\varphi_3 & 0 \\
0 & 0 & \varphi_0 & 0 & 0 & 0 & 0 & \varphi_1 & \varphi_2 & 0 & 0 & 0 & 0 & i\varphi_3 & 0 & 0 \\
0 & 0 & 0 & \varphi_0 & 0 & 0 & \varphi_1 & 0 & 0 & -\varphi_2 & 0 & 0 & -i\varphi_3 & 0 & 0 & 0 \\
0 & -\varphi_1 & 0 & 0 & \varphi_0 & 0 & 0 & 0 & 0 & 0 & 0 & -i\varphi_3 & 0 & 0 & \varphi_2 & 0 \\
-\varphi_1 & 0 & 0 & 0 & 0 & \varphi_0 & 0 & 0 & 0 & 0 & i\varphi_3 & 0 & 0 & 0 & 0 & -\varphi_2 \\
0 & 0 & 0 & -\varphi_1 & 0 & 0 & \varphi_0 & 0 & 0 & -i\varphi_3 & 0 & 0 & \varphi_2 & 0 & 0 & 0 \\
0 & 0 & -\varphi_1 & 0 & 0 & 0 & 0 & \varphi_0 & i\varphi_3 & 0 & 0 & 0 & 0 & -\varphi_2 & 0 & 0 \\
0 & 0 & -\varphi_2 & 0 & 0 & 0 & 0 & i\varphi_3 & \varphi_0 & 0 & 0 & 0 & 0 & -\varphi_1 & 0 & 0 \\
0 & 0 & 0 & \varphi_2 & 0 & 0 & -i\varphi_3 & 0 & 0 & \varphi_0 & 0 & 0 & -\varphi_1 & 0 & 0 & 0 \\
-\varphi_2 & 0 & 0 & 0 & 0 & i\varphi_3 & 0 & 0 & 0 & 0 & \varphi_0 & 0 & 0 & 0 & 0 & -\varphi_1 \\
0 & \varphi_2 & 0 & 0 & -i\varphi_3 & 0 & 0 & 0 & 0 & 0 & 0 & \varphi_0 & 0 & 0 & -\varphi_1 & 0 \\
0 & 0 & 0 & -i\varphi_3 & 0 & 0 & -\varphi_2 & 0 & 0 & \varphi_1 & 0 & 0 & \varphi_0 & 0 & 0 & 0 \\
0 & 0 & i\varphi_3 & 0 & 0 & 0 & 0 & \varphi_2 & \varphi_1 & 0 & 0 & 0 & 0 & \varphi_0 & 0 & 0 \\
0 & -i\varphi_3 & 0 & 0 & -\varphi_2 & 0 & 0 & 0 & 0 & 0 & 0 & \varphi_1 & 0 & 0 & \varphi_0 & 0 \\
i\varphi_3 & 0 & 0 & 0 & 0 & \varphi_2 & 0 & 0 & 0 & 0 & \varphi_1 & 0 & 0 & 0 & 0 & \varphi_0
\end{pmatrix} \tag{6.22}$$

and

$$\overline{\Phi_{\text{PB}}^{16}} = \begin{pmatrix}
\varphi_0 & 0 & 0 & 0 & 0 & -\varphi_1 & 0 & 0 & 0 & 0 & -\varphi_2 & 0 & 0 & 0 & 0 & -i\varphi_3 \\
0 & \varphi_0 & 0 & 0 & -\varphi_1 & 0 & 0 & 0 & 0 & 0 & 0 & \varphi_2 & 0 & 0 & i\varphi_3 & 0 \\
0 & 0 & \varphi_0 & 0 & 0 & 0 & 0 & -\varphi_1 & -\varphi_2 & 0 & 0 & 0 & 0 & -i\varphi_3 & 0 & 0 \\
0 & 0 & 0 & \varphi_0 & 0 & 0 & -\varphi_1 & 0 & 0 & \varphi_2 & 0 & 0 & i\varphi_3 & 0 & 0 & 0 \\
0 & \varphi_1 & 0 & 0 & \varphi_0 & 0 & 0 & 0 & 0 & 0 & 0 & i\varphi_3 & 0 & 0 & -\varphi_2 & 0 \\
\varphi_1 & 0 & 0 & 0 & 0 & \varphi_0 & 0 & 0 & 0 & 0 & -i\varphi_3 & 0 & 0 & 0 & 0 & \varphi_2 \\
0 & 0 & 0 & \varphi_1 & 0 & 0 & \varphi_0 & 0 & 0 & i\varphi_3 & 0 & 0 & -\varphi_2 & 0 & 0 & 0 \\
0 & 0 & \varphi_1 & 0 & 0 & 0 & 0 & \varphi_0 & -i\varphi_3 & 0 & 0 & 0 & 0 & \varphi_2 & 0 & 0 \\
0 & 0 & \varphi_2 & 0 & 0 & 0 & 0 & -i\varphi_3 & \varphi_0 & 0 & 0 & 0 & 0 & \varphi_1 & 0 & 0 \\
0 & 0 & 0 & -\varphi_2 & 0 & 0 & i\varphi_3 & 0 & 0 & \varphi_0 & 0 & 0 & \varphi_1 & 0 & 0 & 0 \\
\varphi_2 & 0 & 0 & 0 & 0 & -i\varphi_3 & 0 & 0 & 0 & 0 & \varphi_0 & 0 & 0 & 0 & 0 & \varphi_1 \\
0 & -\varphi_2 & 0 & 0 & i\varphi_3 & 0 & 0 & 0 & 0 & 0 & 0 & \varphi_0 & 0 & 0 & \varphi_1 & 0 \\
0 & 0 & 0 & i\varphi_3 & 0 & 0 & \varphi_2 & 0 & 0 & -\varphi_1 & 0 & 0 & \varphi_0 & 0 & 0 & 0 \\
0 & 0 & -i\varphi_3 & 0 & 0 & 0 & 0 & -\varphi_2 & -\varphi_1 & 0 & 0 & 0 & 0 & \varphi_0 & 0 & 0 \\
0 & i\varphi_3 & 0 & 0 & \varphi_2 & 0 & 0 & 0 & 0 & 0 & 0 & -\varphi_1 & 0 & 0 & \varphi_0 & 0 \\
-i\varphi_3 & 0 & 0 & 0 & 0 & -\varphi_2 & 0 & 0 & 0 & 0 & -\varphi_1 & 0 & 0 & 0 & 0 & \varphi_0
\end{pmatrix} \tag{6.23}$$

6.5.1 Construction of the Lagrangian

For the free scalar field theory lagrangian density, we have,

$$\mathcal{L} = \frac{1}{16}\text{Tr}\left[\partial^\mu \overline{\Phi_{\text{PB}}^{16}}\, \partial_\mu \Phi_{\text{PB}}^{16} - m^2 \overline{\Phi_{\text{PB}}^{16}} \Phi_{\text{PB}}^{16}\right] \tag{6.24}$$

We can start with the kinect term,

$$\partial^\mu \overline{\Phi_{\text{PB}}^{16}}\, \partial_\mu \Phi_{\text{PB}}^{16} = \eta^{\mu\nu} \partial_\nu \overline{\Phi_{\text{PB}}^{16}}\, \partial_\mu \Phi_{\text{PB}}^{16} \tag{6.25}$$

where $\eta^{\mu\nu}$ is a diagonal matrix with,

$$\eta^{\mu\nu} = \begin{pmatrix} r & 0 & 0 & 0 \\ 0 & 1 & 0 & 0 \\ 0 & 0 & 1 & 0 \\ 0 & 0 & 0 & 1 \end{pmatrix}. \tag{6.26}$$

The parameter r is for an arbitrary metric signature, that is, Minkowskian or Euclidian. Then,

$$\eta^{\mu\nu}\, \partial_\mu \overline{\Phi_{\text{PB}}^{16}}\, \partial_\nu \Phi_{\text{PB}}^{16} = \eta^{00}\, \partial_0 \overline{\Phi_{\text{PB}}^{16}}\, \partial_0 \Phi_{\text{PB}}^{16} + \sum_{i=1}^{3} \eta^{ii}\, \partial_i \overline{\Phi_{\text{PB}}^{16}}\, \partial_i \Phi_{\text{PB}}^{16} \tag{6.27}$$

$$= r\partial_0 \overline{\Phi_{\text{PB}}^{16}}\, \partial_0 \Phi_{\text{PB}}^{16} + \partial_1 \overline{\Phi_{\text{PB}}^{16}}\, \partial_1 \Phi_{\text{PB}}^{16} + \partial_2 \overline{\Phi_{\text{PB}}^{16}}\, \partial_2 \Phi_{\text{PB}}^{16} + \partial_3 \overline{\Phi_{\text{PB}}^{16}}\, \partial_3 \Phi_{\text{PB}}^{16} \tag{6.28}$$

Then we have,

$$\begin{aligned}\frac{1}{16}\operatorname{Tr}\left[\partial^{\mu}\overline{\Phi^{16}_{\mathrm{PB}}}\,\partial_{\mu}\Phi^{16}_{\mathrm{PB}}\right] = r\Big[&\partial_0\varphi_0\,\partial_0\varphi_0+\partial_0\varphi_1\,\partial_0\varphi_1+\partial_0\varphi_2\,\partial_0\varphi_2+\partial_0\varphi_3\,\partial_0\varphi_3\Big]\\ &+\partial_1\varphi_0\,\partial_1\varphi_0+\partial_1\varphi_1\,\partial_1\varphi_1+\partial_1\varphi_2\,\partial_1\varphi_2+\partial_1\varphi_3\,\partial_1\varphi_3\\ &+\partial_2\varphi_0\,\partial_2\varphi_0+\partial_2\varphi_1\,\partial_2\varphi_1+\partial_2\varphi_2\,\partial_2\varphi_2+\partial_2\varphi_3\,\partial_2\varphi_3\\ &+\partial_3\varphi_0\,\partial_3\varphi_0+\partial_3\varphi_1\,\partial_3\varphi_1+\partial_3\varphi_2\,\partial_3\varphi_2+\partial_3\varphi_3\,\partial_3\varphi_3\end{aligned}\tag{6.29}$$

Mass term (auto interaction):

$$\frac{1}{16}\operatorname{Tr}\left[m^2\overline{\Phi^{16}_{\mathrm{PB}}}\Phi^{16}_{\mathrm{PB}}\right] = m^2(\varphi_0^2+\varphi_1^2+\varphi_2^2+\varphi_3^2).\tag{6.30}$$

Now, for a higher order interaction term, we have,

$$\begin{aligned}\frac{1}{16}\operatorname{Tr}\left[\lambda(\overline{\Phi^{16}_{\mathrm{PB}}}\Phi^{16}_{\mathrm{PB}})^2\right] = {}&\lambda\left(\varphi_0^4+\varphi_1^4+\varphi_2^4+\varphi_3^4\right)\\ &+2\lambda\left(\varphi_0^2\varphi_1^2+\varphi_0^2\varphi_2^2+\varphi_0^2\varphi_3^2\right)\\ &+6\lambda\left(\varphi_1^2\varphi_2^2+\varphi_1^2\varphi_3^2+\varphi_2^2\varphi_3^2\right)\end{aligned}\tag{6.31}$$

In the construction of the Lagrangian density for generalized quaternionic scalar field theories, a key distinction arises in the structure of the quartic interaction term. Specifically, the term $\varphi_i^2\varphi_j^2$, with $i,j=1,2,3$, takes different forms in the cases under consideration: the quaternionic bosonic scalar field and the quaternionic parabosonic scalar field. This divergence reflects the differing algebraic properties imposed by the underlying commutation or anticommutation relations, which directly influence the symmetrization of field products and, consequently, the permissible interaction terms in the theory. It is worth noting that the difference we identified in the quartic coupling term between the bosonic and parabosonic scalar field theories echoes similar effects found in the non-relativistic regime. In particular, Kuznetsova and Vasconcellos [82] investigated physical realizations of $\mathbb{Z}_2\times\mathbb{Z}_2$-graded algebras in quantum mechanical systems and showed that such gradings induce modifications in the interaction potential. Although their analysis was carried out in a non-relativistic context, the structural changes observed in the potential reflect the same underlying algebraic deformation of canonical statistics. Our result, which manifests as a correction to the quartic self-interaction of the Lagrangian density, may thus be viewed as a relativistic counterpart to these earlier findings.

6.5.2 Physical operators

As a fundamental premise, we assume that the physical operators, that is, operators associated with physically measurable quantities, are confined to sector 0. Initially, we consider the following operators Θ_i, for $i = 1, 2, 3$.

$$\Theta_i = :\gamma_i M_i \varphi_i :, \quad \text{for} \quad i = 1, 2, 3, \tag{6.32}$$

where γ_i is a constant. Using a standard field expansion, we have,

$$\Theta_i(x) = \gamma_i \mathbb{I}_4 : \int \frac{d^3k\ d^3p}{(2\pi)^3 2\sqrt{\omega_k\ \omega_p}} \left[a_i(k)e^{ik_\mu . x^\mu} + a_i^\dagger(k)e^{-ik_\mu . x^\mu}\right]\left[a_i(p)e^{ip_\mu . x^\mu} + a_i^\dagger(p)e^{-ip_\mu . x^\mu}\right] : \tag{6.33}$$

In the end of the day we have,

$$\begin{aligned}\Theta_i(x) = \gamma_i \mathbb{I}_4 \int \frac{d^3k\ d^3p}{(2\pi)^3 2\sqrt{\omega_k\ \omega_p}} \Bigg[& a_i(k)a_i(p)e^{i(k+p).x} - \epsilon\ a_i(p)a_i^\dagger(k)e^{i(k-p).x} \\ & + a_i^\dagger(k)a_i(p)e^{-i(k-p).x} + a_i^\dagger(k)a_i^\dagger(p)e^{-i(k+p).x} \\ & + \delta^3(k-p)e^{i(k-p)x} \Bigg].\end{aligned} \tag{6.34}$$

It is possible to construct mixed operators, involving components from different sectors, such that the resulting operator resides in sector 0.

Expansion of the Operator $\Omega_{ijk}(x)$

Definitions

Let $\varphi_r(x)$ be real scalar fields, with momentum-space expansion:

$$\varphi_r(x) = \int \frac{d^3p_r}{(2\pi)^3\sqrt{2\omega_{p_r}}} \left[a_r(p_r)\, e^{-ip_r \cdot x} + a_r^\dagger(p_r)\, e^{+ip_r \cdot x}\right], \tag{6.35}$$

where $r = i, j, k$.

The operator $\Omega_{ijk}(x)$ is defined as:

$$\Omega_{ijk}(x) = \alpha \left(M_i M_j M_k + (-1)^{\eta(i,j,k)} M_k M_j M_i\right) : [\varphi_i(x)\, \varphi_j(x)\, \varphi_k(x)] :, \tag{6.36}$$

where $\eta(i, j, k)$ is defined via the $\mathbb{Z}_2^2$-graded structure below.

Graded Algebra: $\mathbb{Z}_2^2$-Lie Color Algebra

Each operator a_r or $a_r^\dagger$ carries a degree $\vec{\alpha}_r \in \mathbb{Z}_2^2$.

The graded sign function is:

$$\varepsilon(\vec{\alpha}_r, \vec{\alpha}_s) = \vec{\alpha}_r \cdot \vec{\alpha}_s \mod 2, \tag{6.37}$$

and the symmetry factor for the matrix term is:

$$\eta(i,j,k) = \varepsilon(k,j) + \varepsilon(j,i) + \varepsilon(k,i) \mod 2. \tag{6.38}$$

Graded commutation relations:

$$a_r a_s = (-1)^{\varepsilon(r,s)} a_s a_r, \quad a_r a_s^\dagger = (-1)^{\varepsilon(r,s)} a_s^\dagger a_r. \tag{6.39}$$

Full Expansion Before Normal Ordering

We expand all combinations from the product:

$$:[\varphi_i(x)\, \varphi_j(x)\, \varphi_k(x)]: \tag{6.40}$$

Each field contributes two terms, yielding 8 terms from $\varphi_i\varphi_j\varphi_k$ and 8 from $\varphi_k\varphi_j\varphi_i$. Explicitly:

$$\begin{aligned}\Omega_{ijk}(x) = \alpha \left(M_i M_j M_k + (-1)^{\eta(i,j,k)} M_k M_j M_i\right) \int \frac{d^3p_i}{(2\pi)^3\sqrt{2\omega_{p_i}}} \frac{d^3p_j}{(2\pi)^3\sqrt{2\omega_{p_j}}} \frac{d^3p_k}{(2\pi)^3\sqrt{2\omega_{p_k}}} \\ \times \Big\{ a_i(p_i)a_j(p_j)a_k(p_k)\, e^{-i(p_i+p_j+p_k)\cdot x} \\ + a_i(p_i)a_j(p_j)a_k^\dagger(p_k)\, e^{-i(p_i+p_j-p_k)\cdot x} \\ + a_i(p_i)a_j^\dagger(p_j)a_k(p_k)\, e^{-i(p_i-p_j+p_k)\cdot x} \\ + a_i(p_i)a_j^\dagger(p_j)a_k^\dagger(p_k)\, e^{-i(p_i-p_j-p_k)\cdot x} \\ + a_i^\dagger(p_i)a_j(p_j)a_k(p_k)\, e^{+i(p_i-p_j-p_k)\cdot x} \\ + a_i^\dagger(p_i)a_j(p_j)a_k^\dagger(p_k)\, e^{+i(p_i-p_j+p_k)\cdot x} \\ + a_i^\dagger(p_i)a_j^\dagger(p_j)a_k(p_k)\, e^{+i(p_i+p_j-p_k)\cdot x} \\ + a_i^\dagger(p_i)a_j^\dagger(p_j)a_k^\dagger(p_k)\, e^{+i(p_i+p_j+p_k)\cdot x} \\ + a_k(p_k)a_j(p_j)a_i(p_i)\, e^{-i(p_k+p_j+p_i)\cdot x} \\ + a_k(p_k)a_j(p_j)a_i^\dagger(p_i)\, e^{-i(p_k+p_j-p_i)\cdot x} \\ + a_k(p_k)a_j^\dagger(p_j)a_i(p_i)\, e^{-i(p_k-p_j+p_i)\cdot x} \\ + a_k(p_k)a_j^\dagger(p_j)a_i^\dagger(p_i)\, e^{-i(p_k-p_j-p_i)\cdot x} \\ + a_k^\dagger(p_k)a_j(p_j)a_i(p_i)\, e^{+i(p_k-p_j-p_i)\cdot x} \\ + a_k^\dagger(p_k)a_j(p_j)a_i^\dagger(p_i)\, e^{+i(p_k-p_j+p_i)\cdot x} \\ + a_k^\dagger(p_k)a_j^\dagger(p_j)a_i(p_i)\, e^{+i(p_k+p_j-p_i)\cdot x} \\ + a_k^\dagger(p_k)a_j^\dagger(p_j)a_i^\dagger(p_i)\, e^{+i(p_k+p_j+p_i)\cdot x} \Big\}\end{aligned} \tag{6.41}$$

After Normal Ordering

Applying the $\mathbb{Z}_2^n$-graded normal ordering and sign conventions:

$$\begin{aligned}\Omega_{ijk}(x) = \alpha \left(M_i M_j M_k + (-1)^{\eta(i,j,k)} M_k M_j M_i\right) \int \frac{d^3p_i\, d^3p_j\, d^3p_k}{(2\pi)^9 \sqrt{8\omega_{p_i}\omega_{p_j}\omega_{p_k}}} \\ \times \Big[+ a_i(p_i)\, a_j(p_j)\, a_k(p_k)\, e^{-i(p_i+p_j+p_k)\cdot x} \\ + (-1)^{\varepsilon(j,k)+\varepsilon(i,k)} a_k^\dagger(p_k)\, a_i(p_i)\, a_j(p_j)\, e^{-i(p_i+p_j-p_k)\cdot x} \\ + (-1)^{\varepsilon(i,j)} a_j^\dagger(p_j)\, a_i(p_i)\, a_k(p_k)\, e^{-i(p_i-p_j+p_k)\cdot x} \\ + (-1)^{\varepsilon(i,j)+\varepsilon(i,k)} a_j^\dagger(p_j)\, a_k^\dagger(p_k)\, a_i(p_i)\, e^{-i(p_i-p_j-p_k)\cdot x} \\ + a_i^\dagger(p_i)\, a_j(p_j)\, a_k(p_k)\, e^{+i(p_i-p_j-p_k)\cdot x} \\ + (-1)^{\varepsilon(j,k)} a_i^\dagger(p_i)\, a_k^\dagger(p_k)\, a_j(p_j)\, e^{+i(p_i-p_j+p_k)\cdot x} \\ + (-1)^{\varepsilon(i,k)} a_i^\dagger(p_i)\, a_j^\dagger(p_j)\, a_k(p_k)\, e^{+i(p_i+p_j-p_k)\cdot x} \\ + (-1)^{\varepsilon(i,k)+\varepsilon(j,k)} a_i^\dagger(p_i)\, a_j^\dagger(p_j)\, a_k^\dagger(p_k)\, e^{+i(p_i+p_j+p_k)\cdot x} \Big]\end{aligned} \tag{6.42}$$

Example

Specifically, for $(i, j, k) = (1, 2, 3)$ and $(2, 3, 1)$, we compute:

Operator $\Omega_{123}(x)$:

$$\begin{aligned}\Omega_{123}(x) = \alpha(M_1M_2M_3 + M_3M_2M_1) \int \frac{d^3p_1\, d^3p_2\, d^3p_3}{(2\pi)^9 \sqrt{8\omega_{p_1}\omega_{p_2}\omega_{p_3}}} \times \Big[\\ + a_1a_2a_3\, e^{-i(p_1+p_2+p_3)\cdot x} \\ - a_3^\dagger a_1 a_2\, e^{-i(p_1+p_2-p_3)\cdot x} \\ + a_2^\dagger a_1 a_3\, e^{-i(p_1-p_2+p_3)\cdot x} \\ - a_2^\dagger a_3^\dagger a_1\, e^{-i(p_1-p_2-p_3)\cdot x} \\ + a_1^\dagger a_2 a_3\, e^{+i(p_1-p_2-p_3)\cdot x} \\ - a_1^\dagger a_3^\dagger a_2\, e^{+i(p_1-p_2+p_3)\cdot x} \\ - a_1^\dagger a_2^\dagger a_3\, e^{+i(p_1+p_2-p_3)\cdot x} \\ + a_1^\dagger a_2^\dagger a_3^\dagger\, e^{+i(p_1+p_2+p_3)\cdot x} \Big]\end{aligned} \tag{6.43}$$

Operator $\Omega_{231}(x)$:

$$\begin{aligned}\Omega_{231}(x) = \alpha(M_2M_3M_1 + M_1M_3M_2)\int \frac{d^3p_2\, d^3p_3\, d^3p_1}{(2\pi)^9\sqrt{8\omega_{p_2}\omega_{p_3}\omega_{p_1}}} \times \Big[& \\ + \; a_2a_3a_1\, e^{-i(p_2+p_3+p_1)\cdot x} & \\ - \; a_1^\dagger a_2a_3\, e^{-i(p_2+p_3-p_1)\cdot x} & \\ + \; a_3^\dagger a_2a_1\, e^{-i(p_2-p_3+p_1)\cdot x} & \\ - \; a_3^\dagger a_1^\dagger a_2\, e^{-i(p_2-p_3-p_1)\cdot x} & \\ + \; a_2^\dagger a_3a_1\, e^{+i(p_2-p_3-p_1)\cdot x} & \\ - \; a_2^\dagger a_1^\dagger a_3\, e^{+i(p_2-p_3+p_1)\cdot x} & \\ + \; a_2^\dagger a_3^\dagger a_1\, e^{+i(p_2+p_3-p_1)\cdot x} & \\ + \; a_2^\dagger a_3^\dagger a_1^\dagger\, e^{+i(p_2+p_3+p_1)\cdot x}\Big] &\end{aligned}$$

Commutator Structure

Each Ω has 8 terms, leading to $8 \times 8 = 64$ pairwise combinations:

$$[\Omega_{123}(x), \Omega_{231}(y)] = \sum_{i=1}^{8}\sum_{j=1}^{8}\left[\mathcal{T}_i(x), \mathcal{T}_j'(y)\right] \tag{6.44}$$

where we have,

$$\begin{aligned}&\textbf{Terms from } \Omega_{123}(x): \\ &\qquad \mathcal{T}_1(x) = a_1a_2a_3\, e^{-i(p_1+p_2+p_3)\cdot x} \\ &\qquad \mathcal{T}_2(x) = -a_3^\dagger a_1a_2\, e^{-i(p_1+p_2-p_3)\cdot x} \\ &\qquad \mathcal{T}_3(x) = +a_2^\dagger a_1a_3\, e^{-i(p_1-p_2+p_3)\cdot x} \\ &\qquad \mathcal{T}_4(x) = -a_2^\dagger a_3^\dagger a_1\, e^{-i(p_1-p_2-p_3)\cdot x} \\ &\qquad \mathcal{T}_5(x) = +a_1^\dagger a_2a_3\, e^{+i(p_1-p_2-p_3)\cdot x} \\ &\qquad \mathcal{T}_6(x) = -a_1^\dagger a_3^\dagger a_2\, e^{+i(p_1-p_2+p_3)\cdot x} \\ &\qquad \mathcal{T}_7(x) = -a_1^\dagger a_2^\dagger a_3\, e^{+i(p_1+p_2-p_3)\cdot x} \\ &\qquad \mathcal{T}_8(x) = +a_1^\dagger a_2^\dagger a_3^\dagger\, e^{+i(p_1+p_2+p_3)\cdot x}\end{aligned} \tag{6.45}$$

Terms from $\Omega_{231}(y)$:

$$\begin{aligned}
\mathcal{T}_1'(y) &= a_2 a_3 a_1 \, e^{-i(q_2+q_3+q_1)\cdot y} \\
\mathcal{T}_2'(y) &= -a_1^\dagger a_2 a_3 \, e^{-i(q_2+q_3-q_1)\cdot y} \\
\mathcal{T}_3'(y) &= +a_3^\dagger a_2 a_1 \, e^{-i(q_2-q_3+q_1)\cdot y} \\
\mathcal{T}_4'(y) &= -a_3^\dagger a_1^\dagger a_2 \, e^{-i(q_2-q_3-q_1)\cdot y} \\
\mathcal{T}_5'(y) &= +a_2^\dagger a_3 a_1 \, e^{+i(q_2-q_3-q_1)\cdot y} \\
\mathcal{T}_6'(y) &= -a_2^\dagger a_1^\dagger a_3 \, e^{+i(q_2-q_3+q_1)\cdot y} \\
\mathcal{T}_7'(y) &= +a_2^\dagger a_3^\dagger a_1 \, e^{+i(q_2+q_3-q_1)\cdot y} \\
\mathcal{T}_8'(y) &= +a_2^\dagger a_3^\dagger a_1^\dagger \, e^{+i(q_2+q_3+q_1)\cdot y}
\end{aligned}$$

The only non-vanishing contributions come from combinations where:

$$[a_r(p), a_r^\dagger(q)] = (2\pi)^3 \delta^3(\vec{p} - \vec{q}) \tag{6.46}$$

We compute representative terms from:

$$[a_1 a_2 a_3, a_1^\dagger a_2^\dagger a_3^\dagger] \tag{6.47}$$

This yields:

$$[\Omega_{123}(x), \Omega_{231}(y)] \supset \int \frac{d^3p_1\, d^3p_2\, d^3p_3}{4096\,\pi^9\,\omega_1\omega_2\omega_3} \Big[\delta^3(\vec{p}_1 - \vec{q}_1) + \delta^3(\vec{p}_2 - \vec{q}_2) + \delta^3(\vec{p}_3 - \vec{q}_3) \Big] \cdot e^{-i(p_1+p_2+p_3)\cdot x} e^{+i(q_1+q_2+q_3)\cdot y} \tag{6.48}$$

After integrating over the delta functions, these terms reconstruct the Pauli–Jordan commutator function:

$$\Delta(x-y) = \int \frac{d^3p}{(2\pi)^3\, 2\omega_p} \left(e^{-ip\cdot(x-y)} - e^{+ip\cdot(x-y)} \right) \tag{6.49}$$

Conclusion: Microcausality

The full commutator between the operators $\Omega_{ijk}(x)$ and $\Omega_{lmn}(y)$ vanishes for spacelike separations:

$$(x-y)^2 < 0 \quad \Rightarrow \quad \Delta(x-y) = 0 \tag{6.50}$$

Thus, we conclude:

$$\boxed{[\Omega_{ijk}(x), \Omega_{lmn}(y)] = 0 \quad \text{for } (x-y)^2 < 0} \tag{6.51}$$

This confirms that the generalized operators $\Omega_{ijk}(x)$ constructed with $\mathbb{Z}_2^2$-graded parastatistics satisfy the fundamental requirement of microcausality in relativistic quantum field theory. It is worth emphasizing that most scientific works concerning paraparticles, or particles beyond the standard fermion and boson categories, have focused on them as emergent excitations in effective theories. One of the guiding questions in this thesis, however, has been to challenge that paradigm: could such particles, characterized by generalized statistics, exist as fundamental constituents of matter?

7 Conclusion and Future Work

This thesis has explored the algebraic and physical implications of $\mathbb{Z}_2^n$-graded Lie (super)algebras, demonstrating their role in classifying inequivalent quantum symmetries, statistical transmutations, and parastatistics. Using a Boolean logic framework, we systematically classified all possible graded brackets through mappings $\mathbb{Z}_2^n \times \mathbb{Z}_2^n \to \mathbb{Z}_2$, obtaining a total of

$$b_n = n + \lfloor n/2 \rfloor + 1$$

inequivalent algebraic structures. These graded brackets provide a rigorous and systematic approach to describing multiparticle quantum systems with exotic statistics, extending beyond the conventional Bose-Fermi dichotomy.

The construction of $\mathbb{Z}_2^n$-graded quantum Hamiltonians has revealed fundamental physical consequences of these algebraic structures, leading to inequivalent multiparticle quantizations. The different graded brackets induce distinct types of parastatistics, where particles can behave as bosons, fermions, parabosons, or parafermions depending on the underlying algebraic structure. These parastatistics are not merely abstract mathematical constructs but are physically distinguishable through specific observables, as shown in our analysis of statistical transmutations. In particular, in supersymmetric and superconformal quantum mechanics, inequivalent graded Lie (super)algebras correspond to alternative formulations of $\mathcal{N}$-extended systems, where the assignment of parastatistical properties to supercharges leads to observable modifications in the spectrum. This was explicitly demonstrated in the $\mathcal{N} = 2$ superconformal model with an $sl(2|1)$ spectrum-generating algebra, where the $\mathbb{Z}_2^2$-graded parastatistics introduce an energy level degeneracy pattern that cannot be realized within standard bosonic or fermionic statistics.

Beyond quantum mechanics, the implications of $\mathbb{Z}_2^n$-graded algebras extend to quantum field theory, where generalized statistics and higher-dimensional supersymmetry could be naturally incorporated into interacting field-theoretic models. The Boolean representation of graded brackets provides an additional computational advantage, offering a structured method for encoding algebraic structures in digital logic circuits. This approach has potential applications not only in theoretical physics but also in quantum computing and information science, where the manipulation of graded symmetries could play a role in quantum algorithms and error correction.

While this work has established a comprehensive classification of Z_2^n-graded Lie (super)algebras and their physical applications, several open problems remain. A major challenge is identifying physical systems where these inequivalent parastatistics can be experimentally observed, possibly in condensed matter systems, optical lattices, or quantum simulations. Extending this algebraic framework to quantum field theory, particularly in the context of non-perturbative effects in supersymmetric models, remains an important direction for future research. Additionally, exploring the potential relevance of higher-dimensional graded structures in theories such as string theory or M-theory could provide new insights into the mathematical formulation of fundamental interactions. Furthermore, the Boolean representation of graded brackets suggests intriguing connections to quantum computing, where graded symmetries might offer novel computational frameworks or improvements in quantum error correction techniques.

As demonstrated in the final chapter on quantum field theory, a distinct difference arises in the structure of the quartic interaction term when comparing conventional bosonic theories to their parabosonic analogues. This distinction reflects the nontrivial impact of generalized statistics on the formulation of interacting field theories. Moreover, as an illustrative case, we have shown that a composite operator constructed from parabosonic scalar fields respects the condition of microcausality, thereby upholding one of the foundational principles of relativistic quantum field theory. It is important to note that existing investigations into paraparticles — entities obeying statistics beyond the standard fermionic and bosonic classifications — have predominantly interpreted them as emergent excitations within effective low-energy theories. In contrast, one of the central questions posed by this thesis is whether such exotic statistical behaviors might instead signal the existence of truly fundamental degrees of freedom in nature, beyond the conventional paradigm of quantum field theory.

The results presented in this thesis contribute to the broader understanding of graded symmetries and their role in fundamental physics, establishing a solid algebraic foundation for the study of exotic quantum statistics. By bridging abstract mathematical formalism with concrete physical applications, this work paves the way for future research in quantum symmetries, parastatistics, and their potential experimental realization.

References

[1] V. G. Kac. Lie superalgebras. *Advances in Mathematics*, 26(1):8–96, 1977. ISSN 0001-8708. doi: https://doi.org/10.1016/0001-8708(77)90017-2. URL https://www.sciencedirect.com/science/article/pii/0001870877900172.

[2] W. Nahm. Supersymmetries and their representations. *Nuclear Physics B*, 135(1):149–166, 1978. ISSN 0550-3213. doi: https://doi.org/10.1016/0550-3213(78)90218-3. URL https://www.sciencedirect.com/science/article/pii/0550321378902183.

[3] J. W. van Holten and A. van Proeyen. $\mathcal{N} = 1$ supersymmetry algebras in $d = 2, 3, 4$ mod 8. *Journal of Physics A: Mathematical and General*, 15(12):3763, Dec 1982. doi: 10.1088/0305-4470/15/12/028. URL https://dx.doi.org/10.1088/0305-4470/15/12/028.

[4] M. A. Vasiliev. Extended higher spin superalgebras and their realizations in terms of quantum operators. *Fortsch. Phys.*, 36:33–62, 1988.

[5] V. Rittenberg and D. Wyler. Generalized superalgebras. *Nuclear Physics B*, 139(3):189–202, 1978. ISSN 0550-3213. doi: https://doi.org/10.1016/0550-3213(78)90186-4. URL https://www.sciencedirect.com/science/article/pii/0550321378901864.

[6] V. Rittenberg and D. Wyler. Sequences of $\mathbb{Z}_2 \otimes \mathbb{Z}_2$ graded Lie algebras and superalgebras. *Journal of Mathematical Physics*, 19(10):2193–2200, 1978.

[7] M. Scheunert. Generalized Lie algebras. *Journal of Mathematical Physics*, 20(4): 712–720, 1979.

[8] S. Silvestrov. On the classification of 3-dimensional coloured Lie algebras. *Banach Center Publications*, 40(1):159–170, 1997. URL http://eudml.org/doc/252193.

[9] M. Marcu. The representations of spl(2,1)—an example of representations of basic superalgebras. *Journal of Mathematical Physics*, 21(6):1277–1283, 06 1980. ISSN 0022-2488. doi: 10.1063/1.524576. URL https://doi.org/10.1063/1.524576.

[10] Y. Su, K. Zhao, and L. Zhu. Classification of derivation-simple color algebras related to locally finite derivations. *Journal of Mathematical Physics*, 45(1):525–536, 01 2004. ISSN 0022-2488. doi: 10.1063/1.1628837. URL https://doi.org/10.1063/1.1628837.

[11] X.-W. Chen, S. D. Silvestrov, and F. Van Oystaeyen. Representations and Cocycle Twists of Color Lie Algebras. *Algebras and Representation Theory*, 2006.

[12] R. Campoamor-Stursberg and M. Rausch de Traubenberg. Color Lie algebras and Lie algebras of order F. *Journal of Generalized Lie Theory and Applications*, 3(2):113–130, 2009. doi: 10.4303/jglta/S090203. URL https://doi.org/10.4303/jglta/S090203.

[13] N. Aizawa, P. S. Isaac, and J. Segar. $\mathbb{Z}_2\times\mathbb{Z}_2$-Generalizations of Infinite-Dimensional Lie Superalgebra of Conformal Type with Complete Classification of Central Extensions. *Reports on Mathematical Physics*, 85(3):351–373, 2020. ISSN 0034-4877. doi: https://doi.org/10.1016/S0034-4877(20)30041-0. URL https://www.sciencedirect.com/science/article/pii/S0034487720300410.

[14] P. S. Isaac, N. I. Stoilova, and J. Van der Jeugt. The $\mathbb{Z}_2 \times \mathbb{Z}_2$-graded general linear Lie superalgebra. *Journal of Mathematical Physics*, 61(1):011702, 01 2020. ISSN 0022-2488. doi: 10.1063/1.5138597. URL https://doi.org/10.1063/1.5138597.

[15] Z. Kuznetsova and F. Toppan. Classification of minimal $\mathbb{Z}_2\times \mathbb{Z}_2$ -graded Lie (super)algebras and some applications. *Journal of Mathematical Physics*, 62(6):063512, 06 2021. ISSN 0022-2488. doi: 10.1063/5.0050200. URL https://doi.org/10.1063/5.0050200.

[16] Z. Kuznetsova and F. Toppan. Beyond the 10-fold Way: 13 Associative $\mathbb{Z}_2\times \mathbb{Z}_2$ -Graded Superdivision Algebras. *Advances in Applied Clifford Algebras*, 33(24), 2023.

[17] N. I. Stoilova and J. Van der Jeugt. On classical $\mathbb{Z}_2 \times \mathbb{Z}_2$-graded Lie algebras. *Journal of Mathematical Physics*, 64(6), 2023.

[18] N. Aizawa, Z. Kuznetsova, H. Tanaka, and F. Toppan. Generalized supersymmetry and Lévy-Leblond equation. *In: Duarte, S., Gazeau, JP., Faci, S., Micklitz, T., Scherer, R., Toppan, F. (eds), Physical and Mathematical Aspects of Symmetries, Springer, Cham*, page 79, 2017.

[19] N. Aizawa, Z. Kuznetsova, H. Tanaka, and F. Toppan. $\mathbb{Z}_2\times \mathbb{Z}_2$-graded Lie symmetries of the Lévy-Leblond equations. *Progress of Theoretical and Experimental Physics*, 2016(12):123A01, Dec 2016. doi: 10.1093/ptep/ptw176. URL https://doi.org/10.1093/ptep/ptw176.

[20] L. Miranda, I. P. De Freitas, and F. Toppan. On the Classification of the Lévy-Leblond Spinors. *Journal of Physics: Conference Series*, 2912(1):012034, Dec 2024. doi: 10.1088/1742-6596/2912/1/012034. URL https://dx.doi.org/10.1088/1742-6596/2912/1/012034.

[21] N. Aizawa, Z. Kuznetsova, and F. Toppan. $\mathbb{Z}_2\times\mathbb{Z}_2$-graded mechanics: the classical theory. *Eur. J. Phys. C*, 80(668), 2020.

[22] A. J. Bruce. $\mathbb{Z}_2 \times \mathbb{Z}_2$-graded supersymmetry: 2-d sigma models. *Journal of Physics A: Mathematical and Theoretical*, 53(45):455201, Oct 2020. doi: 10.1088/1751-8121/abb47f. URL https://dx.doi.org/10.1088/1751-8121/abb47f.

[23] A. J. Bruce and S. Duplij. Double-graded supersymmetric quantum mechanics. *Journal of Mathematical Physics*, 61(6):063503, 06 2020. ISSN 0022-2488. doi: 10.1063/1.5118302. URL https://doi.org/10.1063/1.5118302.

[24] N. Aizawa, Z. Kuznetsova, and F. Toppan. $\mathbb{Z}_2 \times \mathbb{Z}_2$-graded mechanics: The quantization. *Nuclear Physics B*, 967:115426, 2021. ISSN 0550-3213. doi: https://doi.org/10.1016/j.nuclphysb.2021.115426. URL https://www.sciencedirect.com/science/article/pii/S0550321321001231.

[25] F. Toppan. First quantization of braided Majorana fermions. *Nuclear Physics B*, 980:115834, 2022. ISSN 0550-3213. doi: https://doi.org/10.101/nuclphysb.2022.115834. URL https://www.sciencedirect.com/science/article/pii/S0550321322001857.

[26] A. J. Bruce. Is the $\mathbb{Z}_2 \times \mathbb{Z}_2$-graded sine-Gordon equation integrable? *Nuclear Physics B*, 971:115514, 2021.

[27] A. J. Bruce and S. Duplij. Double-Graded Quantum Superplane. *Reports on Mathematical Physics*, 86(3):383–400, 2020. ISSN 0034-4877. doi: https://doi.org/10.1016/S0034-4877(20)30089-6. URL https://www.sciencedirect.com/science/article/pii/S0034487720300896.

[28] S. Doi and N. Aizawa. Comments of $\mathbb{Z}_2^2$-supersymmetry in superfield formalism. *Nuclear Physics B*, 974:115641, 2022. ISSN 0550-3213. doi: https://doi.org/10.1016/j.nuclphysb.2021.115641. URL https://www.sciencedirect.com/science/article/pii/S0550321321003382.

[29] N. Aizawa, R. Ito, Z. Kuznetsova, and F. Toppan. New aspects of the $\mathbb{Z}_2 \times \mathbb{Z}_2$-graded $1D$ superspace: Induced strings and $2D$ relativistic models. *Nuclear Physics B*, 991:116202, 2023. ISSN 0550-3213. doi: https://doi.org/10.1016/j.nuclphysb.2023.116202. URL https://www.sciencedirect.com/science/article/pii/S0550321323001311.

[30] N. Aizawa and R. Ito. Integration on minimal $\mathbb{Z}_2^2$-superspace and emergence of space. *Journal of Physics A: Mathematical and Theoretical*, 56(48):485201, Nov 2023. doi: 10.1088/1751-8121/ad076e. URL https://dx.doi.org/10.1088/1751-8121/ad076e.

[31] N. Aizawa, R. Ito, and T. Tanaka. $\mathbb{Z}_2^2$-graded supersymmetry via superfield on minimal $\mathbb{Z}_2^2$-superspace. *Journal of Physics A: Mathematical and Theoretical*, 57(43):

435201, Oct 2024. doi: 10.1088/1751-8121/ad811a. URL https://dx.doi.org/10.1088/1751-8121/ad811a.

[32] N. Aizawa, R. Ito, Z. Kuznetsova, T. Tanaka, and F. Toppan. Integrable $\mathbb{Z}_2^2$-graded extensions of the Liouville and Sinh–Gordon theories. *Journal of Physics A: Mathematical and Theoretical*, 58(5):055201, Jan 2025. doi: 10.1088/1751-8121/adaab3. URL https://dx.doi.org/10.1088/1751-8121/adaab3.

[33] T. Covolo, S. Kwok, and N. Poncin. Differential calculus on $\mathbb{Z}_2^n$-supermanifolds, 2016. URL https://arxiv.org/abs/1608.00949.

[34] A. J. Bruce and J. Grabowski. Riemannian Structures on $\mathbb{Z}_2^n$-Manifolds. *Mathematics*, 8(9), 2020. ISSN 2227-7390. doi: 10.3390/math8091469. URL https://www.mdpi.com/2227-7390/8/9/1469.

[35] A. J. Bruce and J. Grabowski. Symplectic $\mathbb{Z}_2^n$-manifolds. *Journal of Geometric Mechanics*, 13(3):285–311, 2021. ISSN 1941-4889. doi: 10.3934/jgm.2021020. URL https://www.aimsciences.org/article/id/872e92c6-5dec-4f8c-b021-1496d322cf1a.

[36] R. Lu and Y. Tan. Construction of color Lie algebras from homomorphisms of modules of Lie algebras. *Journal of Algebra*, 620:1–49, 2023. ISSN 0021-8693. doi: https://doi.org/10.1016/j.jalgebra.2022.12.028. URL https://www.sciencedirect.com/science/article/pii/S0021869322006081.

[37] S. Doi and N. Aizawa. $\mathbb{Z}_2^3$-Graded Extensions of Lie Superalgebras and Superconformal Quantum Mechanics. *Symmetry, Integrability and Geometry: Methods and Applications*, Jul 2021. ISSN 1815-0659. doi: 10.3842/sigma.2021.071. URL http://dx.doi.org/10.3842/SIGMA.2021.071.

[38] N. Aizawa, K. Amakawa, and S. Doi. $\mathbb{Z}_2^n$-graded extensions of supersymmetric quantum mechanics via Clifford algebras. *Journal of Mathematical Physics*, 61(5):052105, 05 2020. doi: 10.1063/1.5144325. URL https://doi.org/10.1063/1.5144325.

[39] F. Toppan. Inequivalent quantizations from gradings and $\mathbb{Z}_2\times\mathbb{Z}_2$ parabosons. *Journal of Physics A: Mathematical and Theoretical*, 54(35):355202, Aug 2021. doi: 10.1088/1751-8121/ac17a5. URL https://dx.doi.org/10.1088/1751-8121/ac17a5.

[40] F. Toppan. $\mathbb{Z}_2\times\mathbb{Z}_2$-graded parastatistics in multiparticle quantum Hamiltonians. *Journal of Physics A: Mathematical and Theoretical*, 54(11):115203, Feb 2021. doi: 10.1088/1751-8121/abe2f2. URL https://dx.doi.org/10.1088/1751-8121/abe2f2.

[41] W. Yang and S. Jing. A new kind of graded Lie algebra and parastatistical supersymmetry. *Sci. China Ser. A-Math*, 44:1167–1173, 2021.

[42] V. N. Tolstoy. Once more on parastatistics. *Phys. Part. Nuclei Lett*, 11:933–937, 2014. doi: https://doi.org/10.1134/S1547477114070449.

[43] N. I. Stoilova and J. Van der Jeugt. The $\mathbb{Z}_2 \times \mathbb{Z}_2$-graded Lie superalgebra $\mathfrak{pso}(2m+1|2n)$ and new parastatistics representations. *Journal of Physics A: Mathematical and Theoretical*, 51(13):135201, Feb 2018. doi: 10.1088/1751-8121/aaae9a. URL https://dx.doi.org/10.1088/1751-8121/aaae9a.

[44] N. I. Stoilova and J. Van der Jeugt. The $\mathbb{Z}_2 \times \mathbb{Z}_2$-graded Lie superalgebras $\mathfrak{pso}(2n+1|2n)$ and $\mathfrak{pso}(\infty|\infty)$, and parastatistics Fock spaces. *Journal of Physics A: Mathematical and Theoretical*, 55(4):045201, Jan 2022. doi: 10.1088/1751-8121/ac451d. URL https://dx.doi.org/10.1088/1751-8121/ac451d.

[45] M. M. Balbino, I. P. de Freitas, R. G. Rana, and F. Toppan. Inequivalent $\mathbb{Z}_2^n$-graded brackets, n-bit parastatistics and statistical transmutations of supersymmetric quantum mechanics. *Nuclear Physics B*, 1009:116729, 2024. ISSN 0550-3213. doi: https://doi.org/10.1016/j.nuclphysb.2024.116729. URL https://www.sciencedirect.com/science/article/pii/S0550321324002955.

[46] F. Toppan. Transmuted spectrum-generating algebras and detectable parastatistics of the Superconformal Quantum Mechanics. *Journal of Physics: Conference Series*, 2667(1):012014, Dec 2023. doi: 10.1088/1742-6596/2667/1/012014. URL https://dx.doi.org/10.1088/1742-6596/2667/1/012014.

[47] F. Toppan. On the detectability of paraparticles beyond bosons and fermions, 2024. URL https://arxiv.org/abs/2411.18313.

[48] M. Karnaugh. The map method for synthesis of combinational logic circuits. *Transactions of the American Institute of Electrical Engineers, Part I: Communication and Electronics*, 72(5):593–599, 1953. doi: 10.1109/TCE.1953.6371932.

[49] V. de Alfaro, S. Fubini, and G. Furlan. Conformal Invariance in Quantum Mechanics. *Nuovo Cim. A*, 34:569, 1976. doi: 10.1007/BF02785666.

[50] E. Witten. Constraints on supersymmetry breaking. *Nuclear Physics B*, 202(2):253–316, 1982. ISSN 0550-3213. doi: https://doi.org/10.1016/0550-3213(82)90071-2. URL https://www.sciencedirect.com/science/article/pii/0550321382900712.

[51] E. C. Marino. *Quantum field theory approach to condensed matter physics*. Cambridge University Press, 2017.

[52] A. J. Bruce and S. Duplij. Double-graded supersymmetric quantum mechanics. *Journal of Mathematical Physics*, 61(6):063503, 06 2020. doi: 10.1063/1.5118302. URL https://doi.org/10.1063/1.5118302.

[53] A. Pashnev and F. Toppan. On the classification of N-extended supersymmetric quantum mechanical systems. *Journal of Mathematical Physics*, 42(11):5257–5271, 11 2001. doi: 10.1063/1.1409349. URL https://doi.org/10.1063/1.1409349.

[54] Z. Kuznetsova, M. Rojas, and F. Toppan. Classification of irreps and invariants of the N-extended Supersymmetric Quantum Mechanics. *Journal of High Energy Physics*, 2006(03):098, Mar 2006. doi: 10.1088/1126-6708/2006/03/098. URL https://dx.doi.org/10.1088/1126-6708/2006/03/098.

[55] I. E. Cunha, N. L. Holanda, and F. Toppan. From worldline to quantum superconformal mechanics with and without oscillatorial terms: $D(2,1;\alpha)$ and $sl(2|1)$ models. *Phys. Rev. D*, 96(6):065014, Sep 2017. doi: 10.1103/PhysRevD.96.065014. URL https://link.aps.org/doi/10.1103/PhysRevD.96.065014.

[56] M. Gonzales, S. Khodaee, and F. Toppan. On nonminimal $\mathcal{N}$=4 supermultiplets in 1D and their associated σ-models. *Journal of Mathematical Physics*, 52(1):013514, 01 2011. doi: 10.1063/1.3533761. URL https://doi.org/10.1063/1.3533761.

[57] N. Aizawa, Z. Kuznetsova, and F. Toppan. The quasi-nonassociative exceptional F(4) deformed quantum oscillator. *Journal of Mathematical Physics*, 59(2):022101, Feb 2018. doi: 10.1063/1.5016915. URL https://doi.org/10.1063/1.5016915.

[58] S. Fedoruk, E. Ivanov, and O. Lechtenfeld. Superconformal mechanics. *Journal of Physics A: Mathematical and Theoretical*, 45(17):173001, Apr 2012. doi: 10.1088/1751-8113/45/17/173001. URL https://dx.doi.org/10.1088/1751-8113/45/17/173001.

[59] N. Aizawa, I. E. Cunha, Z. Kuznetsova, and F. Toppan. On the spectrum-generating superalgebras of the deformed one-dimensional quantum oscillators. *Journal of Mathematical Physics*, 60(4):042102, Apr 2019. doi: 10.1063/1.5085164. URL https://doi.org/10.1063/1.5085164.

[60] S. Majid. *Foundations of Quantum Group Theory*. Cambridge University Press, 1995.

[61] W. Pauli. The Connection Between Spin and Statistics. *Phys. Rev.*, 58:716, 1940. doi: 10.1103/PhysRev.58.716.

[62] R. F. Streater and A. S. Wightman. *PCT, Spin and Statistics, and All That*. Princeton University Press, 1989.

[63] S. Doplicher, R. Haag, and J. E. Roberts. Local observables and particle statistics. I. *Commun. Math. Phys.*, 23:199–230, 1971.

[64] M. Chaichian, K. Nishijima, and A. Tureanu. Spin-statistics and cpt theorems in noncommutative field theory. *Physics Letters B*, 568(1):146–152, 2003. ISSN

0370-2693. doi: https://doi.org/10.1016/j.physletb.2003.06.009. URL https://www.sciencedirect.com/science/article/pii/S0370269303008979.

[65] S. Coleman and J. Mandula. All possible symmetries of the s matrix. *Phys. Rev.*, 159(5):1251–1256, 1967. doi: 10.1103/PhysRev.159.1251. URL https://link.aps.org/doi/10.1103/PhysRev.159.1251.

[66] R. Haag, J. T. Łopuszański, and M. Sohnius. All possible generators of supersymmetries of the s-matrix. *Nuclear Physics B*, 88(2):257–274, 1975. ISSN 0550-3213. doi: https://doi.org/10.1016/0550-3213(75)90279-5. URL https://www.sciencedirect.com/science/article/pii/0550321375902795.

[67] R. Ito and A. Nago. Novel possible symmetries of s-matrix generated by $\mathbb{Z}_2^n$-graded lie superalgebras, 2025. URL https://arxiv.org/abs/2501.07311.

[68] C. H. Alderete, A. M. Green, N. H. Nguyen, Y. Zhu, B. M. Rodríguez-Lara, and N. M. Linke. Experimental realization of para-particle oscillators, 2021. URL https://arxiv.org/abs/2108.05471.

[69] C. H. Alderete, A. M. Green, N. H. Nguyen, Y. Zhu, N. M. Linke, and B. M. Rodríguez-Lara. Para-particle oscillator simulations on a trapped ion quantum computer, 2022. URL https://arxiv.org/abs/2207.02430.

[70] Z. Wang and K. R. A. Hazzard. Particle exchange statistics beyond fermions and bosons. *Nature*, 637:314–318, 2025. doi: https://doi.org/10.1038/s41586-024-08262-7.

[71] S. L. Adler. *Quaternionic quantum mechanics and quantum fields*. Oxford University Press, 1988.

[72] S. Giardino. Quaternionic Klein–Gordon equation. *Eur. Phys. J. Plus*, 136(612), 2021.

[73] S. Giardino. Quaternionic scalar field in the real Hilbert space. *International Journal of Modern Physics A*, 37(15):2250101, 2022. doi: 10.1142/S0217751X22501019. URL https://doi.org/10.1142/S0217751X22501019.

[74] S. Doplicher, R. Haag, and J. E. Roberts. Local observables and particle statistics. I. *Commun. Math. Phys.*, 23:199–230, 1971.

[75] H. Stehouwer. The Spin-Statistics Theorem for Topological Quantum Field Theories. *Commun. Math. Phys.*, 370:201–235, 2019.

[76] S. Weinberg. *The Quantum theory of fields. Vol. 1: Foundations*. Cambridge University Press, 6 2005. ISBN 978-0-521-67053-1, 978-0-511-25204-4. doi: 10.1017/CBO9781139644167.

[77] I. Duck and E. C. G. Sudarshan. Toward an understanding of the spin-statistics theorem. *American Journal of Physics*, 66(4):284–303, 04 1998. ISSN 0002-9505. doi: 10.1119/1.18860. URL https://doi.org/10.1119/1.18860.

[78] S. Giardino. Four-dimensional conformal field theory using quaternions. *Adv. Appl. Clifford Algebras*, 27:2457–2471, 2015. doi: https://doi.org/10.1007/s00006-017-0781-3.

[79] K. Morita. Quaternionic Formulation of Dirac Theory in Special and General Relativity. *Progress of Theoretical Physics*, 70(6):1648–1665, 12 1983. ISSN 0033-068X. doi: 10.1143/PTP.70.1648. URL https://doi.org/10.1143/PTP.70.1648.

[80] S. De Leo and G. C. Ducati. Quaternionic groups in physics. *International Journal of Theoretical Physics*, 38:2197–2220, 1999. doi: https://doi.org/10.1023/A:1026626424174.

[81] J. C. Baez. The Octonions. *Bull. Am. Math. Soc.*, 39:145–205, 2002. doi: 10.1090/S0273-0979-01-00934-X. [Erratum: Bull. Am. Math. Soc. 42, 213 (2005)].

[82] Z. Kuznetsova and L. V. de Souza. $\mathbb{Z}_2 \times \mathbb{Z}_2$-graded Lie algebras and supseralgebras and related physical models. *J. Phys.: Conf. Ser.*, 2667:012017, 2023. doi: 10.1088/1742-6596/2667/1/012017.

[83] Kevin McCrimmon. *A taste of Jordan algebras*. Springer, 2004.

[84] Z. Kuznetsova and F. Toppan. Superalgebras of (split-)division algebras and the split octonionic M-theory in $(6,5)$-signature. *arXiv:hep-th/0610122*, 2006.

A Tables of Inequivalent Graded Lie Brackets

In detail, we present the tables of inequivalent graded Lie brackets that are compatible with the n-bit construction of $\mathbb{Z}_2^n$ structures (for $n \leq 4$). Specifically, we present the mappings $\mathbb{Z}_2^n \times \mathbb{Z}_2^n \to \mathbb{Z}_2$.

- The $b_1 = 2$ inequivalent brackets of $n = 1$:

1_1 case: (an ordinary Lie algebra),

	0	1
0	0	0
1	0	0

1_2 case: (an ordinary Lie superalgebra);

	0	1
0	0	0
1	0	1

- The $b_2 = 4$ inequivalent brackets of $n = 2$:

2_1 case: (an ordinary Lie algebra),

	00	10	01	11
00	0	0	0	0
10	0	0	0	0
01	0	0	0	0
11	0	0	0	0

2_2 case: (an ordinary $\mathbb{Z}_2$-graded Lie superalgebra),

	00	10	01	11
00	0	0	0	0
10	0	1	1	0
01	0	1	1	0
11	0	0	0	0

2_3 case: (the $\mathbb{Z}_2^2$ color Lie algebra),

	00	10	01	11
00	0	0	0	0
10	0	0	1	1
01	0	1	0	1
11	0	1	1	0

2_4 case:

	00	10	01	11
00	0	0	0	0
10	0	1	0	1
01	0	0	1	1
11	0	1	1	0

(the $\mathbb{Z}_2^2$ color Lie superalgebra);

- The $b_3 = 5$ inequivalent brackets of $n = 3$:

The rows (columns) are labeled by 3-bit, $\alpha_1, \alpha_2, \alpha_3$ (and, respectively, $\beta_1, \beta_2, \beta_3$). The 1-bit entries are expressed as *mod* 2 formulas.

3_1 case:

	000	100	010	001	110	101	011	111
000	0	0	0	0	0	0	0	0
100	0	0	0	0	0	0	0	0
010	0	0	0	0	0	0	0	0
001	0	0	0	0	0	0	0	0
110	0	0	0	0	0	0	0	0
101	0	0	0	0	0	0	0	0
011	0	0	0	0	0	0	0	0
111	0	0	0	0	0	0	0	0

(Lie algebra),

3_2 case:

	000	100	010	001	110	101	011	111
000	0	0	0	0	0	0	0	0
100	0	0	1	0	1	0	1	1
010	0	1	0	0	1	1	0	1
001	0	0	0	0	0	0	0	0
110	0	1	1	0	0	1	1	0
101	0	0	1	0	1	0	1	1
011	0	1	0	0	1	1	0	1
111	0	1	1	0	0	1	1	0

(from $\alpha_1\beta_2 + \alpha_2\beta_1$ mod 2),

3_3 case:

	000	100	010	001	110	101	011	111
000	0	0	0	0	0	0	0	0
100	0	1	0	0	1	1	0	1
010	0	0	0	0	0	0	0	0
001	0	0	0	0	0	0	0	0
110	0	1	0	0	1	1	0	1
101	0	1	0	0	1	1	0	1
011	0	0	0	0	0	0	0	0
111	0	1	0	0	1	1	0	1

(from $\alpha_1\beta_1$ mod 2),

3_4 case: (from $\alpha_1\beta_1 + \alpha_2\beta_2 \mod 2$),

	000	100	010	001	110	101	011	111
000	0	0	0	0	0	0	0	0
100	0	1	0	0	1	1	0	1
010	0	0	1	0	1	0	1	1
001	0	0	0	0	0	0	0	0
110	0	1	1	0	0	1	1	0
101	0	1	0	0	1	1	0	1
011	0	0	1	0	1	0	1	1
111	0	1	1	0	0	1	1	0

3_5 case: ($\alpha_1\beta_1 + \alpha_2\beta_2 + \alpha_3\beta_3 \mod 2$).

	000	100	010	001	110	101	011	111
000	0	0	0	0	0	0	0	0
100	0	1	0	0	1	1	0	1
010	0	0	1	0	1	0	1	1
001	0	0	0	1	0	1	1	1
110	0	1	1	0	0	1	1	0
101	0	1	0	1	1	0	1	0
011	0	0	1	1	1	1	0	0
111	0	1	1	1	0	0	0	1

The inequivalence of the 5 graded brackets is spotted in terms of:

- i) the number $R(n_k)$ of nonvanishing rows and
- ii) the trace $Tr(n_k)$ of the above matrices.

We have

$$Tr(3_1) = Tr(3_2) = 0, \quad Tr(3_3) = Tr(3_4) = Tr(3_5) = 4,$$

which implies that the cases 3_1 and 3_2 correspond to (para)bosonic Lie algebras.

The numbers of nonvanishing rows are given by

$$R(3_1) = 0, \quad R(3_2) = 6, \quad R(3_3) = 4, \quad R(3_4) = 6, \quad R(3_5) = 7.$$

The $b_4 = 7$ inequivalent brackets of $n = 4$:

The rows (columns) are labeled by 4-bit, $\alpha_1, \alpha_2, \alpha_3, \alpha_4$ (and, respectively, $\beta_1, \beta_2, \beta_3, \beta_4$). The 1-bit entries are expressed as $\mod 2$ formulas.

4_1 case:

	0000	1000	0100	0010	0001	1100	1010	1001	0110	0101	0011	1110	1101	1011	0111	1111
0000	0	0	0	0	0	0	0	0	0	0	0	0	0	0	0	0
1000	0	0	0	0	0	0	0	0	0	0	0	0	0	0	0	0
0100	0	0	0	0	0	0	0	0	0	0	0	0	0	0	0	0
0010	0	0	0	0	0	0	0	0	0	0	0	0	0	0	0	0
0001	0	0	0	0	0	0	0	0	0	0	0	0	0	0	0	0
1100	0	0	0	0	0	0	0	0	0	0	0	0	0	0	0	0
1010	0	0	0	0	0	0	0	0	0	0	0	0	0	0	0	0
1001	0	0	0	0	0	0	0	0	0	0	0	0	0	0	0	0
0110	0	0	0	0	0	0	0	0	0	0	0	0	0	0	0	0
0101	0	0	0	0	0	0	0	0	0	0	0	0	0	0	0	0
0011	0	0	0	0	0	0	0	0	0	0	0	0	0	0	0	0
1110	0	0	0	0	0	0	0	0	0	0	0	0	0	0	0	0
1101	0	0	0	0	0	0	0	0	0	0	0	0	0	0	0	0
1011	0	0	0	0	0	0	0	0	0	0	0	0	0	0	0	0
0111	0	0	0	0	0	0	0	0	0	0	0	0	0	0	0	0
1111	0	0	0	0	0	0	0	0	0	0	0	0	0	0	0	0

4_2 case:

	0000	1000	0100	0010	0001	1100	1010	1001	0110	0101	0011	1110	1101	1011	0111	1111
0000	0	0	0	0	0	0	0	0	0	0	0	0	0	0	0	0
1000	0	0	1	0	0	1	0	0	1	1	0	1	1	0	1	1
0100	0	1	0	0	0	1	1	1	0	0	0	1	1	1	0	1
0010	0	0	0	0	0	0	0	0	0	0	0	0	0	0	0	0
0001	0	0	0	0	0	0	0	0	0	0	0	0	0	0	0	0
1100	0	1	1	0	0	0	1	1	1	1	0	0	0	1	1	0
1010	0	0	1	0	0	1	0	0	1	1	0	1	1	0	1	1
1001	0	0	1	0	0	1	0	0	1	1	0	1	1	0	1	1
0110	0	1	0	0	0	1	1	1	0	0	0	1	1	1	0	1
0101	0	1	0	0	0	1	1	1	0	0	0	1	1	1	0	1
0011	0	0	0	0	0	0	0	0	0	0	0	0	0	0	0	0
1110	0	1	1	0	0	0	1	1	1	1	0	0	0	1	1	0
1101	0	1	1	0	0	0	1	1	1	1	0	0	0	1	1	0
1011	0	0	1	0	0	1	0	0	1	1	0	1	1	0	1	1
0111	0	1	0	0	0	1	1	1	0	0	0	1	1	1	0	1
1111	0	1	1	0	0	0	1	1	1	1	0	0	0	1	1	0

4_3 case:

	0000	1000	0100	0010	0001	1100	1010	1001	0110	0101	0011	1110	1101	1011	0111	1111
0000	0	0	0	0	0	0	0	0	0	0	0	0	0	0	0	0
1000	0	0	1	0	0	1	0	0	1	1	0	1	1	0	1	1
0100	0	1	0	0	0	1	1	1	0	0	0	1	1	1	0	1
0010	0	0	0	0	1	0	0	1	0	1	1	0	1	1	1	1
0001	0	0	0	1	0	0	1	0	1	0	1	1	0	1	1	1
1100	0	1	1	0	0	0	1	1	1	1	0	0	0	1	1	0
1010	0	0	1	0	1	1	0	1	1	0	1	1	0	1	0	0
1001	0	0	1	1	0	1	1	0	0	1	1	0	1	1	0	0
0110	0	1	0	0	1	1	1	0	0	1	1	1	0	0	1	0
0101	0	1	0	1	0	1	0	1	1	0	1	0	1	0	1	0
0011	0	0	0	1	1	0	1	1	1	1	0	1	1	0	0	0
1110	0	1	1	0	1	0	1	0	1	0	1	0	1	0	0	1
1101	0	1	1	1	0	0	0	1	0	1	1	1	0	0	0	1
1011	0	0	1	1	1	1	1	1	0	0	0	0	0	0	1	1
0111	0	1	0	1	1	1	0	0	1	1	0	0	0	1	0	1
1111	0	1	1	1	1	0	0	0	0	0	0	1	1	1	1	0

4_4 case:

	0000	1000	0100	0010	0001	1100	1010	1001	0110	0101	0011	1110	1101	1011	0111	1111
0000	0	0	0	0	0	0	0	0	0	0	0	0	0	0	0	0
1000	0	1	0	0	0	1	1	1	0	0	0	1	1	1	0	1
0100	0	0	0	0	0	0	0	0	0	0	0	0	0	0	0	0
0010	0	0	0	0	0	0	0	0	0	0	0	0	0	0	0	0
0001	0	0	0	0	0	0	0	0	0	0	0	0	0	0	0	0
1100	0	1	0	0	0	1	1	1	0	0	0	1	1	1	0	1
1010	0	1	0	0	0	1	1	1	0	0	0	1	1	1	0	1
1001	0	1	0	0	0	1	1	1	0	0	0	1	1	1	0	1
0110	0	0	0	0	0	0	0	0	0	0	0	0	0	0	0	0
0101	0	0	0	0	0	0	0	0	0	0	0	0	0	0	0	0
0011	0	0	0	0	0	0	0	0	0	0	0	0	0	0	0	0
1110	0	1	0	0	0	1	1	1	0	0	0	1	1	1	0	1
1101	0	1	0	0	0	1	1	1	0	0	0	1	1	1	0	1
1011	0	1	0	0	0	1	1	1	0	0	0	1	1	1	0	1
0111	0	0	0	0	0	0	0	0	0	0	0	0	0	0	0	0
1111	0	1	0	0	0	1	1	1	0	0	0	1	1	1	0	1

4_5 case:

	0000	1000	0100	0010	0001	1100	1010	1001	0110	0101	0011	1110	1101	1011	0111	1111
0000	0	0	0	0	0	0	0	0	0	0	0	0	0	0	0	0
1000	0	1	0	0	0	1	1	1	0	0	0	1	1	1	0	1
0100	0	0	1	0	0	1	0	0	1	0	0	1	1	0	1	1
0010	0	0	0	0	0	0	0	0	0	0	0	0	0	0	0	0
0001	0	0	0	0	0	0	0	0	0	0	0	0	0	0	0	0
1100	0	1	1	0	0	0	1	1	1	1	0	0	0	1	1	0
1010	0	1	0	0	0	1	1	1	0	0	0	1	1	1	0	1
1001	0	1	0	0	0	1	1	1	0	0	0	1	1	1	0	1
0110	0	0	1	0	0	1	0	0	1	1	0	1	1	0	1	1
0101	0	0	1	0	0	1	0	0	1	1	0	1	1	0	1	1
0011	0	0	0	0	0	0	0	0	0	0	0	0	0	0	0	0
1110	0	1	1	0	0	0	1	1	1	1	0	0	0	1	1	0
1101	0	1	1	0	0	0	1	1	1	1	0	0	0	1	1	0
1011	0	1	0	0	0	1	1	1	0	0	0	1	1	1	0	1
0111	0	0	1	0	0	1	0	0	1	1	0	1	1	0	1	1
1111	0	1	1	0	0	0	1	1	1	1	0	0	0	1	1	0

4_6 case:

	0000	1000	0100	0010	0001	1100	1010	1001	0110	0101	0011	1110	1101	1011	0111	1111
0000	0	0	0	0	0	0	0	0	0	0	0	0	0	0	0	0
1000	0	1	0	0	0	1	1	1	0	0	0	1	1	1	0	1
0100	0	0	1	0	0	1	0	0	1	1	0	1	1	0	1	1
0010	0	0	0	1	0	0	1	0	1	0	1	1	0	1	1	1
0001	0	0	0	0	0	0	0	0	0	0	0	0	0	0	0	0
1100	0	1	1	0	0	0	1	1	1	1	0	0	0	1	1	0
1010	0	1	0	1	0	1	0	1	1	0	1	0	1	0	1	0
1001	0	1	0	0	0	1	1	1	0	0	0	1	1	1	0	1
0110	0	0	1	1	0	1	1	0	0	1	1	0	1	1	0	0
0101	0	0	1	0	0	1	0	0	1	1	0	1	1	0	1	1
0011	0	0	0	1	0	0	1	0	1	0	1	1	0	1	1	1
1110	0	1	1	1	0	0	0	1	0	1	1	1	0	0	0	1
1101	0	1	1	0	0	0	1	1	1	1	0	0	0	1	1	0
1011	0	1	0	1	0	1	0	1	1	0	1	0	1	0	1	0
0111	0	0	1	1	0	1	1	0	0	1	1	0	1	1	0	0
1111	0	1	1	1	0	0	0	1	0	1	1	1	0	0	0	1

4_7 case:

	0000	1000	0100	0010	0001	1100	1010	1001	0110	0101	0011	1110	1101	1011	0111	1111
0000	0	0	0	0	0	0	0	0	0	0	0	0	0	0	0	0
1000	0	1	0	0	0	1	1	1	0	0	0	1	1	1	0	1
0100	0	0	1	0	0	1	0	0	1	1	0	1	1	0	1	1
0010	0	0	0	1	0	0	1	0	1	0	1	1	0	1	1	1
0001	0	0	0	0	1	0	0	1	0	1	1	0	1	1	1	1
1100	0	1	1	0	0	0	1	1	1	1	0	0	0	1	1	0
1010	0	1	0	1	0	1	0	1	1	0	1	0	1	0	1	0
1001	0	1	0	0	1	1	1	0	0	1	1	1	0	0	1	0
0110	0	0	1	1	0	1	1	0	0	1	1	0	1	1	0	0
0101	0	0	1	0	1	1	0	1	1	0	1	1	0	1	0	0
0011	0	0	0	1	1	0	1	1	1	1	0	1	1	0	0	0
1110	0	1	1	1	0	0	0	1	0	1	1	1	0	0	0	1
1101	0	1	1	0	1	0	1	0	1	0	1	0	1	0	0	1
1011	0	1	0	1	1	1	0	0	1	1	0	0	0	1	0	1
0111	0	0	1	1	1	1	1	1	0	0	0	0	0	0	1	1
1111	0	1	1	1	1	0	0	0	0	0	0	1	1	1	1	0

The entries of the corresponding cases are given by

$$
\begin{aligned}
&4_1 : 0,\\
&4_2 : \alpha_1\beta_2 + \alpha_2\beta_1 \mod 2,\\
&4_3 : \alpha_1\beta_2 + \alpha_2\beta_1 + \alpha_3\beta_4 + \alpha_4\beta_3 \mod 2,\\
&4_4 : \alpha_1\beta_1 \mod 2,\\
&4_5 : \alpha_1\beta_1 + \alpha_2\beta_2 \mod 2,\\
&4_6 : \alpha_1\beta_1 + \alpha_2\beta_2 + \alpha_3\beta_3 \mod 2,\\
&4_7 : \alpha_1\beta_1 + \alpha_2\beta_2 + \alpha_3\beta_3 + \alpha_4\beta_4 \mod 2.
\end{aligned}
$$

The inequivalence of the 7 graded brackets is spotted in terms of:

i) the number $R(n_k)$ of nonvanishing rows and

ii) the trace $Tr(n_k)$ of the above matrices.

We have

$$
\begin{aligned}
&Tr(4_1) = Tr(4_2) = Tr(4_3) = 0,\\
&Tr(4_4) = Tr(4_5) = Tr(4_6) = Tr(4_7) = 8,
\end{aligned}
$$

which implies that the cases 4_1, 4_2, and 4_3 correspond to (para)bosonic Lie algebras.

The numbers of nonvanishing rows are given by

$$
\begin{aligned}
&R(4_1) = 0, \quad R(4_2) = 12, \quad R(4_3) = 15, \quad R(4_4) = 8,\\
&R(4_5) = 12, \quad R(4_6) = 14, \quad R(4_7) = 15.
\end{aligned}
$$

B Assignments of $\mathbb{Z}_2^3$ graded sectors

The combinatorics which are used to derive the 16 inequivalent graded Lie (super)algebras of the biquaternions and the 10 inequivalent parastatistics of the $\mathcal{N}=4$ supersymmetric quantum mechanics are based on the admissible 3-bit assignments of the $\mathbb{Z}_2^3$ graded sectors. Here we present two tables which clarify this feature. The $\mathbb{Z}_2^3$ grading of 8×8 matrices implies that the $\underline{0}=000$ (i.e., zero-vector) graded elements belong to the diagonal, while the 7 remaining sectors are expressed in terms of any choice of three fundamental gradings α,β,γ according to the following *mod* 2 relations. The $*$ symbol denotes, for each graded sector, which entries of the 8×8 matrices can be nonvanishing:

$$
\begin{array}{rlrl}
\underline{0}\equiv 000: & \begin{pmatrix} \ast &&&&&&& \\ & \ast &&&&&& \\ && \ast &&&&& \\ &&& \ast &&&& \\ &&&& \ast &&& \\ &&&&& \ast && \\ &&&&&& \ast & \\ &&&&&&& \ast \end{pmatrix} & \alpha: & \begin{pmatrix} && \ast &&&&& \\ &&& \ast &&&& \\ \ast &&&&&&& \\ & \ast &&&&&& \\ &&&&&& \ast & \\ &&&&&&& \ast \\ &&&& \ast &&& \\ &&&&& \ast && \end{pmatrix} \\
\beta: & \begin{pmatrix} &&& \ast &&&& \\ && \ast &&&&& \\ & \ast &&&&&& \\ \ast &&&&&&& \\ &&&&&&& \ast \\ &&&&&& \ast & \\ &&&&& \ast && \\ &&&& \ast &&& \end{pmatrix} & \gamma: & \begin{pmatrix} &&&& \ast &&& \\ &&&&& \ast && \\ &&&&&& \ast & \\ &&&&&&& \ast \\ \ast &&&&&&& \\ & \ast &&&&&& \\ && \ast &&&&& \\ &&& \ast &&&& \end{pmatrix} \\
\alpha+\beta: & \begin{pmatrix} & \ast &&&&&& \\ \ast &&&&&&& \\ &&& \ast &&&& \\ && \ast &&&&& \\ &&&&& \ast && \\ &&&& \ast &&& \\ &&&&&&& \ast \\ &&&&&& \ast & \end{pmatrix} & \alpha+\gamma: & \begin{pmatrix} &&&&&& \ast & \\ &&&&&&& \ast \\ &&&& \ast &&& \\ &&&&& \ast && \\ && \ast &&&&& \\ &&& \ast &&&& \\ \ast &&&&&&& \\ & \ast &&&&&& \end{pmatrix} \\
\beta+\gamma: & \begin{pmatrix} &&&&&&& \ast \\ &&&&&& \ast & \\ &&&&& \ast && \\ &&&& \ast &&& \\ &&& \ast &&&& \\ && \ast &&&&& \\ & \ast &&&&&& \\ \ast &&&&&&& \end{pmatrix} & \alpha+\beta+\gamma: & \begin{pmatrix} &&&&& \ast && \\ &&&& \ast &&& \\ &&&&&&& \ast \\ &&&&&& \ast & \\ & \ast &&&&&& \\ \ast &&&&&&& \\ &&& \ast &&&& \\ && \ast &&&&& \end{pmatrix}
\end{array}
\tag{B.0}
$$

In another schematical presentation, the 3-bit nonzero vectors can be assigned to the 7 vertices of the Fano's plane. For each one of the 7 edges, the sum *mod* 2 of the vectors of any two vertices gives the 3-bit vector of the third vertex lying on the edge:

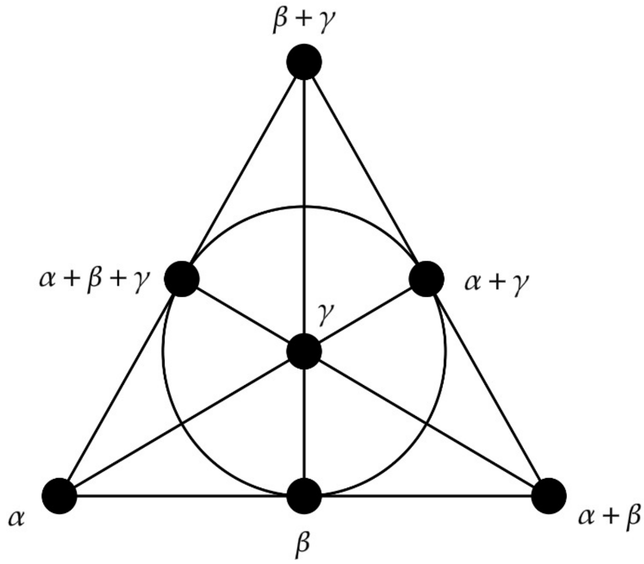

Figure 1 – Assignments on Fano's plane

Bellow, we present the non-trivial $\mathbb{Z}_2^3$ maps through diagrams. Starting with $\mathbb{Z}_2^2$ graded algebra embedded on a $\mathbb{Z}_2^3$ structure, we have

$\alpha_1.\beta_2 - \alpha_2.\beta_1$	000	001	010	011	100	101	110	111
000	0	0	0	0	0	0	0	0
001	0	0	0	0	0	0	0	0
010	0	0	0	0	1	1	1	1
011	0	0	0	0	1	1	1	1
100	0	0	1	1	0	0	1	1
101	0	0	1	1	0	0	1	1
110	0	0	1	1	1	1	0	0
111	0	0	1	1	1	1	0	0

Table 7 – (Anti)commutator table for $\alpha_1.\beta_2 - \alpha_2.\beta_1$

B.0.1 Subalgebras of 3_2 case: **2 Bosons, 6 Parabosons**

$\boxed{001, 010, 011}$

2_1 **case**:

$[001, 001]$	$[001, 010]$	$[010, 010]$
$[001, 011]$	$[011, 011]$	$[010, 011]$

	001	010	011
001	0	0	0
010	0	0	0
011	0	0	0

Ordinary Lie algebra

$\boxed{001, 100, 101}$

2_1 **case**:

$[001, 001]$	$[001, 100]$	$[100, 100]$
$[001, 101]$	$[101, 101]$	$[100, 101]$

	001	100	101
001	0	0	0
100	0	0	0
101	0	0	0

Ordinary Lie algebra

$\boxed{001, 110, 111}$

2_1 **case**:

$[001, 001]$	$[001, 110]$	$[110, 110]$
$[001, 111]$	$[111, 111]$	$[110, 111]$

	001	110	111
001	0	0	0
110	0	0	0
111	0	0	0

Ordinary Lie algebra

$\boxed{010, 100, 110}$

2_3 **case**:

$[010, 010]$	$\{010, 100\}$	$[100, 100]$
$\{010, 110\}$	$[100, 110]$	$\{110, 110\}$

	010	100	110
010	0	1	1
100	1	0	1
110	1	1	0

$\mathbb{Z}_2^2$ graded algebra

$\boxed{010, 101, 111}$

2_3 **case**:

$[010, 010]$	$\{010, 101\}$	$[101, 101]$
$\{010, 111\}$	$[111, 111]$	$\{101, 111\}$

	010	101	111
010	0	1	1
101	1	0	1
111	1	1	0

$\mathbb{Z}_2^2$ graded algebra

$\boxed{011, 100, 111}$

2_3 **case**:

$[011, 011]$ $\{011, 100\}$ $[100, 100]$
$\{011, 111\}$ $[111, 111]$ $\{100, 111\}$

	011	100	111
011	0	1	1
100	1	0	1
111	1	1	0

$\mathbb{Z}_2^2$ **graded algebra**

$\boxed{011, 110, 101}$

2_3 **case**:

$[011, 011]$ $\{011, 110\}$ $[110, 110]$
$\{011, 101\}$ $[101, 101]$ $\{110, 101\}$

	011	110	101
011	0	1	1
110	1	0	1
101	1	1	0

$\mathbb{Z}_2^2$ **graded algebra**

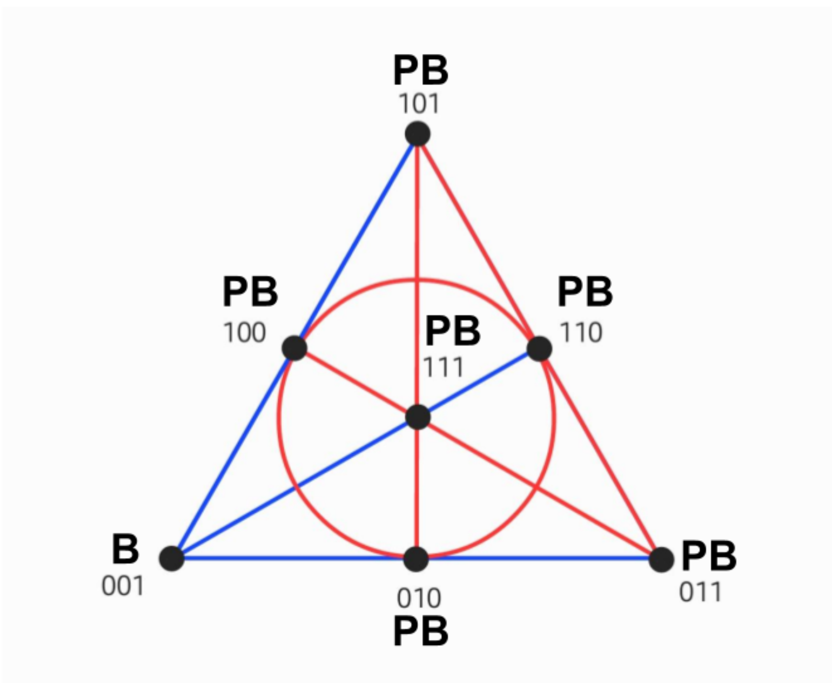

Figure 2 – Fano plane for 3_2 case

Summary:

- 3 ordinary Lie algebras
- 4 $\mathbb{Z}_2^2$ algebras

For the 3_3 case, we have:

$\alpha_1.\beta_1$	000	001	010	011	100	101	110	111
000	0	0	0	0	0	0	0	0
001	0	0	0	0	0	0	0	0
010	0	0	0	0	0	0	0	0
011	0	0	0	0	0	0	0	0
100	0	0	0	0	1	1	1	1
101	0	0	0	0	1	1	1	1
110	0	0	0	0	1	1	1	1
111	0	0	0	0	1	1	1	1

Table 8 – (Anti)commutator table for $\alpha_1.\beta_1$

B.0.2 Subalgebras of 3_3 case: **4 Bosons, 4 Fermions**

$\boxed{001, 010, 011}$

2_1 **case**:

[001, 001] [001, 010] [010, 010]
[001, 011] [011, 011] [010, 011]

	001	010	011
001	0	0	0
010	0	0	0
011	0	0	0

Ordinary Lie algebra

$\boxed{001, 100, 101}$

2_2 **case**:

[001, 001] [001, 100] {100, 100}
[001, 101] {101, 101} {100, 101}

	001	100	101
001	0	0	0
100	0	1	1
101	0	1	1

$\mathbb{Z}_2$ **superalgebra**

$\boxed{001, 110, 111}$

2_2 **case**:

[001, 001] [001, 110] {110, 110}
[001, 111] {111, 111} {110, 111}

	001	110	111
001	0	0	0
110	0	1	1
111	0	1	1

$\mathbb{Z}_2$ **superalgebra**

$\boxed{010, 100, 110}$

2_2 **case**:

$[010, 010]$ $[010, 100]$ $\{100, 100\}$
$[010, 110]$ $\{110, 110\}$ $\{110, 100\}$

	010	100	110
010	0	0	0
100	0	1	1
110	0	1	1

$\mathbb{Z}_2$ **superalgebra**

$\boxed{010, 101, 111}$

2_2 **case**:

$[010, 010]$ $[010, 101]$ $\{101, 101\}$
$[010, 111]$ $\{111, 111\}$ $\{101, 111\}$

	010	101	111
010	0	0	0
101	0	1	1
111	0	1	1

$\mathbb{Z}_2$ **superalgebra**

$\boxed{011, 100, 111}$

2_2 **case**:

$[011, 011]$ $[011, 100]$ $\{100, 100\}$
$[011, 111]$ $\{111, 111\}$ $\{100, 111\}$

	011	100	111
011	0	0	0
100	0	1	1
111	0	1	1

$\mathbb{Z}_2$ **superalgebra**

$\boxed{011, 110, 101}$

2_2 **case**:

$[011, 011]$ $[011, 110]$ $\{110, 110\}$
$[011, 101]$ $\{101, 101\}$ $\{110, 101\}$

	011	110	101
011	0	0	0
110	0	1	1
101	0	1	1

$\mathbb{Z}_2$ **superalgebra**

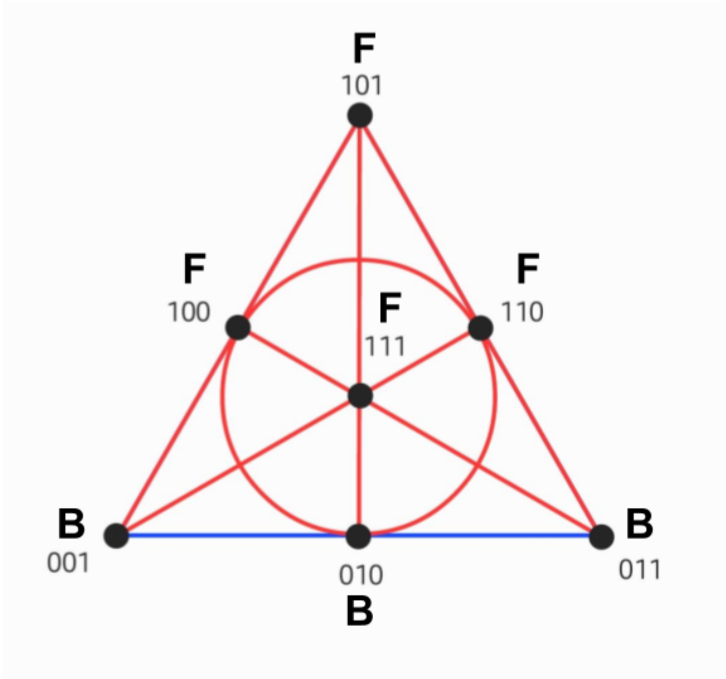

Figure 3 – Fano plane for 3_3 case

Summary:

- 1 ordinary Lie algebra
- 6 $\mathbb{Z}_2$ superalgebras

For the 3_4 case, we have:

$\alpha_1.\beta_1 + \alpha_2.\beta_2$	000	001	010	011	100	101	110	111
000	0	0	0	0	0	0	0	0
001	0	0	0	0	0	0	0	0
010	0	0	1	1	0	0	1	1
011	0	0	1	1	0	0	1	1
100	0	0	0	0	1	1	1	1
101	0	0	0	0	1	1	1	1
110	0	0	1	1	1	1	0	0
111	0	0	1	1	1	1	0	0

Table 9 – (Anti)commutator table for $\alpha_1.\beta_1 + \alpha_2.\beta_2$

B.0.3 Subalgebras of 3_4 case: **2 Bosons, 4 Parabosons, 4 Parafermions**

$\boxed{001, 010, 011}$

2_2 **case**:

$[001, 001]$	$[001, 010]$	$\{010, 010\}$
$[001, 011]$	$\{011, 011\}$	$\{010, 011\}$

	001	010	011
001	0	0	0
010	0	1	1
011	0	1	1

$\mathbb{Z}_2$ **superalgebra**

$\boxed{001, 100, 101}$

2_2 **case**:

$[001, 001]$	$[001, 100]$	$\{100, 100\}$
$[001, 101]$	$\{101, 101\}$	$\{100, 101\}$

	001	100	101
001	0	0	0
100	0	1	1
101	0	1	1

$\mathbb{Z}_2$ **superalgebra**

$\boxed{001, 110, 111}$

2_1 **case**:

$[001, 001]$	$[001, 110]$	$\{110, 110\}$
$[001, 111]$	$\{111, 111\}$	$\{110, 111\}$

	001	110	111
001	0	0	0
110	0	0	0
111	0	0	0

Ordinary Lie algebra

$\boxed{010, 100, 110}$

2_4 **case**:

$\{010, 010\}$	$[010, 100]$	$\{100, 100\}$
$\{010, 110\}$	$[110, 110]$	$\{110, 100\}$

	010	100	110
010	1	0	1
100	0	1	1
110	1	1	0

$\mathbb{Z}_2^2$ **superalgebra**

$\boxed{010, 101, 111}$

2_4 **case**:

$\{010, 010\}$	$[010, 101]$	$\{101, 101\}$
$\{010, 111\}$	$[111, 111]$	$\{101, 111\}$

	010	101	111
010	1	0	1
101	0	1	1
111	1	1	0

$\mathbb{Z}_2^2$ **superalgebra**

$\boxed{011, 100, 111}$

2_4 **case**:

$$\begin{array}{|lll}
\{011, 011\} & [011, 100] & \{100, 100\} \\
\{011, 111\} & [111, 111] & \{100, 111\}
\end{array}$$

	011	100	111
011	1	0	1
100	0	1	1
111	1	1	0

$\mathbb{Z}_2^2$ **superalgebra**

$\boxed{011, 110, 101}$

2_4 **case**:

$$\begin{array}{|lll}
\{011, 011\} & [011, 110] & \{110, 110\} \\
\{011, 101\} & [101, 101] & \{110, 101\}
\end{array}$$

	011	110	101
011	1	0	1
110	0	1	1
101	1	1	0

$\mathbb{Z}_2^2$ **superalgebra**

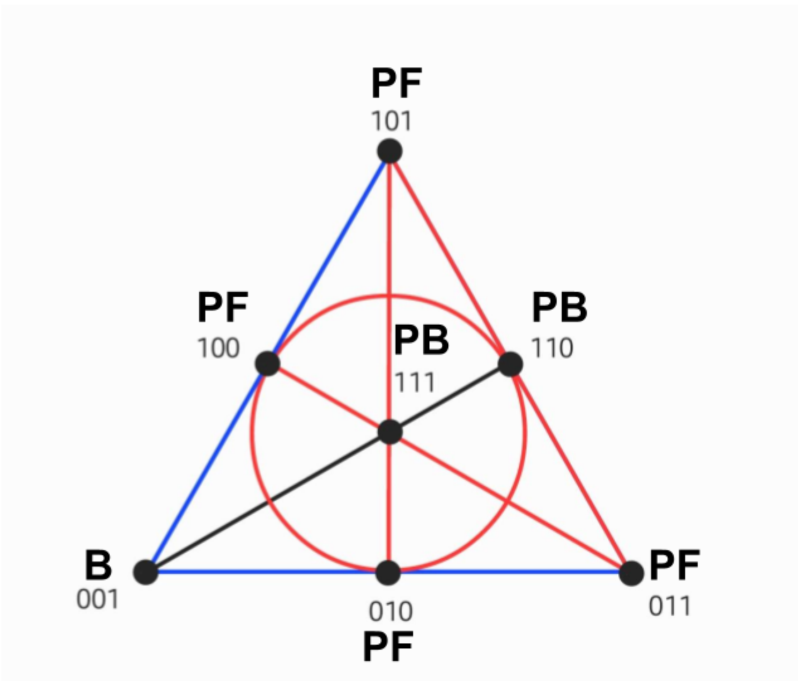

Figure 4 – Fano plane for 3_4 case

Summary:

- 1 ordinary Lie algebra
- 2 $\mathbb{Z}_2$ superalgebra
- 4 $\mathbb{Z}_2^2$ superalgebras

For the 3_5 case, we have:

$\alpha_1.\beta_1+\alpha_2.\beta_2+\alpha_3.\beta_3$	000	001	010	011	100	101	110	111
000	0	0	0	0	0	0	0	0
001	0	1	0	1	0	1	0	1
010	0	0	1	1	0	0	1	1
011	0	1	1	0	0	1	1	0
100	0	0	0	0	1	1	1	1
101	0	1	0	1	1	0	1	0
110	0	0	1	1	1	1	0	0
111	0	1	1	0	1	0	0	1

Table 10 – (Anti)commutators table for $\alpha_1.\beta_1+\alpha_2.\beta_2+\alpha_3.\beta_3$

B.0.4 Subalgebras of 3_5 case: **1 Boson, 3 Parabosons, 4 Parafermions**

$\boxed{001, 010, 011}$

2_4 **case**:

$\{001,001\}$ $[001,010]$ $\{010,010\}$
$[001,011]$ $[011,011]$ $\{010,011\}$

	001	010	011
001	1	0	1
010	0	1	1
011	1	1	0

$\mathbb{Z}_2^2$ **superalgebra**

$\boxed{001, 100, 101}$

2_4 **case**:

$\{001,001\}$ $[001,100]$ $\{100,100\}$
$\{001,101\}$ $[101,101]$ $\{100,101\}$

	001	100	101
001	1	0	1
100	0	1	1
101	1	1	0

$\mathbb{Z}_2^2$ **superalgebra**

$\boxed{001, 110, 111}$

2_2 **case**:

$\{001,001\}$ $[001,110]$ $[110,110]$
$\{001,111\}$ $\{111,111\}$ $[110,111]$

	001	110	111
001	1	0	1
110	0	0	0
111	1	0	1

$\mathbb{Z}_2$ **superalgebra**

$\boxed{010, 100, 110}$

2_4 **case**:

$$\begin{array}{ccc} \{010,010\} & [010,100] & \{100,100\} \\ \{010,110\} & [110,110] & \{110,100\} \end{array}$$

	010	100	110
010	1	0	1
100	0	1	1
110	1	1	0

$\mathbb{Z}_2^2$ **superalgebra**

$\boxed{010, 101, 111}$

2_2 **case**:

$$\begin{array}{ccc} \{010,010\} & [010,101] & [101,101] \\ \{010,111\} & \{111,111\} & [101,111] \end{array}$$

	010	101	111
010	1	0	1
101	0	0	0
111	1	0	1

$\mathbb{Z}_2$ **superalgebra**

$\boxed{011, 100, 111}$

2_2 **case**:

$$\begin{array}{ccc} [011,011] & [011,100] & \{100,100\} \\ [011,111] & \{111,111\} & \{100,111\} \end{array}$$

	011	100	111
011	0	0	0
100	0	1	1
111	0	1	1

$\mathbb{Z}_2$ **superalgebra**

$\boxed{011, 110, 101}$

2_3 **case**:

$$\begin{array}{ccc} [011,011] & \{011,110\} & [110,110] \\ \{011,101\} & [101,101] & \{110,101\} \end{array}$$

	011	110	101
011	0	1	1
110	1	0	1
101	1	1	0

$\mathbb{Z}_2^2$ **graded algebra**

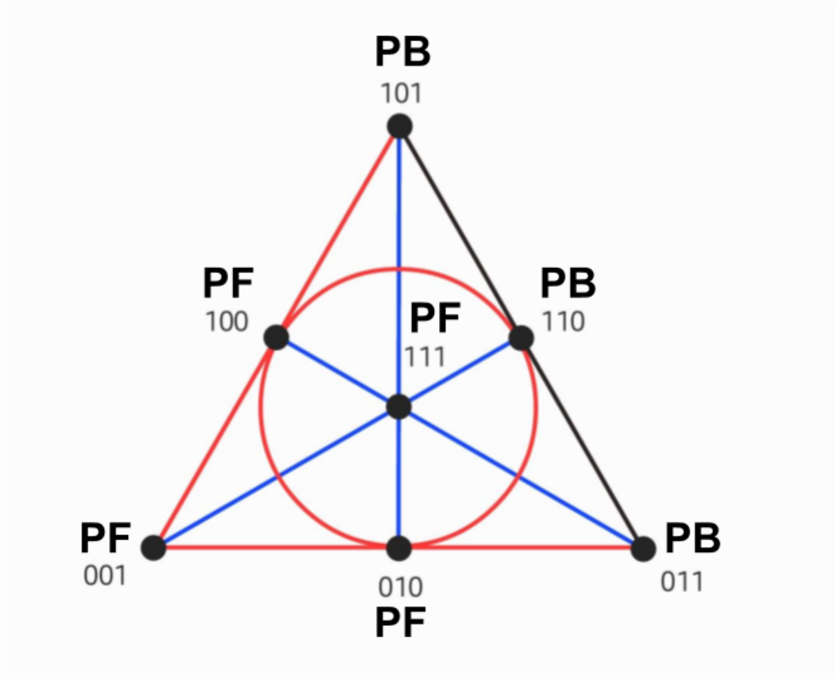

Figure 5 – Fano plane for 3_5 case

Summary:

- 1 $\mathbb{Z}_2^2$ graded algebra
- 3 $\mathbb{Z}_2$ superalgebras
- 3 $\mathbb{Z}_2^2$ superalgebras

C Details of Boolean Logic Representations

In this appendix, we illustrate how the tables of inequivalent graded Lie brackets can be reformulated using Boolean logic gates.

The Boolean logic representation follows a systematic procedure: first, the graded sectors appearing in the tables of Appendix A are reordered according to a Gray code (where only one bit changes at a time). This rearrangement enables the use of Karnaugh maps, which, when further simplified, allow the graded-bracket tables to be expressed in terms of the logical gates AND, OR, XOR along with the NOT operation.

The truth tables for these logical operations, acting on binary inputs $a, b \in \{0, 1\}$, are as follows:

NOT:

a	$\overline{a}$
0	1
1	0

AND:

a	b	$a \cdot b$
0	0	0
0	1	0
1	0	0
1	1	1

OR:

a	b	$a + b$
0	0	0
0	1	1
1	0	1
1	1	1

XOR:

a	b	$a \oplus b$
0	0	0
0	1	1
1	0	1
1	1	0

The symbols used to denote these operations are:

$$\text{NOT:} \quad a \mapsto \overline{a}, \qquad \text{AND:} \quad a, b \mapsto a \cdot b, \qquad \text{OR:} \quad a, b \mapsto a + b, \qquad \text{XOR:} \quad a, b \mapsto a \oplus b.$$

For $n = 2$, Gray code representations of the 2_2, 2_3, and 2_4 cases from Appendix A are given below:

- 2_2 case:

$\alpha_1\, \alpha_2 \setminus \beta_1\, \beta_2$	00	01	11	10
00	0	0	0	0
01	0	1	1	0
11	0	1	1	0
10	0	0	0	0

- 2_3 case:

$\alpha_1\ \alpha_2 \setminus \beta_1\ \beta_2$	00	01	11	10
00	0	0	0	0
01	0	0	1	1
11	0	1	0	1
10	0	1	1	0

- 2_4 case:

$\alpha_1\ \alpha_2 \setminus \beta_1\ \beta_2$	00	01	11	10
00	0	0	0	0
01	0	1	1	0
11	0	1	0	1
10	0	0	1	1

The 1 entries in the above tables are encircled to indicate how they are grouped together in a Karnaugh map. Whenever possible, horizontally or vertically adjacent 1 entries are grouped in even numbers, except when an isolated 1 remains.

After grouping the entries into pairs, we examine which bit (denoted as $\alpha_1, \alpha_2, \beta_1, \beta_2$ in the above tables) remains constant and which varies as we move from one encircled row or column to another.

For example, consider the encircled row in table where $\alpha_1 = 0$, $\alpha_2 = 1$. In this row, the β_2 bit remains constant ($\beta_2 = 1$), while β_1 changes from 0 to 1. Thus, the non-varying bits in this encircled row are $\alpha_1, \alpha_2, \beta_2$.

The Karnaugh map assigns to this row the following mod 2 expression in terms of the non-varying bits:

$$\overline{\alpha}_1 \cdot \alpha_2 \cdot \beta_2.$$

Here, the bar over α_1 indicates the NOT operation, since in the encircled row, $\alpha_1 = 0$ (while $\alpha_2 = 1$ and $\beta_2 = 1$).

The expressions for the different encircled pairs are combined using the OR operation. Thus, the table (C) is encoded as the mod 2 equation:

$$\langle \alpha, \beta \rangle = \overline{\alpha}_1 \cdot \alpha_2 \cdot \beta_2 + \alpha_1 \cdot \overline{\alpha}_2 \cdot \beta_1 + \alpha_2 \cdot \overline{\beta}_1 \cdot \beta_2 + \alpha_1 \cdot \beta_1 \cdot \overline{\beta}_2.$$

Further simplifications allow us to express $\langle \alpha, \beta \rangle$ as:

$$\langle \alpha, \beta \rangle = \alpha_2 \cdot \beta_2 \cdot (\overline{\alpha}_1 + \overline{\beta}_1) + \alpha_1 \cdot \beta_1 \cdot (\overline{\alpha}_2 + \overline{\beta}_2).$$

Using De Morgan's theorem, which states that:

$$\overline{a} + \overline{b} = \overline{a \cdot b},$$

we can rewrite $\langle \alpha, \beta \rangle$ as:

$$\langle \alpha, \beta \rangle = \alpha_2 \cdot \beta_2 \cdot (\overline{\alpha_1 \cdot \beta_1}) + \alpha_1 \cdot \beta_1 \cdot (\overline{\alpha_2 \cdot \beta_2}).$$

The final simplification uses the XOR operation, which satisfies (mod 2):

$$a \oplus b = a \cdot \overline{b} + \overline{a} \cdot b.$$

Thus, the table (C) is simplified to:

$$\langle \alpha, \beta \rangle = (\alpha_1 \cdot \beta_1) \oplus (\alpha_2 \cdot \beta_2).$$

By using the standard logic gate representation, the simplification can be depicted as:

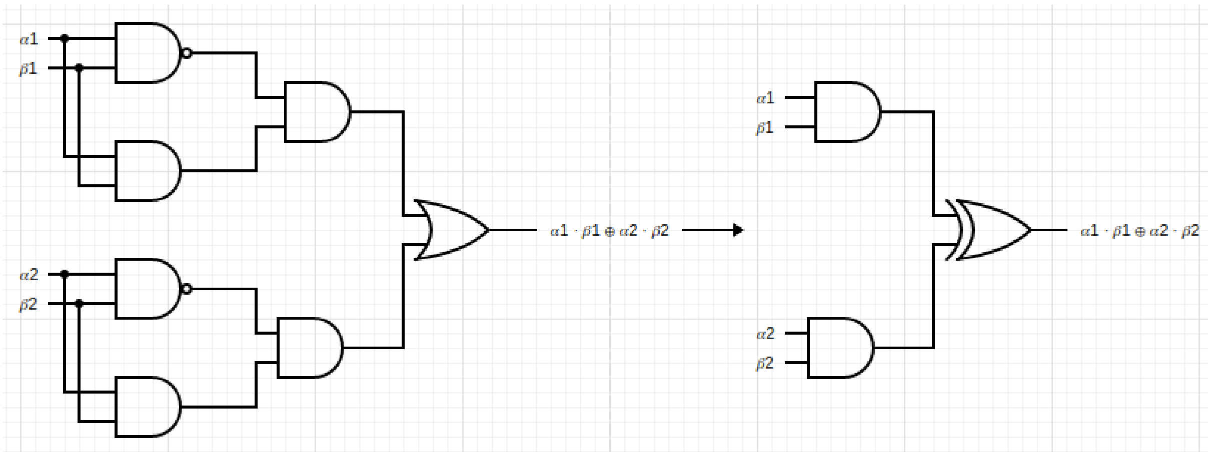

The NAND operation (a combination of NOT and AND), which maps a, b to $\overline{a \cdot b}$, appears on the left in the above diagram.

This construction can be extended to other $n = 2$ cases, as well as to $n > 2$ tables.

In the Boolean logic graphical representation, the $\langle \alpha, \beta \rangle$ scalar products for the cases $2_2, 2_3, 2_4$ are:

$2_2 : \quad \langle \alpha, \beta \rangle = \alpha_2 \cdot \beta_2 \quad \Rightarrow$

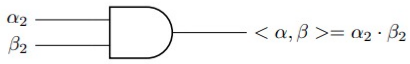

$2_3 : \quad \langle \alpha, \beta \rangle = (\alpha_1 \cdot \beta_2) \oplus (\alpha_2 \cdot \beta_1) \quad \Rightarrow$

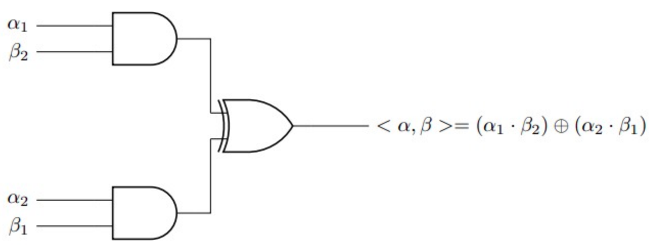

$2_4 : \quad \langle \alpha, \beta \rangle = (\alpha_1 \cdot \beta_1) \oplus (\alpha_2 \cdot \beta_2) \quad \Rightarrow$

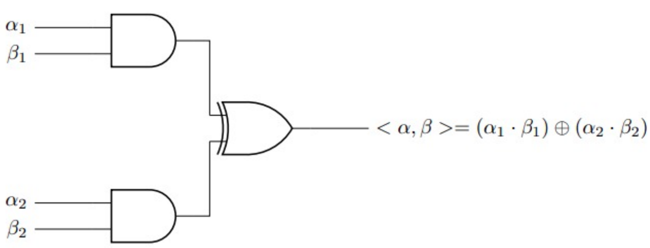

In terms of Boolean logic operators, the $\langle \alpha, \beta \rangle$ scalar products of the five 3-bit cases are expressed as:

$$
\begin{aligned}
3_1 : &\qquad \langle \alpha, \beta \rangle = 0, \\
3_2 : &\qquad \langle \alpha, \beta \rangle = (\alpha_1 \cdot \beta_2) \oplus (\alpha_2 \cdot \beta_1), \\
3_3 : &\qquad \langle \alpha, \beta \rangle = \alpha_1 \cdot \beta_1, \\
3_4 : &\qquad \langle \alpha, \beta \rangle = (\alpha_1 \cdot \beta_1) \oplus (\alpha_2 \cdot \beta_2), \\
3_5 : &\qquad \langle \alpha, \beta \rangle = (\alpha_1 \cdot \beta_1) \oplus (\alpha_2 \cdot \beta_2) \oplus (\alpha_3 \cdot \beta_3).
\end{aligned}
$$

The extension of this Boolean logic representation to n-bit scalar products for $n > 3$ is straightforward.

D Analysis of Specific Examples (biquaternions and (split-)quaternions)

D.1 (Split-)quaternions

As a preliminary step toward the construction and classification of the 3-bit compatible $\mathbb{Z}_2^n$-graded ($n = 0, 1, 2, 3$) Lie (super)algebras of biquaternions, we discuss in detail the recovery of the 2-bit $\mathbb{Z}_2^n$-graded compatible Lie (super)algebras over $\mathbb{R}$ induced by quaternions and split-quaternions.

Quaternions and split-quaternions arise from an ε-dependent Cayley-Dickson doubling of the complex numbers, with $\varepsilon = \pm 1$. The choice $\varepsilon = -1$ yields the division algebra of quaternions, while $\varepsilon = +1$ produces its split version (see [83, 84] for details on the construction).

We denote the four generators of the quaternions as e_0, e_i, and the four generators of the split-quaternions as $\widetilde{e}_0, \widetilde{e}_i$, where $i = 1, 2, 3$. The elements e_0 and $\widetilde{e}_0$ serve as the respective identities. The $\mathbb{Z}_2^2$ multiplicative grading of quaternions and split-quaternions is preserved by faithful 4×4 real matrix representations.

Without loss of generality, we express these algebras in terms of the following 2×2 real matrices:

$$I = \begin{pmatrix} 1 & 0 \\ 0 & 1 \end{pmatrix}, \qquad X = \begin{pmatrix} 1 & 0 \\ 0 & -1 \end{pmatrix}, \qquad Y = \begin{pmatrix} 0 & 1 \\ 1 & 0 \end{pmatrix}, \qquad A = \begin{pmatrix} 0 & 1 \\ -1 & 0 \end{pmatrix}.$$

We can set for the quaternions:

$$e_0 = I \otimes I, \quad e_1 = A \otimes I, \quad e_2 = Y \otimes A, \quad e_3 = X \otimes A.$$

so that

$$e_0 = \begin{pmatrix} 1 & 0 & 0 & 0 \\ 0 & 1 & 0 & 0 \\ 0 & 0 & 1 & 0 \\ 0 & 0 & 0 & 1 \end{pmatrix}, \quad e_1 = \begin{pmatrix} 0 & 0 & 1 & 0 \\ 0 & 0 & 0 & 1 \\ -1 & 0 & 0 & 0 \\ 0 & -1 & 0 & 0 \end{pmatrix},$$
$$e_2 = \begin{pmatrix} 0 & 0 & 0 & 1 \\ 0 & 0 & -1 & 0 \\ 0 & 1 & 0 & 0 \\ -1 & 0 & 0 & 0 \end{pmatrix}, \quad e_3 = \begin{pmatrix} 0 & 1 & 0 & 0 \\ -1 & 0 & 0 & 0 \\ 0 & 0 & 0 & -1 \\ 0 & 0 & 1 & 0 \end{pmatrix}.$$

And for the split-quaternions:

$$\widetilde{e}_0 = I \otimes I, \quad \widetilde{e}_1 = A \otimes I, \quad \widetilde{e}_2 = Y \otimes Y, \quad \widetilde{e}_3 = X \otimes Y.$$

so that

$$\widetilde{e}_0 = \begin{pmatrix} 1 & 0 & 0 & 0 \\ 0 & 1 & 0 & 0 \\ 0 & 0 & 1 & 0 \\ 0 & 0 & 0 & 1 \end{pmatrix}, \quad \widetilde{e}_1 = \begin{pmatrix} 0 & 0 & 1 & 0 \\ 0 & 0 & 0 & 1 \\ -1 & 0 & 0 & 0 \\ 0 & -1 & 0 & 0 \end{pmatrix},$$

$$\widetilde{e}_2 = \begin{pmatrix} 0 & 0 & 0 & 1 \\ 0 & 0 & 1 & 0 \\ 0 & 1 & 0 & 0 \\ 1 & 0 & 0 & 0 \end{pmatrix}, \quad \widetilde{e}_3 = \begin{pmatrix} 0 & 1 & 0 & 0 \\ 1 & 0 & 0 & 0 \\ 0 & 0 & 0 & -1 \\ 0 & 0 & -1 & 0 \end{pmatrix}.$$

The identity operators e_0 and $\widetilde{e}_0$ always belong to the 2-bit 00-graded sector, while the remaining operators are distributed among the 10, 01, and 11-graded sectors. The four compatible graded Lie (super)algebras, denoted as $2_1, 2_2, 2_3, 2_4$, are explicitly presented in Appendix A.

Remark: In the cases 2_1 and 2_3, the graded sectors 10, 01, and 11 are treated symmetrically. However, in the cases 2_2 and 2_4, the 11-graded sector is distinguished from the 10 and 01 sectors. Specifically:

- In the 2_2 case, the 11-graded sector corresponds to a bosonic generator, while the 10 and 01 sectors contain fermionic generators.
- In the 2_4 case, the 11-graded sector contains an "exotic boson" (see [15]), while the 10 and 01 sectors correspond to parafermions.

For the graded Lie (super)algebras derived from quaternions, this distinction is irrelevant. The three imaginary quaternionic generators e_1, e_2, e_3 are completely symmetric and can be interchanged freely.

However, the distinction becomes significant when constructing the graded Lie (super)algebras induced by split-quaternions. In this case, one of the generators, $\widetilde{e}_1$, is inherently different from $\widetilde{e}_2$ and $\widetilde{e}_3$. This asymmetry arises from the relations:

$$\widetilde{e}_1^2 = -\widetilde{e}_0, \quad \widetilde{e}_2^2 = \widetilde{e}_3^2 = \widetilde{e}_0.$$

Thus, $\widetilde{e}_1$ can be considered a "marked" generator, distinguishing it from the others.

This observation leads to the classification of four inequivalent graded Lie (super)algebras derived from quaternions and six inequivalent graded Lie (super)algebras derived from split-quaternions. Each of these algebras is uniquely defined by its set of (anti)commutators.

The four inequivalent quaternionic graded Lie (super)algebras are denoted as $\mathfrak{q}_1$, $\mathfrak{q}_2$, $\mathfrak{q}_3$, and $\mathfrak{q}_4$. Their definitions, based on their respective grading sector assignments, are as follows:

$\mathfrak{q}_1$ **from** 2_1 In this case, the generators are assigned as follows: $e_0 \in [00]$, $e_1 \in [10]$, $e_2 \in [01]$, and $e_3 \in [11]$. The commutation relations defining $\mathfrak{q}_1$ are:

$$[e_0, e_1] = [e_0, e_2] = [e_0, e_3] = 0, \quad [e_1, e_2] = 2e_3, \quad [e_2, e_3] = 2e_1, \quad [e_3, e_1] = 2e_2.$$

$\mathfrak{q}_2$ **from** 2_2 For $\mathfrak{q}_2$, the same grading sector assignments are used: $e_0 \in [00]$, $e_1 \in [10]$, $e_2 \in [01]$, and $e_3 \in [11]$. However, the defining (anti)commutation relations differ:

$$\begin{aligned} &[e_0, e_1] = [e_0, e_2] = [e_0, e_3] = 0, \quad [e_1, e_3] = -2e_2, \quad [e_2, e_3] = 2e_1, \\ &\{e_1, e_1\} = \{e_2, e_2\} = -2e_0, \quad \{e_1, e_2\} = 0. \end{aligned}$$

$\mathfrak{q}_3$ **from** 2_3 The sector assignments remain the same: $e_0 \in [00]$, $e_1 \in [10]$, $e_2 \in [01]$, and $e_3 \in [11]$. The defining relations for $\mathfrak{q}_3$ are:

$$[e_0, e_1] = [e_0, e_2] = [e_0, e_3] = 0, \quad \{e_1, e_2\} = \{e_2, e_3\} = \{e_3, e_1\} = 0.$$

$\mathfrak{q}_4$ **from** 2_4 The grading sector assignments are unchanged: $e_0 \in [00]$, $e_1 \in [10]$, $e_2 \in [01]$, and $e_3 \in [11]$. However, the defining (anti)commutators are:

$$\begin{aligned}&[e_0, e_1] = [e_0, e_2] = [e_0, e_3] = 0, \quad [e_1, e_2] = 2e_3,\\ &\{e_1, e_1\} = \{e_2, e_2\} = -2e_0, \quad \{e_1, e_3\} = \{e_2, e_3\} = 0.\end{aligned}$$

Comment: $\mathfrak{q}_3$ and $\mathfrak{q}_4$ enter the [15] classification of minimal $\mathbb{Z}_2^2$-graded Lie (super)algebras ($\mathfrak{q}_3$ corresponds to the algebra $A7$ and $\mathfrak{q}_4$ to the superalgebra $S10_{\varepsilon=+1}$).

The six inequivalent split-quaternionic graded Lie (super)algebras are denoted as $\widetilde{\mathfrak{q}}_1$, $\widetilde{\mathfrak{q}}_{2\alpha}$, $\widetilde{\mathfrak{q}}_{2\beta}$, $\widetilde{\mathfrak{q}}_3$, $\widetilde{\mathfrak{q}}_{4\alpha}$, and $\widetilde{\mathfrak{q}}_{4\beta}$. Their definitions, based on their respective grading sector assignments, are as follows:

$\widetilde{\mathfrak{q}}_1$ **from** 2_1 In this case, the sector assignments are given by $\widetilde{e}_0 \in [00]$, $\widetilde{e}_1 \in [10]$, $\widetilde{e}_2 \in [01]$, and $\widetilde{e}_3 \in [11]$. The defining commutation relations are:

$$[\widetilde{e}_0, \widetilde{e}_1] = [\widetilde{e}_0, \widetilde{e}_2] = [\widetilde{e}_0, \widetilde{e}_3] = 0, \quad [\widetilde{e}_1, \widetilde{e}_2] = 2\widetilde{e}_3, \quad [\widetilde{e}_2, \widetilde{e}_3] = -2\widetilde{e}_1, \quad [\widetilde{e}_3, \widetilde{e}_1] = 2\widetilde{e}_2.$$

$\widetilde{\mathfrak{q}}_{2\alpha}$ **from** 2_2 The sector assignments remain the same: $\widetilde{e}_0 \in [00]$, $\widetilde{e}_1 \in [10]$, $\widetilde{e}_2 \in [01]$, and $\widetilde{e}_3 \in [11]$. The defining (anti)commutation relations are:

$$\begin{aligned}&[\widetilde{e}_0, \widetilde{e}_1] = [\widetilde{e}_0, \widetilde{e}_2] = [\widetilde{e}_0, \widetilde{e}_3] = 0, \quad [\widetilde{e}_1, \widetilde{e}_3] = -2\widetilde{e}_2, \quad [\widetilde{e}_2, \widetilde{e}_3] = -2\widetilde{e}_1,\\ &\{\widetilde{e}_1, \widetilde{e}_1\} = -2\widetilde{e}_0, \quad \{\widetilde{e}_2, \widetilde{e}_2\} = 2\widetilde{e}_0, \quad \{\widetilde{e}_1, \widetilde{e}_2\} = 0.\end{aligned}$$

$\widetilde{\mathfrak{q}}_{2\beta}$ **from** 2_2 In this case, the sector assignments differ slightly: $\widetilde{e}_0 \in [00]$, $\widetilde{e}_1 \in [11]$, $\widetilde{e}_2 \in [10]$, and $\widetilde{e}_3 \in [01]$. The defining relations are:

$$\begin{aligned}&[\widetilde{e}_0, \widetilde{e}_1] = [\widetilde{e}_0, \widetilde{e}_2] = [\widetilde{e}_0, \widetilde{e}_3] = 0, \quad [\widetilde{e}_1, \widetilde{e}_2] = 2\widetilde{e}_3, \quad [\widetilde{e}_1, \widetilde{e}_3] = -2\widetilde{e}_2,\\ &\{\widetilde{e}_2, \widetilde{e}_2\} = \{\widetilde{e}_3, \widetilde{e}_3\} = 2\widetilde{e}_0, \quad \{\widetilde{e}_2, \widetilde{e}_3\} = 0.\end{aligned}$$

$\widetilde{\mathfrak{q}}_3$ **from** 2_3 The sector assignments return to: $\widetilde{e}_0 \in [00]$, $\widetilde{e}_1 \in [10]$, $\widetilde{e}_2 \in [01]$, and $\widetilde{e}_3 \in [11]$. The defining relations are:

$$[\widetilde{e}_0, \widetilde{e}_1] = [\widetilde{e}_0, \widetilde{e}_2] = [\widetilde{e}_0, \widetilde{e}_3] = 0, \quad \{\widetilde{e}_1, \widetilde{e}_2\} = \{\widetilde{e}_2, \widetilde{e}_3\} = \{\widetilde{e}_3, \widetilde{e}_1\} = 0.$$

$\widetilde{\mathfrak{q}}_{4\alpha}$ **from** 2_4 Here, the generators are assigned to the same sectors as before: $\widetilde{e}_0 \in [00]$, $\widetilde{e}_1 \in [10]$, $\widetilde{e}_2 \in [01]$, and $\widetilde{e}_3 \in [11]$. The defining relations are:

$$\begin{aligned}&[\widetilde{e}_0, \widetilde{e}_1] = [\widetilde{e}_0, \widetilde{e}_2] = [\widetilde{e}_0, \widetilde{e}_3] = 0, \quad [\widetilde{e}_1, \widetilde{e}_2] = 2\widetilde{e}_3,\\ &\{\widetilde{e}_1, \widetilde{e}_1\} = -2\widetilde{e}_0, \quad \{\widetilde{e}_2, \widetilde{e}_2\} = 2\widetilde{e}_0, \quad \{\widetilde{e}_1, \widetilde{e}_3\} = \{\widetilde{e}_2, \widetilde{e}_3\} = 0.\end{aligned}$$

$\widetilde{\mathfrak{q}}_{4\beta}$ **from** 2_4 In this case, the sector assignments are: $\widetilde{e}_0 \in [00]$, $\widetilde{e}_1 \in [11]$, $\widetilde{e}_2 \in [10]$, and $\widetilde{e}_3 \in [01]$. The defining relations are:

$$\begin{aligned}&[\widetilde{e}_0, \widetilde{e}_1] = [\widetilde{e}_0, \widetilde{e}_2] = [\widetilde{e}_0, \widetilde{e}_3] = 0, \quad [\widetilde{e}_2, \widetilde{e}_3] = -2\widetilde{e}_1,\\ &\{\widetilde{e}_2, \widetilde{e}_2\} = \{\widetilde{e}_3, \widetilde{e}_3\} = 2\widetilde{e}_0, \quad \{\widetilde{e}_1, \widetilde{e}_2\} = \{\widetilde{e}_1, \widetilde{e}_3\} = 0.\end{aligned}$$

Comment: $\widetilde{\mathfrak{q}}_3$, $\widetilde{\mathfrak{q}}_{4\alpha}$, $\widetilde{\mathfrak{q}}_{4\beta}$ enter the [15] classification of minimal $\mathbb{Z}_2^2$-graded Lie (super)algebras ($\widetilde{\mathfrak{q}}_3$ corresponds to the algebra $A7$, $\widetilde{\mathfrak{q}}_{4\alpha}$ to the superalgebra $S10_{\varepsilon=-1}$ and $\widetilde{\mathfrak{q}}_{4\beta}$ to the superalgebra $S10_{\varepsilon=+1}$).

D.2 Biquaternions

The algebra $\mathbb{H}_B$ of biquaternions can be regarded as the tensor product $\mathbb{C} \times \mathbb{H}$ of the complex numbers with the quaternions (over $\mathbb{R}$). This algebra has eight generators, which can be arranged within a $\mathbb{Z}_2^3$ multiplicative grading (allowing for a 3-bit assignment).

A faithful 8×8 matrix representation that preserves this grading can be constructed using the 2×2 matrices I, X, Y, A introduced in the beginning of this appendix. We define the generators as follows:

$$\begin{aligned} &f_0 = I \otimes I \otimes I, \quad f_1 = I \otimes A \otimes I, \quad f_2 = I \otimes Y \otimes A, \quad f_3 = I \otimes X \otimes A, \\ &g_0 = A \otimes I \otimes I, \quad g_1 = A \otimes A \otimes I, \quad g_2 = A \otimes Y \otimes A, \quad g_3 = A \otimes X \otimes A. \end{aligned}$$

Taking into account the definitions of the I, X, Y, A matrices, the multiplication table for these generators can be derived:

	f_0	f_1	f_2	f_3	g_0	g_1	g_2	g_3
f_0	f_0	f_1	f_2	f_3	g_0	g_1	g_2	g_3
f_1	f_1	$-f_0$	f_3	$-f_2$	g_1	$-g_0$	g_3	$-g_2$
f_2	f_2	$-f_3$	$-f_0$	f_1	g_2	$-g_3$	$-g_0$	g_1
f_3	f_3	f_2	$-f_1$	$-f_0$	g_3	g_2	$-g_1$	$-g_0$
g_0	g_0	g_1	g_2	g_3	$-f_0$	$-f_1$	$-f_2$	$-f_3$
g_1	g_1	$-g_0$	g_3	$-g_2$	$-f_1$	f_0	$-f_3$	f_2
g_2	g_2	$-g_3$	$-g_0$	g_1	$-f_2$	f_3	f_0	$-f_1$
g_3	g_3	g_2	$-g_1$	$-g_0$	$-f_3$	$-f_2$	f_1	f_0

In the above table, each entry represents the result of the left action of a row generator on a column generator.

The generator f_0 corresponds to the identity operator, while g_0 represents the imaginary unit, as it commutes with all other generators. The quaternionic subalgebra is spanned by the set $\{f_0, f_1, f_2, f_3\}$.

The remaining seven generators (excluding the identity) fall into three distinct equivalence classes (A, B, C), which "mark" them according to the classification presented. These classes are determined by the transformations that leave the multiplication table (D.2) invariant. These transformations include permutations within a given class combined with a possible ± 1 sign normalization. The class structure is as follows:

$$f_1, f_2, f_3 \in A, \quad g_0 \in B, \quad g_1, g_2, g_3 \in C.$$

The identity operator f_0 is assigned to the 000-graded sector:

$$[f_0] = 000.$$

The 3-bit grading assignments of the remaining generators can be deduced from those of f_1, f_2, and g_0. Let us define $[f_1] = \alpha$, $[f_2] = \beta$, and $[g_0] = \gamma$. Consistency with the $\mathbb{Z}_2^3$-grading requires:

$$\begin{aligned} &[f_0] = 000, \quad [f_1] = \alpha, \quad\quad [f_2] = \beta, \quad\quad [f_3] = \alpha + \beta, \\ &[g_0] = \gamma, \quad\quad [g_1] = \alpha + \gamma, \quad [g_2] = \beta + \gamma, \quad [g_3] = \alpha + \beta + \gamma, \end{aligned}$$

where the sums are taken modulo 2.

The inequivalent graded Lie (super)algebras compatible with the multiplicative $\mathbb{Z}_2^3$ grading assignments are the five algebras denoted as $3_1, 3_2, 3_3, 3_4, 3_5$.

We can extend the analysis performed before for the 2-bit assignments to determine which graded sectors (besides 000) are distinguished in each of the five cases given in Appendix A. The results are as follows:

3_1 *case*: All seven graded sectors $100, 010, 001, 110, 101, 011, 111$ are on equal footing and correspond to bosonic particles.

3_2 *case*: The sector 001 is singled out as it corresponds to a bosonic particle, whereas the remaining six sectors $100, 010, 110, 101, 011, 111$ correspond to parabosons and are treated symmetrically.

3_3 *case*: The three sectors $010, 001, 011$ correspond to bosonic particles, while the remaining four sectors $100, 110, 101, 111$ correspond to fermions.

3_4 *case*: The seven graded sectors divide into three distinct types: 001 corresponds to a bosonic particle, 110 and 111 to parabosons, and $100, 010, 101, 011$ to parafermions.

3_5 *case*: The three sectors $110, 101, 011$ correspond to parabosons, while the remaining four sectors $100, 010, 001, 111$ correspond to parafermions.

Thus, the seven additional graded sectors (besides 000) are distributed as follows:

$$3_1:\ 7, \quad 3_2:\ 1+6, \quad 3_3:\ 3+4, \quad 3_4:\ 1+2+4, \quad 3_5:\ 3+4.$$

Inequivalent graded Lie (super)algebras are obtained by assigning the seven marked generators (D.2), which belong to classes A, B, C, to the different graded sector classes listed above. The classification results in the following subcases:

3_1 *case* - A single graded Lie algebra, which can be expressed as:

$$3_{1,i}: \quad \alpha = 100,\ \beta = 010,\ \gamma = 001$$

(All other assignments are equivalent.)

3_2 *case* - Three inequivalent graded Lie algebras:

$$\begin{aligned} 3_{2,i}&: \quad \alpha = 100,\ \beta = 010,\ \gamma = \underline{001}, \\ 3_{2,ii}&: \quad \alpha = \underline{001},\ \beta = 010,\ \gamma = 100, \\ 3_{2,iii}&: \quad \alpha = 111,\ \beta = 010,\ \gamma = 100 \end{aligned}$$

(The underlined sector 001 is the distinguished bosonic sector. In case $3_{2,iii}$, it is assigned to the C generator g_3, whose grading is $\alpha + \beta + \gamma$.)

3_3 *case* - Three inequivalent graded Lie superalgebras, considering the $3 + 4$ split $(010, 001, 011$ vs. $100, 110, 101, 111)$:

$$\begin{aligned} 3_{3,i}&: \quad \alpha = 010,\ \beta = 001,\ \gamma = 111, \\ 3_{3,ii}&: \quad \alpha = 010,\ \beta = 100,\ \gamma = 111, \\ 3_{3,iii}&: \quad \alpha = 010,\ \beta = 100,\ \gamma = 011 \end{aligned}$$

(Either all three A generators f_1, f_2, f_3 are assigned to the $010, 001, 011$ sectors, or just one of them. In the latter case, there are two inequivalent possibilities for the grading of γ in g_0: either it belongs to $010, 001, 011$ or it does not.)

3_4 *case* - Six inequivalent graded Lie superalgebras, considering the 1+2+4 split $(001/110, 111/100, 010, 101, 011)$:

$$\begin{aligned}
3_{4,i}&: \quad \alpha = 001,\ \beta = 110,\ \gamma = 100,\\
3_{4,ii}&: \quad \alpha = 001,\ \beta = 100,\ \gamma = 110,\\
3_{4,iii}&: \quad \alpha = 001,\ \beta = 100,\ \gamma = 011,\\
3_{4,iv}&: \quad \alpha = 110,\ \beta = 100,\ \gamma = 001,\\
3_{4,v}&: \quad \alpha = 110,\ \beta = 100,\ \gamma = 111,\\
3_{4,vi}&: \quad \alpha = 110,\ \beta = 100,\ \gamma = 011
\end{aligned}$$

(Define a, b, c as the respective graded sectors of the $1 + 2 + 4$ decomposition. Either all three A generators f_1, f_2, f_3 belong to sectors a, b, forcing γ into c, or only one of them is assigned to a or b. If this generator is in a, then γ can be in b or c. If this generator is in c, then γ has three inequivalent placements: a, b, or c.)

3_5 *case* - Three inequivalent graded Lie superalgebras arise from the 3+4 split $(110, 101, 011/100, 010, 001, 111)$. These algebras can be presented as follows:

$$\begin{aligned}
3_{5,i}&: \quad \alpha = 110,\ \beta = 101,\ \gamma = 100,\\
3_{5,ii}&: \quad \alpha = 110,\ \beta = 100,\ \gamma = 111,\\
3_{5,iii}&: \quad \alpha = 110,\ \beta = 100,\ \gamma = 011
\end{aligned}$$

(The classification follows the same reasoning as in the 3_3 case, which is also based on a $3 + 4$ graded sector split.)

Thus, the total number n_B of inequivalent graded Lie (super)algebras compatible with the $\mathbb{Z}_2^3$ multiplicative grading of the biquaternions is:

$$n_B = 1 + 3 + 3 + 6 + 3 = 16.$$

To save space, we explicitly present the defining (anti)commutators only for the three inequivalent superalgebras from the 3_5 case. Each of these algebras is defined by 32 (anti)commutators, of which the following seven are common to all cases:

$$[f_0, z] = 0 \quad \text{for any } z \in \mathbb{H}_B.$$

The remaining (anti)commutators are given below.

For $3_{5,i}$: Nine defining brackets vanish:

$$[g_0, g_1] = [g_0, g_2] = [g_0, f_3] = \{g_1, f_3\} = \{g_2, f_3\} = \{f_1, f_2\} = \{f_1, f_3\} = \{f_2, f_3\} = [f_3, g_3] = 0.$$

The remaining sixteen are nonvanishing:

$$\begin{aligned}
&\{g_0, g_0\} = -2f_0,\ \{g_0, f_1\} = 2g_1,\ \{g_0, f_2\} = 2g_2,\ \{g_0, g_3\} = -2f_3,\ \{g_1, g_1\} = 2f_0,\\
&[g_1, g_2] = -2f_3,\ \{g_1, f_1\} = -2g_0,\ [g_1, f_2] = 2g_3,\ \{g_1, g_3\} = -2f_2,\ \{g_2, g_2\} = 2f_0,\\
&[g_2, f_1] = -2g_3,\ \{g_2, f_2\} = -2g_0,\ \{g_2, g_3\} = -2f_1,\ [f_1, g_3] = -2g_2,\ [f_2, g_3] = 2g_1,\\
&\{g_3, g_3\} = 2f_0.
\end{aligned}$$

For $3_{5,ii}$: Fifteen defining brackets vanish:

$$\begin{aligned}
&\{f_2, f_1\} = \{f_2, g_3\} = [f_2, g_2] = \{f_3, f_1\} = [f_3, g_3] = \{f_3, g_2\} = [g_1, f_1] = \{g_1, g_3\} =\\
&= \{g_1, g_2\} = \{f_1, g_3\} = \{f_1, g_2\} = [f_1, g_0] = \{g_3, g_2\} = [g_3, g_0] = [g_2, g_0] = 0.
\end{aligned}$$

The remaining ten are nonvanishing:

$$\{f_2, f_2\} = -2f_0,\ [f_2, f_3] = 2f_1,\ [f_2, g_1] = -2g_3,\ \{f_2, g_0\} = 2g_2,\ \{f_3, f_3\} = -2f_0,$$
$$[f_3, g_1] = 2g_2,\ \{f_3, g_0\} = 2g_3,\ \{g_1, g_1\} = 2f_0,\ \{g_1, g_0\} = -2f_1,\ \{g_0, g_0\} = -2f_0.$$

For $3_{5,iii}$: Nine defining brackets vanish:

$$\{f_2, f_1\} = \{f_2, g_1\} = [f_2, g_0] = [f_3, g_3] = \{f_3, f_1\} = [f_3, g_2] = \{g_3, g_1\} = \{g_3, g_2\} = [g_0, g_2] = 0.$$

The remaining sixteen are nonvanishing:

$$\{f_2, f_2\} = -2f_0,\ [f_2, f_3] = 2f_1,\ [f_2, g_3] = 2g_1,\ \{f_2, g_2\} = -2g_0, \{f_3, f_3\} = -2f_0,$$
$$[f_3, g_1] = 2g_2,\ \{f_3, g_0\} = 2g_3,\ \{g_3, g_3\} = 2f_0,\ [g_3, f_1] = 2g_2,\ \{g_3, g_0\} = -2f_3,$$
$$\{f_1, g_1\} = -2g_0,\ \{f_1, g_0\} = 2g_1,\ [f_1, g_2] = 2g_3,\ \{g_1, g_0\} = -2f_1,\ [g_1, g_2] = -2f_3,$$
$$\{g_2, g_2\} = 2f_0.$$

Comment: The difference between the $3_{5,i}$ and $3_{5,iii}$ cases is related to the diagonal signature of the parafermionic generators. Since f_0 is the identity operator, the graded superalgebra $3_{5,i}$ has the signature $(-1, +1, +1, +1)$ for the squared values of g_0, g_1, g_2, g_3, while in the $3_{5,iii}$ case, the squared values of f_2, f_3, g_3, g_2 produce the signature $(-1, -1, +1, +1)$. Thus, $3_{5,i}$ and $3_{5,iii}$ are different real forms of a graded superalgebra.